THERMAL DECOMPOSITION OF HYDRAZOIC ACID

by 45

WILLIAM C. RICHARDSON

B. S., Fordham College, 1965

A MASTER'S THESIS

submitted in partial fulfillment of the

requirements for the degree

MASTER OF SCIENCE

Department of Chemistry

KANSAS STATE UNIVERSITY
Manhattan, Kansas

1969

Approved by:

D. W. Setser

Major Professor

Table of Contents

List of Tables

List of Figures

INTRODUCTION

The original purpose of this investigation may be divided into two parts. (1) At the present time it is a frank appraisal of NH radical chemistry to state that not one single elementary reaction of NH has been well characterized (See Appendix III). Elucidation of some NH radical chemistry in a classical system was a first step goal of this study. (2) NH is an inorganic radical isoelectronic with methylene (CH_2), and oxygen atoms. Intuitively it may be expected to possess a similar chemistry. Generation of CH_2 from diazomethane (CH_2N_2) and ketene (CH_2CO) followed by its reaction with various substrates has enabled researchers in this laboratory and others to study non-equilibrium unimolecular decomposition of a variety of chemically activated species. Resultant experimental rate constants could then be compared with those calculated from the Rice-Ramsperger-Kassel-Marcus theory of unimolecular decay by proposition of an activated complex. Similar studies could, in principle, be done with the NH radical, and this was attempted in this study.

Pyrolysis of hydrazoic acid vapor was selected as the source of NH radicals. The reactions of the NH radical would be expected to depend upon its electronic state ($^3\Sigma$ or $^1\Delta$) and will be an important aspect of NH_3 pyrolysis, as well as being pertinent to the two main goals just outlined.

Previous investigations of hydrazoic acid decomposition in pyrolysis[1-3] and photolysis[4-8] systems are consistent with the formation of NH in the primary dissociation. Product analysis

in photolytic systems[9] is made difficult by the formation of a white solid on the walls of the vessel. This solid is attributed to ammonium azide, arising from an acid-base complexation of product ammonia and undecomposed hydrazoic acid. In pyrolysis systems the NH_4N_3 which makes quantitative analysis difficult, would be eliminated because of the complete dissociation of ammonium azide at temperatures above 100°C.[10] A recent infrared study[11] of ammonium azide at room temperature showed that the vapor over solid NH_4N_3 contained predominantly HN_3 and NH_3.

Early pyrolysis studies[1-3] indicated that decomposition occurred by two different routes depending upon the experimental parameters of temperature and pressure. Above certain limits of temperature and pressure the reaction was explosive. Nitrogen and hydrogen were the only observed products, and the yield was in accord with an overall stoichiometry given by equation (1).

$$HN_3 \rightarrow 1/2\ H_2 + 3/2\ N_2 \qquad (1)$$

$$HN_3 \rightarrow 1/3\ NH_3 + 4/3\ N_2 \qquad (2)$$

Equation (2) represents the stoichiometry for the slow thermal decomposition; no hydrogen was observed. There is evidence that the slow thermal decomposition is affected by surface conditions. The role of surface in thermal systems and the fate of NH with regard to surface have not been ascertained. A more recent report[12] has indicated a third mode of decomposition, just below the explosion limits, yet near the boundary. Decomposition was observed to be slow and accompanied by a white luminescence after

a brief induction period. Thus the decomposition of hydrazoic acid in pyrolysis systems offers some promise as a source of NH radicals under a variety conditions for study of reactions with substrates.

In the absence of definitive data on the thermal decomposition of HN_3, results from the pyrolysis studies of the isoelectronic molecules diazomethane and nitrous oxide are helpful. Thermal decomposition of diazomethane[13,14] gives nitrogen and methylene in its low lying $^1A_1$ spin state in the primary dissociation with rate constant[15] $1.2 \times 10^{12} \exp(-3400/RT)$ sec^{-1} at 2.5 cm pressure. Although the energy separation between the $^3\Sigma$ ground state and $^1A_1$ state of CH_2 is not known exactly, it is believed to be small, perhaps near 5 kcal.[15] The thermal decomposition thus proceeds with conservation of spin. The thermal decomposition of nitrous oxide has been of much theoretical interest, and the reaction has been widely studied. Johnston[16] has updated, corrected, and reviewed the experimental work on N_2O thermal decomposition. The high pressure rate is $10^{11.9} \exp(-60000/RT)$ sec^{-1}. It is generally agreed that nitrous oxide-decomposition exemplifies a non-adiabatic reaction involving formation of the spin forbidden $O(^3P)$.[17] The low preexponential factor reflects this feature. The energy separation of $O(^3P)$ - $O(^1D)$ is about 45 kcal.[18] HN_3 lies between CH_2N_2 and N_2O when one considers the heavier atom of the radical formed (i.e. C, N, O) in the primary dissociation, and also the thermochemistry of the singlet-triplet radicals. It becomes an interesting

question as to which spin state of NH is formed in the primary dissociation of HN_3.

From a vast body of information compiled[13,15,19] on the reactions of CH_2 ($^1A_1$) it is apparent that singlet methylene reacts with C-H bonds in alkanes by a mechanism leading to a product corresponding to the insertion of CH_2 between the C and H of the hydrocarbon (3).

$$CH_2(^1A_1) + R\text{-}H \rightarrow R\text{-}CH_2\text{-}H \quad (R = CH_3 \text{ to } C_3H_7) \tag{3}$$

Also a $CH_2(^3\Sigma)$ reacts with C-H bonds by an abstraction reaction (4).

$$CH_2(^3\Sigma) + RH \rightarrow R + CH_3 \tag{4}$$

However, recent work has indicated that $CH_2(^3\Sigma)$ may insert[20], and $CH_2(^1A_1)$ may abstract[21] under certain conditions, but reactions (3) and (4) are certainly the predominant reactions with simple alkanes. Studies[22,23,24] of oxygen atom reactions and methylene radical reactions in a variety of olefinic systems have indicated that singlet diradicals add directly across double bonds (5), while triplet diradicals add in a non-stereo-specific fashion (6).

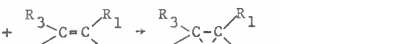

(5)

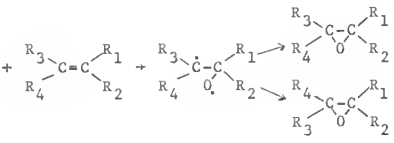

(6)

With alkanes $O(^1D)$ reacts by an insertion similar to (3), and $O(^3P)$ by an abstraction mechanism similar to (4).[25] More recently studies[26] of sulfur atoms generated from carbonyl sulfide, COS, photolysis have indicated an insertion mechanism for $S(^1D)$ reaction with hydrocarbons. $S(^3P)$ has been shown to be inert in these systems due to unfavorable energetics for abstraction and/or slow rate of insertion.

From the chemistry of CH_2, O, and S, there appears to be an important trend relating the spin state of a species to its mode of reaction with hydrocarbons. In each case, $CH_2(^1A_1)$, $O(^1D)$, and $S(^1D)$ react predominantly by an insertion mechanism and $CH_2(^3\Sigma)$ and $O(^3P)$ react by an abstraction mechanism. It should be emphasized that exact details of the singlet-triplet reactions of CH_2, O, and S are still being investigated, and there is some conflict over detailed interpretations. By examination of HN_3 decomposition with alkane and alkene substrates one can argue intuitively from the background of trends noted above as to which spin state of NH is important. For example singlet NH would be expected to react by (7), triplet NH by (8) with alkanes.

$$NH\ (^1\Delta) + R\text{-}H \rightarrow R\text{-}NH_2 \qquad (7)$$

$$NH\ (^3\Sigma) + R\text{-}H \rightarrow R + NH_2 \qquad (8)$$

CALCULATIONS

In 1951 Marcus and Rice[27] reformulated the Rice-Ramsperger-Kassel theory of unimolecular reactions[28]; this theory is based upon classical statistical mechanical arguments with quantum restrictions. This improvement, generally referred to as RRKM theory, when applied to actual examples has shown that all the vibrational degrees of freedom are involved in the internal energy distribution processes of activated molecules. The theory has enjoyed a considerable amount of success when quantitatively applied to a variety of data[29], and has been able to predict results in advance of experimental data.[30] It was with this view that calculations were carried out for certain reactions expected to occur in this study (i.e. for N_2H_4 and CH_3NH_2); the calculations were expected to aid in the interpretation of some very complicated experimental data from this study and from the existing literature.

The RRKM theory of unimolecular reactions has been discussed in detail elsewhere[27,31-33], and only the equations are listed here. The microscopic specific rate constants are given as a function of energy by

$$k_\varepsilon = \frac{\sigma}{h} \frac{Z_1^\dagger}{Z_1^*} \frac{\Sigma P(\varepsilon_{vr}^\dagger)}{N_\varepsilon^*} \qquad \text{(I)}$$

Where $Z_1^\dagger$ and Z_1^* are the products of the partition functions for the adiabatic degrees of freedom of the activated complex and

molecule, respectively; $\Sigma P(\epsilon^{\dagger}_{vr})$ is the sum of the degeneracies of all possible energy eigenstates of the active (vibrational and rotational) degrees of freedom of the activated comples at total energy $\epsilon^{\dagger}_{vr}$; $N^{*}(\epsilon_{vr})$ is the number of eigenstates per unit energy of the active degrees of freedom for the molecule at energy ϵ_{vr}; h is Planck's constant; σ is the reaction path degeneracy; and $\epsilon^{\dagger}_{vr} = \epsilon_{vr} - \epsilon_{o}$, where ϵ_{o} is the critical energy for reaction, and ϵ_{vr} is the total energy.

All vibrational degrees of freedom are considered active. Overall rotations may be adiabatic. An adiabatic degree of freedom does not exchange energy with any other degree of freedom, whereas free flow of energy exists among the active degrees of freedom.

Marcus and Rice[27,31,32,34] have developed expressions for $\Sigma P(\epsilon^{\dagger}_{vr})$ and N^{*}_{ϵ}:

$$P(\epsilon^{\dagger}_{vr}) = \frac{Z^{\dagger}_{r}}{(kT)^{r^{\dagger}/2}\Gamma(1+r^{\dagger}/2)} \sum_{\epsilon^{\dagger}_{v}=0}^{\epsilon^{\dagger}} P(\epsilon_{v})(\epsilon^{\dagger}-\epsilon^{\dagger}_{v})^{r^{\dagger}/2}; r^{\dagger}\neq 0 \qquad \text{(II)}$$

$$N^{*}_{\epsilon} = \frac{Z^{*}_{r}}{(kT)^{r^{*}/2}\Gamma(r^{*}/2)} \Sigma P(\epsilon^{*}_{vr})(\epsilon-\epsilon_{v})^{r^{*}/2-1}; r^{*}\neq 0 \quad . \qquad \text{(III)}$$

For either complex or molecule, Z_{r} is the appropriate partition function expression for r active internal and overall degrees of freedom; $\Gamma(x)$ is the Gamma function of x; and the pre-sum factors in equations (II) and (III) are denoted $A^{\dagger}$ and A^{*}, respectively.

To be strictly correct, the sums and densities of states should be calculated for anharmonic vibrations. However, a harmonic oscillator approximation was used in these calculations; below 100 kcal mole^{-1} the magnitude of k_ε is much less strongly affected by anharmonic corrections.[35] The procedure was as follows: given a model of the activated complex, the fundamental vibrational frequencies were used to calculate $\Sigma\ P^\dagger(\varepsilon_{vr})$ at several values of $\varepsilon^\dagger_{vr}$ using a direct count method. The Haarhoff[36] approximation was used to calculate the density of states from the vibrational frequencies of the molecule. The direct count was matched to the Haarhoff approximation at intermediate energies before the latter was used. The values of N^*_ε and $\Sigma\ P(\varepsilon^\dagger_{vr})$ were then substituted into equation (I) to obtain k_ε as a function of energy.

In any real system the molecules are formed with a distribution of energies and the specific rate constants must be averaged according to the distribution function. The distribution function in thermal activation systems is simply the thermal quantum Boltzmann distribution

$$k(\varepsilon_{vr})\ d\varepsilon_{vr} = \frac{N^*(\varepsilon_{vr})\ \exp[-(\varepsilon_{vr}/RT)]}{Z^*_{vr}}\ d\varepsilon_{vr} \qquad \text{(IV)}$$

where Z^*_{vr} is the partition function for the active degrees of freedom of the molecule. For the chemical activation system in which the energized molecules are formed by the combination of

thermalized free radicals, the distribution function is given by

$$f(\varepsilon_{vr})\ d\varepsilon_{vr} = k'_{\varepsilon}\ K(\varepsilon_{vr})\ d\varepsilon_{vr} / \int_{\varepsilon'_o}^{\infty} k'_{\varepsilon}\ K(\varepsilon_{vr})\ d\varepsilon_{vr} \quad . \tag{V}$$

The primed terms refer to the decomposition reaction which is the reverse of the combination reaction leading to the formation of the molecules. $K(\varepsilon_{vr})$ is defined as in equation (IV). The temperatures of the experiments in which the combination reactions were studied is used in equation (IV).

The non-equilibrium experimental rate constant for chemically activated systems is defined for strong collisions as

$$k_a = \omega \frac{D}{S} = \omega \frac{\int_{E_{min}}^{\infty} \frac{k_{\varepsilon}}{k_{\varepsilon} + \omega} f(\varepsilon)\ d\varepsilon}{\int_{E_{min}}^{\infty} \frac{\omega}{k_{\varepsilon} + \omega} f(\varepsilon)\ d\varepsilon} \quad , \tag{VI}$$

Where ω is the collision frequency, D/S is the ratio of decomposition to stabilization products, and $f(\varepsilon)\ d\varepsilon$ is the distribution function for the chemically activated molecule. The average energy of the formed molecules, $\langle \varepsilon^{\dagger} \rangle$, is

$$\langle \varepsilon^{\dagger} \rangle = \frac{\int_{o}^{\infty} \varepsilon\ f(\varepsilon)\ d\varepsilon}{\int_{o}^{\infty} f(\varepsilon)\ d\varepsilon} \quad , \tag{VII}$$

while the average energy of the reacting molecules is

$$\langle \varepsilon_r^{\dagger} \rangle = \frac{\int_{\varepsilon_o}^{\infty} \frac{k_\varepsilon}{k_\varepsilon + \omega} \varepsilon \, d(\varepsilon) \, d\varepsilon}{\int_{\varepsilon_o}^{\infty} \frac{k_\varepsilon}{k_\varepsilon + \omega} f(\varepsilon) \, d\varepsilon} . \qquad \text{(VIII)}$$

Where $\langle \varepsilon_r^{\dagger} \rangle$ is measured from ε_o, i.e., $\langle \varepsilon_r \rangle = \varepsilon_o + \langle \varepsilon_r^{\dagger} \rangle$

Calculations are done for hydrazine and methylamine unimolecular decomposition; such reactions belong to a general class of reactions characterized by little or no activation energy for the reverse process, i.e., for the combination of free radicals. A profile of the potential energy surface for this class of reactions and associated thermochemical quantities are given in Fig. 1.

The calculations demand a knowledge of the thermochemistry and molecular parameters of the molecules and radicals, and a description of the transition state; thermochemistry is especially important. Pertinent data for the molecules and radicals are presented in Appendices I and II. A reasonable description of the transition state was obtained for hydrazine in the following way. Consider the unimolecular decomposition of hydrazine,

$$N_2H_4 + M \rightleftarrows N_2H_4^{*} + M \qquad (9)$$

$$N_2H_4^{*} \rightarrow N_2H_4^{\dagger} \qquad (10)$$

$$N_2H_4^{\dagger} \rightarrow NH_2 + NH_2 , \qquad (11)$$

where M is any bath molecule capable of imparting vibrational

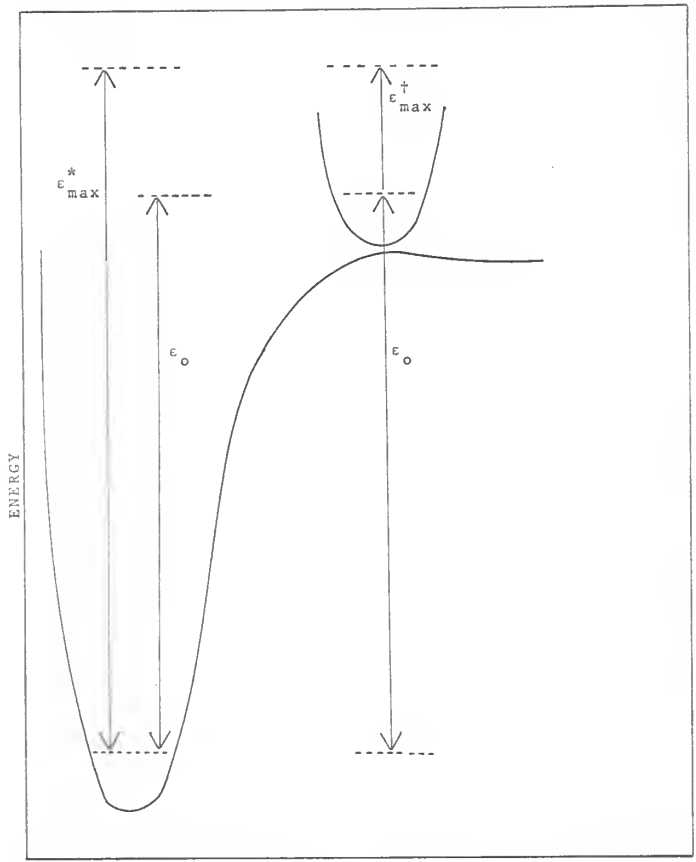

Figure 1. Potential energy profile for reaction: $R^{*} \rightarrow$ products.

energy to hydrazine, $N_2H_4^*$ denotes a molecule with sufficient energy to dissociate, i.e., an energized or active molecule, and $N_2H_4^\dagger$ denotes an activated complex. In a high pressure thermal equilibrium system hydrazine molecules would be in equilibrium with products, i.e.,

$$N_2H_4 \underset{k_{bi}}{\overset{k_{uni}}{\rightleftharpoons}} NH_2 + NH_2 \quad , \tag{12}$$

where k_{uni} is the unimolecular decomposition rate constant for N_2H_4 ($=k_\infty$ in this case), and k_{bi} is the bimolecular rate constant for the combination of NH_2 radicals. The equilibrium constant for this reaction is a measure of the k_{uni}/k_{bi} ratio and K_{eq} may be calculated as usual from partition functions[38].

$$K_{eq} = k_{uni}/k_{bi} = \frac{Q^{NH_2} Q^{NH_2}}{Q^{N_2H_4}} \exp[-\Delta H_o^o/RT] \quad , \tag{IX}$$

The equilibrium high pressure unimolecular rate constant, may be calculated from partition functions[38] by

$$k_\infty = \frac{kT}{h} \frac{Q^\dagger_{N_2H_4}}{Q^*_{N_2H_4}} \exp(-\varepsilon_o/RT) = \frac{ekT}{h} \exp(\Delta S^\dagger/R)\exp(-Ea/RT) \tag{X}$$

Here $Q^\dagger_{N_2H_4}$ and $Q^*_{N_2H_4}$ are the total partition function expressions for the activated complex and molecule respectively, $\Delta S^\dagger$ is the entropy of activation, ε_o is the critical energy, and E_a is the experimental activation energy.

The bimolecular rate constant from collision theory for combination of two radicals assuming no activation barrier is given[39] by

$$k_{bi} = K \zeta \pi r_*^2 (8kT/\pi\mu)^{1/2} \quad , \qquad (XI)$$

where r_* is approximately the sum of the radii of the colliding particles assuming rigid spheres, K is the steric factor, ζ is unity or 1/2 depending upon whether the radicals are different or identical, μ is the reduced mass, and k is Boltzmann's constant.

K_{eq} may be calculated without prejudice. The bimolecular rate constant for many doublet state free radicals such as CH_3, CF_3, etc. has been measured and is nearly always $10^{13.5}$ cc mole^{-1} sec^{-1}. This corresponds to the prediction of either the Gorin model[40] or simply collision theory (XI) with a steric factor of 0.1 to 0.01. Calculation of k_∞ (k_{uni} at high pressure limit) by equation (x) is guided by the results obtained from $K_{eq} \times k_{bi}$. Thus the description, in terms of $Q^\dagger$ or $\Delta S^\dagger$ of the $N_2H_4^\dagger$ transition state is determined within certain limitations. Once the transition model is established calculation of k_ε, k_a, $\langle\varepsilon_r\rangle$, and D/S is a routine procedure using the IBM 360 digital computer.

A summary of the pre-exponential factors for K_{eq} and k_{bi} used to define the hydrazine and methylamine complexes is given in Tables I and II.

TABLE I. For hydrazine. Pre-exponential factors (calculated) for K_{eq} and k_{bi} and their comparison to k_{uni} for complex models chosen.

Temperature (°K)	K_{eq}[a]	k_{bi}[b,c]	$K_{eq} x k_{bi}$	k_{uni}(I)[d]	k_{uni}(II)
553	3.84×10^{26}	4.49×10^{-10}	1.72×10^{17}	1.50×10^{16}	1.29×10^{15}
723	5.02×10^{26}	5.14×10^{-10}	2.58×10^{17}	3.34×10^{16}	2.52×10^{15}
1000	5.58×10^{26}	6.04×10^{-10}	3.37×10^{17}	7.41×10^{16}	4.95×10^{15}
1500	4.60×10^{26}	7.39×10^{-10}	3.40×10^{17}	15.5×10^{16}	9.24×10^{15}

a. In units of molecule cc^{-1}. b. In units of cc molccule^{-1} sec^{-1}. c. A value[54] of 4.42A was used for the sum of radii of colliding particles. A symmetry factor of 1/2 was used because the colliding partners are identical. No steric factor has been added to this calculation. d. In units of sec^{-1}. (I) and (II) refer to the hydrazine complex models used.

TABLE II. For methylamine. Pre-exponential factors (calculated) for K_{eq} and k_{bi} and their comparison to k_{uni} for complex models chosen.

Temperature (°K)	k_{eq}[a]	k_{bi}[b,c]	$k_{eq} x k_{bi}$	k_{uni}(I)[d]	k_{uni}(II)
553	9.50×10^{25}	3.95×10^{-10}	3.75×10^{16}	1.33×10^{15}	2.93×10^{14}
723	1.26×10^{26}	4.52×10^{-10}	5.69×10^{16}	2.84×10^{15}	5.64×10^{14}
1000	1.46×10^{26}	5.32×10^{-10}	7.77×10^{16}	6.13×10^{15}	1.10×10^{15}

a, b, and d as in Table I. c. A value of 3.2A was used for sum of radii of colliding particles. A symmetry factor of 1 was used. No steric factor has been added.

The model for the hydrazine molecule used for computing the RRKM specific rate constants is listed in Table III, from the data in Appendix II. The 18 internal degrees of freedom are divided into 15 active and 3 adiabatic overall rotational degrees of freedom. The torsional motion was treated as a vibration. The barrier to internal rotation is >2.50 kcal $mole^{-1}$, and thus a vibration is a reasonable representation. If the vibration is changed to a free rotation the density of states is reduced by a factor of 2. The true density lies between these bounds. The vibrational frequencies are grouped in the usual way. The bond dissociation energy plus 1 kcal for the energy barrier for NH_2 recombination is 56.8 kcal $mole^{-1}$ at 0°K, which is the value for ϵ_o.

TABLE III. Vibrations and moments of inertia for hydrazine.

Frequencies	(Degeneracies)	moments of Inertia (g cm^2)	(amu A^2)
3282 cm^{-1}	(4)	$6.18X10^{-40}$	3.72
1549	(2)	$35.3X10^{-40}$	21.2
1183	(2)	$37.0X10^{-40}$	22.3
860	(2)		
780	(1)		
377	(1)		

Two loose models of the activated complex were used in these computations. The complex models are simply viewed as two NH_2 groups loosely bound together. The reported vibrational frequencies of NH_2 are used along with two doubly degencrate arbitrarily-chosen low bending frequencies, which when used in the calculations reproduce k_{bi} with a steric factor of 0.1 (Model I) or 0.01 (Model II) at 300°K. An active internal rotor and the two doubly degenerate low bending frequencies are common to both models; however, the bending frequencies differ in magnitude. The models are tabulated in Table IV. The moments of inertia of the complex were obtained by extending the N-N bond distance from 1.47A to 3.0A, assuming the complex planar, with N-H = 1.04A, $\angle$NNH = 110°, and $\angle$HNH = 110° (from hydrazine[41]). The nature of the NH_2 internal rotation deserves further mention. The nitrogen atom in hydrazine is approximated by sp^3 hybridization. In the complex models used in the calculations the extended nitrogen atom in the transition complex is also assumed to be sp^3 hybridized, although one orbital will be only half filled, and the NH_2's are twisted to a planar configuration resembling ethylene. Such a model is a simplification for computations; however, other models, although more difficult to handle, would affect the overall calculations very little.

The methylamine molecule model is given in TABLE V. The bond dissociation energy plus 1 kcal activation barrier for radical recombination is 78.0 kcal $mole^{-1}$ at 0°K, which is the value for ε_o. It is interesting to note that this is about 10

kcal mole^{-1} below the dissociation energy for ethane. Details are given in Appendix II.

Table IV. $N_2H_4^+$ Complex Models.

Model I		Moments of Inert.		Model II	
Freq.	(Deg.)	(g cm^2)	(amu A^2)	Freq.	(Deg.)
3220 cm^{-1}	(2)	4.86X10^{-40}	2.93	3220 cm^{-1}	(2)
3173	(2)	138.0 X10^{-40}	83.5	3173	(2)
1499	(2)	134.0 X10^{-40}	80.8	1499	(2)
150	(2)	1.21X10^{-40}[a]	0.732[a]	275	(2)
80	(2)			200	(2)

a. Active rotor. A symmetry number of 2 was used for NH_2 internal rotation.

Table V. Vibrational frequencies and moments of inertia for methylamine.

Frequencies	(Deg.)	Moments of inertia (g cm^2)	(amu A^2)
3374 cm^{-1}	(2)	8.14X10^{-40}	4.90
2875	(3)	37.1 X10^{-40}	22.3
1662	(1)	38.7 X10^{-40}	23.3
1426	(3)		
1136	(3)		
684	(2)		
235	(1)		

The methylamine complex models were treated in a manner similar to hydrazine. The models consist of the known frequencies for free CH_3 and NH_2 groups to which four extra frequencies associated with a loosely held complex are added to fit k_{bi} with a steric factor of 0.1 (model I) and 0.01 (model II). A C-H bond distance of 1.09A and an sp^2 hybridized model for methyl in the transition state were used. The C-N bond was extended from 1.47A in the complex to 3A. The models are summarized in Table VI.

TABLE VI. Methylamine complex models.

Model I		Moments of Inertia		Model II	
Freq.	(Deg.)	($g\ cm^2$)	($amu\ A^2$)	Freq.	(Deg.)
3112 cm^{-1}	(5)	8.40×10^{-40}	5.06	3112 cm^{-1}	(5)
1432	(3)	126.0×10^{-40}	75.8	1432	(3)
730	(1)	127.0×10^{-40}	77.2	730	(1)
200	(2)	1.73×10^{-40} [a]	1.04 [a]	300	(2)
125	(2)			225	(2)

a. Active rotor. The symmetry number for internal rotation was taken as 6.

The results of the S/D calculations at the particular temperatures of this study are given in Tables VII and VIII for hydrazine and methylamine systems activated by means of the equations below.

Table VII. Calculated S/D values for hydrazine.

Temperature	Calculation[a]	Model	Pressure (cm Hg) 10^6	10^5	10^4	10^3	10^2	10	1.0	0.1
298°K[b]	S/D	I	1.89×10^{3}	193	22.2	3.48	0.737	0.164	3.15×10^{-2}	4.68×10^{-3}
		II	3.38×10^{4}	3.38×10^{3}	342	37.3	5.28	1.03	0.220	3.53×10^{-2}
	k_a^c, sec^{-1}	I	5.07×10^{10}	5.00×10^{10}	4.32×10^{10}	2.75×10^{10}	1.30×10^{10}	5.83×10^{9}	3.04×10^{9}	2.05×10^{9}
		II	2.84×10^{9}	2.83×10^{9}	2.80×10^{9}	2.57×10^{9}	1.82×10^{9}	9.27×10^{8}	4.35×10^{8}	2.72×10^{8}
	$\langle\varepsilon\rangle^{\dagger}_{vr}$,d,e (kcal mole-1)	I	5.00	4.94	4.65	4.00	3.32	2.90	2.73	2.69
		II	4.40	4.40	4.37	4.17	3.60	2.91	2.42	2.21
553°K	S/D	I	117	14.2	2.42	0.526	0.114	2.07×10^{-2}	3.06×10^{-3}	3.77×10^{-4}
		II	2.13×10^{3}	2.18×10^{2}	24.7	3.80	0.782	0.170		4.32×10^{-3}
	k_a^c, sec^{-1}	I	6.01×10^{11}	4.94×10^{11}	2.90×10^{11}	1.34×10^{11}	6.20×10^{10}	3.40×10^{10}	2.30×10^{10}	1.87×10^{10}
		II	3.30×10^{10}	3.23×10^{10}	2.84×10^{10}	1.85×10^{10}	9.00×10^{9}	4.13×10^{9}		1.63×10^{9}
	$\langle\varepsilon\rangle^{\dagger}_{vr}$, d,e ($kcal\ mole^{-1}$)	I	10.1	9.29	7.90	6.64	5.94	5.69	5.62	5.61
		II	9.61	9.51	8.95	7.67	6.31	5.47		5.04
723°K	S/D	I	34.4	5.05	1.02	0.227	4.49×10^{-2}	7.24×10^{-3}	9.72×10^{-4}	1.13×10^{-4}
		II	591	62.9	8.34	1.55	0.343	7.02×10^{-2}	1.16×10^{-2}	1.47×10^{-3}
	k_a^c, sec^{-1}	I	1.79×10^{12}	1.22×10^{12}	6.04×10^{11}	2.71×10^{11}	1.37×10^{11}	8.50×10^{10}	6.33×10^{10}	5.46×10^{10}
		II	1.04×10^{11}	9.79×10^{10}	7.38×10^{10}	3.96×10^{10}	1.79×10^{10}	8.77×10^{9}	5.29×10^{9}	4.17×10^{9}
	$\langle\varepsilon\rangle^{\dagger}_{vr}$, d,e ($kcal\ mole^{-1}$)	I	13.5	11.8	9.89	8.57	8.00	7.83	7.80	7.80
		II	13.5	13.1	11.7	9.75	8.23	7.48	7.24	7.19

a. A collision cross section of 3.5A was used, and is independent of temperature. b. The calculated results at 1200°K for 10^4 cm Hg are: S/D = 0.184, $k_a = 2.60\times10^{12}$ sec^{-1}, $\langle\varepsilon\rangle^{\dagger}_{vr} = 16.2$ kcal $mole^{-1}$ for Model (I), and S/D = 1.27, $k_a = 3.77\times10^{11}$ sec^{-1}, $\langle\varepsilon\rangle^{\dagger}_{vr} = 18.7$ kcal $mole^{-1}$ for Model (II). c. k_a is the apparent rate constant, i.e., the specific rate constant, k_ε, averaged over the distribution function for the chemically activated $N_2H_4^a$. d. $\langle\varepsilon\rangle^{\dagger}_{vr}$ is the average energy of the reacting molecules above ε_o, which is 56.7 kcal $mole^{-1}$. e. The average energy of the formed molecules for complex models (I) and (II) is 2.68 and 2.16 kcal $mole^{-1}$ at 298°K, 5.61 and 5.02 kcal $mole^{-1}$ at 553°K, 7.80 and 7.15 kcal $mole^{-1}$ at 723°K, respectively.

TABLE VIII. Calculated S/D Values for Methylamine.

Temperature	Calculation[a]	Model	Pressure (cm Hg) 10^4	10^3	10^2	10	1.0	0.1	10^{-2}	10^{-3}
298°K[b]	S/D	I	4.15×10^4	4.16×10^3	4.23×10^2	46.9	6.79	1.37	0.317	6.58×10^{-2}
		II	2.64×10^5	2.64×10^4	2.65×10^3	2.71×10^2	31.0	4.76	0.980	0.207
	k_a, sec^{-1}	I	2.32×10^7	2.31×10^7	2.28×10^7	2.05×10^7	1.42×10^7	7.04×10^6	3.04×10^6	1.46×10^6
		II	3.64×10^6	3.64×10^6	3.63×10^6	3.55×10^6	3.11×10^6	2.02×10^6	9.82×10^5	4.65×10^5
	$\langle\varepsilon\rangle^{\dagger}_{vr,}$ (kcal $mole^{-1}$)[c,d]	I	5.24	5.23	5.18	4.92	4.27	3.48	2.91	2.63
		II	4.75	4.75	4.74	4.67	4.35	3.64	2.89	2.38
553°K	S/D	I	1.38×10^3	1.45×10^2	18.5	3.33	0.777	0.186	3.81×10^{-2}	6.19×10^{-3}
		II	9.21×10^3	9.29×10^2	99.6	13.3	2.54	0.601	0.139	2.61×10^{-2}
	k_a, sec^{-1}	I	5.12×10^8	4.87×10^8	3.82×10^8	2.12×10^8	9.09×10^7	3.80×10^7	1.86×10^7	1.14×10^7
		II	7.67×10^7	7.60×10^7	7.10×10^7	5.29×10^7	2.79×10^7	1.18×10^7	5.08×10^6	2.71×10^6
	$\langle\varepsilon\rangle^{\dagger}_{vr,}$ (kcal $mole^{-1}$)	I	11.8	11.5	10.5	8.89	7.38	6.43	6.02	5.90
		II	11.3	11.3	10.9	9.75	8.09	6.67	5.83	5.50
723°K	S/D	I	2.78×10^2	32.5	5.34	1.20	0.301	6.75×10^{-2}	1.22×10^{-2}	1.77×10^{-3}
		II	1.88×10^3	1.94×10^2	23.5	4.07	0.945	0.234	5.01×10^{-2}	8.37×10^{-3}
	k_a, sec^{-1}	I	2.22×10^9	1.90×10^9	1.16×10^9	5.14×10^8	2.05×10^8	9.15×10^7	5.06×10^7	3.49×10^7
		II	3.29×10^8	3.19×10^8	2.63×10^8	1.52×10^8	6.54×10^7	2.65×10^7	1.23×10^7	7.39×10^6
	$\langle\varepsilon\rangle_{vr,}$ (kcal $mole^{-1}$)	I	16.2	15.4	13.4	11.2	9.63	8.84	8.58	8.52
		II	15.6	15.4	14.5	12.5	10.3	8.92	8.26	8.05

a. A collision cross section of 3.5A was used, and is independent of temperature. b. The calculated results at 300°K for 0.1 cm Hg are: S/D = 1.34 and 4.65, $k_a = 7.16\times10^6$ sec^{-1} and 2.06×10^6 sec^{-1}, $\langle\varepsilon\rangle^{\dagger}_{vr} = 3.50$ kcal $mole^{-1}$ and 3.67 kcal $mole^{-1}$ for models (I) and (II) respectively. c. $\langle\varepsilon\rangle^{\dagger}_{vr}$ is the average energy of the reacting above ε_o, which is 77.0 kcal $mole^{-1}$. d. The average energy of the formed molecules for models (I) and (II) is 2.52 and 2.12 kcal $mole^{-1}$ at 298°K, 5.86 and 5.40 kcal $mole^{-1}$ at 553°K, 8.48 and 8.00 kcal $mole^{-1}$ at 723°K, respectively.

$$NH_2 + NH_2 \rightarrow (N_2H_4)^* \begin{matrix} k_{\varepsilon \rightarrow NH_2} + NH_2 & (D) \\ \omega \rightarrow N_2H_4 & (S) \end{matrix} \qquad (13)$$

$$CH_3 + NH_2 \rightarrow (CH_3NH_2)^* \begin{matrix} k_{\varepsilon \rightarrow CH_3} + NH_2 & (D) \\ \omega \rightarrow CH_3NH_2 & (S) \end{matrix} \qquad (14)$$

The specific rate constants as a function of energy are given for hydrazine and methylamine in Figs. 2 and 3, respectively. These model calculations should provide rough upper and lower limits to the true rate constants for these energized molecules.

Application of the results of these calculations to the data of this thesis and the data of the literature is made in the discussion section.

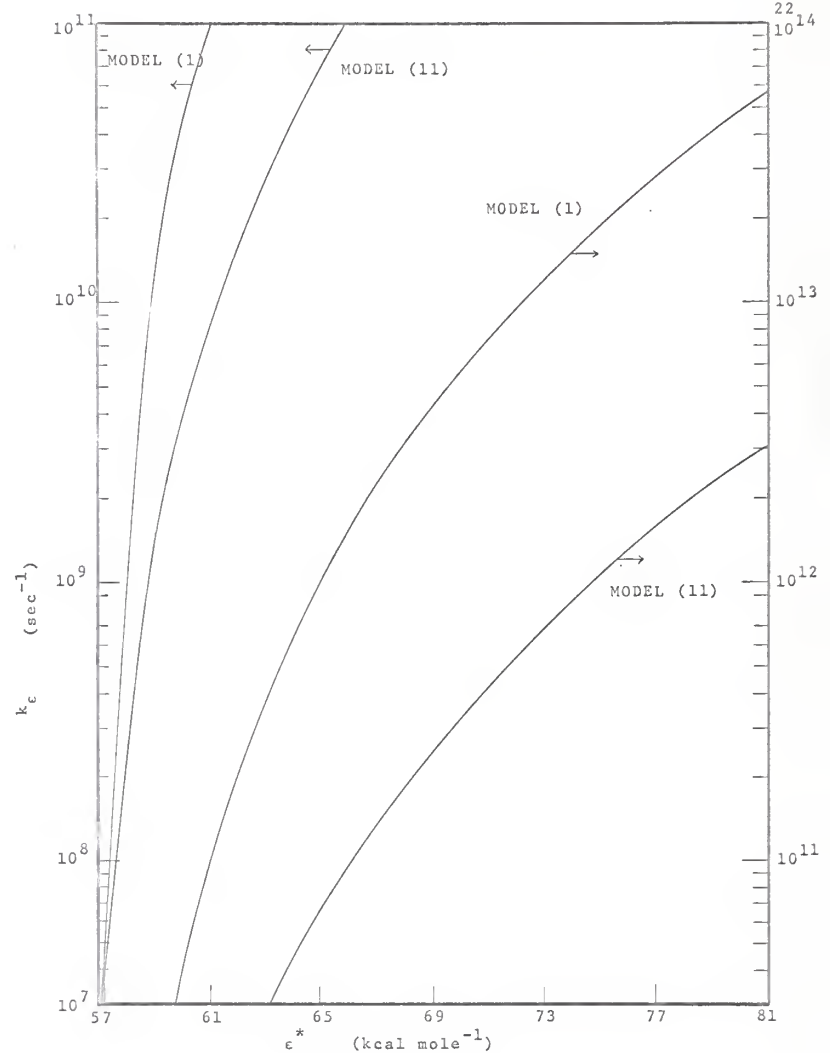

Figure 2. k_ε vs. ε^* for hydrazine models (I) and (II).

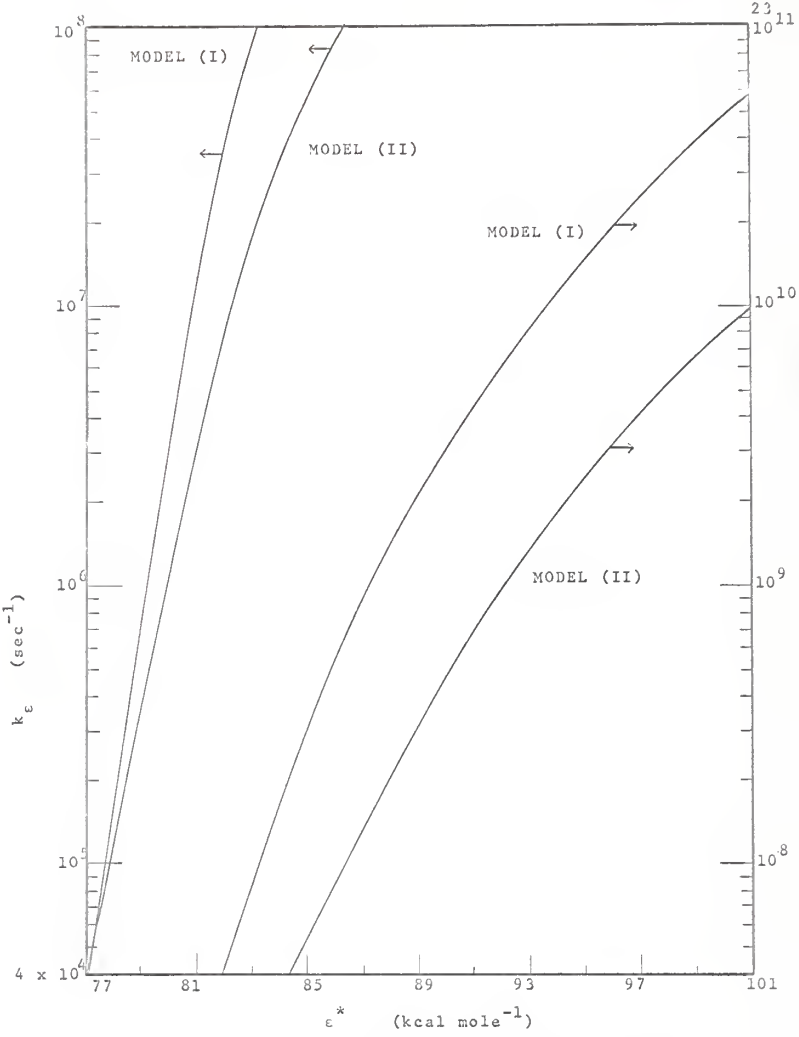

Figure 3. k_ε vs. ε^* for methylamine models (I) and (II).

EXPERIMENTAL

A. The Vacuum System. The vacuum system was made of Pyrex glass. The pumping system consisted of a Ruggles, Kurth, two stage mercury diffusion pump backed by a Welch Duo-Seal forepump. No precautions were taken to keep the system free of mercury. All stopcocks were Pyrex glass except two Springer valves, fitted with Viton A diaphragms, on the gas burette. Apiezon N grease was used on stopcocks; Apiezon M grease was used on all standard taper joints.

Gases were stored in 500 ml or one liter round bottom flasks attached to the system with stopcocks. The hydrazoic acid reservoir was enclosed in a small wire mesh cage for protection in case of an explosion.

B. Hydrazoic Acid Preparations. Hydrazoic acid is an extremely unstable compound with a positive heat of formation. The early literature is filled with reports of explosions of the liquid form and other hazards associated with its handling. After years of use, the safest manner of storage appears to be as a gas at a pressure no greater than 200 Torr.

There are a number of methods of HN_3 preparation, and in this study two were tried. The first method requires the reaction of sodium azide and sulfuric acid according to the stoichometric equation

$$2NaN_3 + H_2SO_4 \longrightarrow 2HN_3 + Na_2SO_4 \ . \qquad (15)$$

The apparatus used in this study (Fig. 4) was based on a generator designed by Miller.[9] The procedure is given below: 1 g of NaN_3 (Fisher Laboratory Chemical, purified grade) was placed in a mixing bulb and the bulb was evacuated; 2.0 ml of concentrated sulfuric acid (Baker Analyzed Reagent, 97.4%, specific gravity 1.84) was admitted through an external side arm to the NaN_3. The mixture became quite warm, and gas was evolved. The gas was passed through a drying U-tube 40 cm long and 1 cm in diameter filled with Drierite and phosphorus pentoxide, and collected in a trap at -198°C. A small amount of non-condensable gas passed through the -198°C trap and was pumped away. Upon completion of the reaction, the -198°C trap was allowed to warm, and a large middle fraction of gas was transferred to the storage resevoir. As a safety precaution, the generator was equipped with a sodium hydroxide trap as a means of disposing of excess HN_3, and as an aid to quenching a rapid HN_3 build up.

More recently Jacox and Mulligan[42] reported preparation of Ar:HN_3 mixtures by passing gaseous mixtures of Ar:HCl through a column packed with 20 cm of finely divided powdered sodium azide. Conversion was reported to be complete. An attempt was made to follow this procedure; the apparatus was essentially the same as Fig. 4, except the mixing bulb was replaced by an HCl resevoir. The drying tube was filled to give a 20 cm plug of NaN_3 previously pulverized in a mortar and pestle. The remainder of the tube was filled with phosphorous pentoxide as a precaution against possible water contamination. The generator was then evacuated,

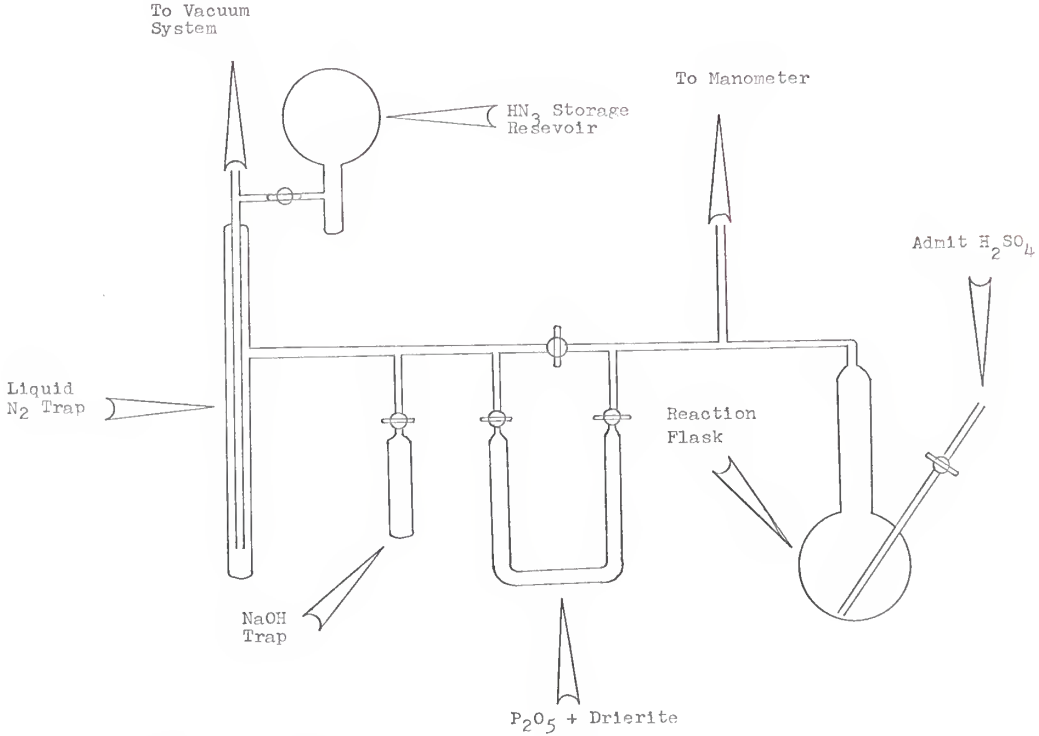

Figure IV. Hydrazoic Acid Generator.

and the HCl opened to the U-tube. Since the column was tightly packed, the flow of gas through the tube was slow. The emergent gas was condensed in a trap at -198°C. After the HCl resevoir was exhausted, a Dry-Ice Trichloroethylene bath, at -78°C, was applied to the trap while pumping on it. A gas with a high vapor pressure, probably unreacted HCl, was released. To insure purity the collected gas was passed through the U-tube twice more, and finally stored in a resevoir. It became apparent that this method of passing pure HCl through NaN_3 did not quantitatively convert HCl to HN_3. An estimate of the yield gave less than 25% conversion. Also, the slightest contamination of HCl was very crucial to product analysis in the studies of HN_3 pyrolysis. The presence of HCl in the reaction system significantly altered the distribution of basic products.

Preparations of hydrazoic acid are usually dangerous adventures; however, the latter method appears to be quite safe, and gives the experimentor more control over the reaction conditions at any time during the preparation. This must be weighed against the other problems encountered with this method. Proper clothing and head protection should be worn for protection in case of an explosion.

The infrared spectrum of HN_3 from both preparations was taken on a Perkin-Elmer model 337 spectrophotometer. A gas cell 10 cm long fitted with NaCl and KBr windows was used with a pressure of HN_3 of 180 Torr. No major impurities were indicated. The spectrum corresponded to the reported vibrational spectrum.[43]

The spectrum obtained on a Perkin-Elmer 137 is given in Fig. 5 for reference. Mass spectral analysis on a Bendix-Time-Of-Flight indicated no major impurities from either preparation. However, small H_2O impurities were noted in cracking patterns from both preparations, and HN_3 from the H_2SO_4-NaN_3 preparation contained minor impurities at m/e = 48 and m/e = 64. These impurities were not investigated.# Mass spectral data for HN_3 is given in Table IX, along with reported electron impact data.[44]

Table IX. Mass spectrum of hydrazoic acid.

m/e	Ion	Relative Abundance[a]	Literature Value[b]
43	HN_3^+	100	100
42	N_3^+	11	5.8
29	HN_2^+	16	8.3
28	N_2^+	39[c]	7.3
15	HN^+	21	16.8
14	N^+	9	4.9

a. Taken on Bendix-Time-Of-Flight, this work. b. Reported[44] intensities from an electron impact mass spectrometric study. c. Uncorrected for an air impurity.

C. Other Chemicals. Other gases used in this work included CH_4, CH_3NH_2, C_2H_6, $C_2H_5NH_2$, C_2H_4, C_3H_8, C_4H_8, C_4H_{10}, O_2, N_2, NO, C_2D_4,

#Indcpendent spectroscopic research by Dr. D. H. Stedman of these laboratories has identified S-O emission bands in a HN_3 (prepared by H_2SO_4-NaN_3)-argon metastable flow system. The source of this contaminant is thought to be SO_2. Therefore, it was concluded that the peak at m/e = 64 was due to SO_2^+ and that at m/e = 48 was due to SO^+.

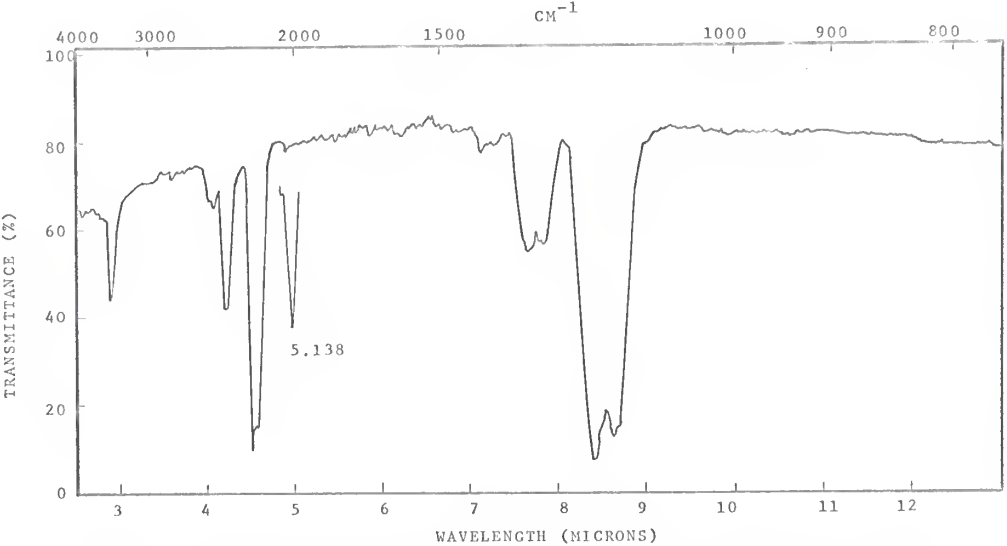

Figure 5. Gas phase infrared spectrum of HN_3 (p = 23 mm), taken on a Perkin-Elmer 137 spectrometer to include complete spectrum in one trace. Absorption of polystyrene at 5.138 microns included for reference.

and D_2. CH_4 was Matheson Ultra High Pure and showed traces (0.1%) of C_2H_4 and C_2H_6 as detected by gas chromatography. O_2 and N_2 were obtained directly from standard cylinders and not purified. All other gases were obtained from Matheson lecture bottles and not purified further except C_2H_6. This was purified by gas chromatography using a silver nitrate polyethylene glycol column, which separated C_2H_6 and C_2H_4. C_2D_4 was generously provided by Dr. H. Okabe of the National Bureau of Standards.

D. Measuring and Collecting Sections. Condensable gases were measured in a versatile gas burette provided with two Springer valves using Viton A diaphragms, and transferred by liquid N_2 cooled traps. Non-condensable gases were handled by using a U-tube packed with Linde activated molecular Sieve 5A, which absorbed non-condensable gases at liquid N_2 temperatures and quantitatively desorbed at room temperature.

E. Reaction Bulbs. Reaction vessels were made of Pyrex glass blown to about spherical shape and of a volume of about 10 cc. The vessels were fused to 15x3 mm tubing with a stopcock on the end, and could be transferred very easily from the vacuum system to the furnace. However, the stopcocks on the reaction vessel could not be heated, so there existed a portion of the vessel that was not in the furnace. The dead volume was kept to less than 10% of the total volume.

A number of experiments were performed with sealed Pyrex vessels allowing complete immersion into the furnace. These

vessels were provided with break seals and could be manipulated using standard vacuum techniques.

Since it was thought that vessel surface may have an effect on the course of the reaction, a 'seasoned' vessel was made. The term 'seasoned' is arbitrarily assigned to a vessel in which propylene was pyrolyzed for four hours at a temperature of 450°C. The vessel was left brown even after pumping down to 10^{-4} Torr. The residue was probably carbon and a C-H polymer known to form in propylene pyrolysis. To contrast with this, unseasoned, fresh vessels were also used.

To further check the effect of vessel surface, a fresh vessel was packed with glass tubing calculated to increase the vessel surface by a factor of two.

F. Furnace and Temperature Measurement. The furnace was originally constructed by J. C. Hassler and was not modified. It consisted of a cylindrical transite core wound with nichrome wire #20, and packed with glass wool inside two standard size reagent cans. Temperatures as high as 550°C could be achieved with no difficulty by fitting the top of the core with a transite plate. Because of the large size of the furnace and the uniform winding, large temperature gradients existed between the top and the bottom, but the temperature gradient over the reaction flask was less than 10°C.

The temperature was measured with a movable Chromel A - Alumel A thermocouple calibrated from the cooling curve of 99% zinc (Mallinckrodt Analytical Reagent, 20 mesh). The thermocouple

was always external to the reaction vessel and consequently represents the temperature of the furnace and not necessarily the temperature inside the vessel. However, the thermocouple was introduced to the same depth as the reaction vessel, and maintained directly next to it. Upon opening the lid for vessel introduction the temperature of the furnace naturally dropped, but it could be controlled over an hour period to within 5° of the temperature reading taken two minutes after introduction. Reactions were run at three different temperatures.

A definite possibility in all runs at higher temperatures, i.e., above 400°C where complete reaction took place in less than two minutes, is that an explosion or near explosion may have occurred possibly accompanied by adiabatic heating of the final products. In the limit of an explosion of HN_3 in the presence of substrate, simplified thermodynamic considerations give an upper limit to the temperature that may be attained. Assuming instantaneous decomposition at constant volume and 298°K of HN_3 in a 1 to 10 mixture of HN_3:CH_4 to form NH_3, N_2, and CH_4 in a 1/3:4/3: 10 ratio respectively, and adiabatic heating of the final components in the system, pertinent enthalpy (Appendix I) and heat capacity data (Table X) predict a maximum attainable temperature of 1031°C starting with reactants at 298°K. For the same calculation but starting with reactants at 700°K the maximum temperature is 1010°C. This treatment applied to a $1HN_3/10C_2H_4$ mixture exploding to give $1/3NH_3$, $4/3N_2$, and $10C_2H_4$ starting with reactants at 298°K yields a maximum temperature of 828°C.

Table X. Heat capacity data for HN_3 explosion in CH_4 and C_2H_4.

Substance	C_p, cal deg^{-1} $mole^{-1a}$	C_p, cal deg^{-1} $mole^{-1b}$	Reference
CH_4	8.518	13.813	(75)
C_2H_4	10.250	18.574	(75)
N_2	6.961	7.350	(75)
NH_3	8.38	11.538	(75)

a. At 298°K. b. At 700°K.

Starting with reactants at 700°K the maximum temperature is 852°C. Obviously this treatment is crude and simplified, however, it may indicate that the temperature in the reaction vessel is somewhat higher than the temperature of the furnace for the short reaction time runs. For anything but an explosion the temperature rise will be too small to be important. A return to this view will be made when discussing possible processes occuring in the ethylene-hydrazoic acid pyrolysis system, where its consideration may be important.

C. Analytical Methods. Non-condensable gas analysis was carried out on an Aerograph A-90P gas chromatograph using a 6 ft. activated Molecular Sieve 5A column at 25°C and a helium flow of 25 cc/min. Under such conditions separation of O_2 (Retention Time 2.5 min.), N_2 (R.T. 7.8 min.), and CH_4 (R.T. 10 min.) was possible. The column was activated in a purified helium flow

at 300°C for 6 hours. Helium was purified against possible H_2O content by passage through an activated silica gel column at -78°C. The instrument employed 4 filament thermal conductivity detectors. Sensitivities for O_2, N_2, and CH_4 were 0.0012 cc/scale division of chart paper, 0.0015 cc/div., and 0.0045 cc/div. respectively.

Condensable gas analysis was performed on a Perkin-Elmer 820 gas chromatograph equipped with a 4 wire thermal conductivity detector. Columns, their preparation and operating conditions for condensable analysis were: (1) A 10 ft. column of Porapak Q plus 20% tetraethylenepentamine: Porapak Q was coated with tetraethylenepentamine using an absolute ether solvent. At 25° and 50 cc/min. He, separation of ammonia, propylene, and small amounts of ethane and ethylene was possible. The sensitivity for ammonia was 0.00062 cc/div with a retention time of 15 min. At 64°C and a flow of 70 cc/min CH_3NH_2 (R.T. 23 min.) and $C_2H_5NH_2$ (R.T. 30 min.) could be separated. At higher temperatures column bleeding became a problem. (2) A 1 meter Porapak Q + 6% polyethyleneimine column: Porapak Q was coated with polyethyleneimine dissolved in hot methanol. At 60°C and a flow of 50 cc/min He, separation of C_4H_{10}, C_3H_6, CH_3CN, CH_3NH_2, $C_2H_5NH_2$, and CH_2CH_2NH was possible. The sensitivity for CH_3CN was 0.00045 cc/div at a retention of 29.5 min. The maximum temperature of the column is advertized to be 250°C. (3) A 2 meter column of Gas-Chrom CL (Applied Science Labs), a Celite type support, +20% Carbowax 400 + 5% NaOH: The solid support was first coated with

Carbowax 400 dissolved in chloroform. Then the material was treated with an ethanol-water solution containing NaOH. The method is after Bighi and Saglietto.[45] At 68°C and a flow of 60 cc/min He, separation of NH_3, CH_3CN, CH_3NH_2, $C_2H_5NH_2$, and CH_2CH_2NH was possible. This column was found to deteriorate after about a month as evidenced by a severe change in ammonia sensitivity. (4) Qualitative hydrocarbon analysis utilized a silver nitrate polyethylene glycol column operated at room temperature and at a He flow of 30 cc/min. Separation of C_2H_6 (R.T. 4 min.), C_2H_4 (R.T. 12 min.), and C_4H_{10} (R.T. 16 min.) was possible.

A Bendix-Time-Of-Flight mass spectometer was used to aid in identification of product species trapped from g. c. effluent.

H. Run Procedure. Condensable gases were measured out in the gas burette and cryogenically pumped into the reaction vessel. Non-condensable gases were confined to the small calibrated inlet portion of the vacuum line provided with an open-end manometer, and simultaneously accommodating the reaction vessel. In this way, non-condensable gases could be measured out, and a portion transferred by expansion into the reaction vessel with a minimum of wasted gas. For methane handling, this process was even more efficient, since the vapor pressure of methane will drop to about 9 mm at liquid nitrogen temperatures. Samples were such that the pressure in the reaction vessel at the temperatures of reaction was always in the range 2-4 atm. After warming to

room temperature and mixing, the vessel was introduced into the furnace and a temperature reading taken. The temperature was also monitored 5 minutes after introduction and before removal from the furnace. After reaction, the vessel was transferred to the vacuum line containing a glass-wool-packed trap maintained at -196°C for removal of condensable gases and a trap containing activated molecular Sieve 5A for removal of non-condensable gases. The reaction vessel was opened slowly to the traps, both maintained at -196°C. After complete trapping (pressure $\leq 4 \times 10^{-3}$ Torr), the traps were transferred to the gas chromatograph inlet lines for analysis.

RESULTS

A. General Features. A number of HN_3-substrate systems have been examined in varying degrees of completeness and with different views in mind. It seems best to divide the results according to the system, and then integrate the date into an overall interpretation in the discussion section. Some features common to all substrates are presented first.

In most runs hydrazoic acid was at partial pressures of 130 to 360 Torr and the total pressure in the reaction vessel was generally in the range 1-2.5 atm. At $p(HN_3)$ equal 300 Torr, vessels containing pure HN_3 shattered when introduced into the furnace. The explosive decomposition of HN_3 is not well understood but undoubtedly proceeds by a radical chain mechanism. However, at lower pressures and in the presence of substrates, no explosion took place even at the highest temperatures (450°-460°). This study then, is concerned with thermal decomposition of HN_3 in the presence of hydrocarbon substrates.

For the case of complete HN_3 decomposition, ammonia was one of the products; however, at less than complete HN_3 decomposition ammonia could not be found and a white solid was found in reaction vessels when cooled to room temperature. The solid exhibited a small vapor pressure and could be transferred in vacuum lines by cryogenic pumping. This solid is undoubtedly NH_4N_3. A reference sample of this white solid was formed in experiments where equal amounts of HN_3 and NH_3 were brought together. Attempts were made to analyze the NH_3 of this solid by transferring

a small sample to the g.c. inlet by heating (100°C, boiling water) the gas injector of the gas chromatograph inlet system. The disappearance of the white solid was slow, but it could be injected. The resulting peaks obtained were similar to those encountered in analysis of condensible product fractions from runs in which the HN_3 was not completely decomposed.

B. Pyrolysis of Hydrazoic Acid With Methane. The hydrazoic acid-methane system was extensively investigated because methane is the first member of the homologous series of saturated hydrocarbons, and its thermal stability extends to higher temperatures than either ethane or propane. Blank runs with no HN_3 over long periods of time (1 hr.) at 450°C showed that only a small amount (<0.1%) of ethane was formed. The quantities were sufficiently small that the thermal decomposition of methane may be ignored. Extensive analysis of condensible and non-condensible gases were made at complete HN_3 reaction, obviating the difficulty of working with ammonium azide. Nitrogen and ammonia were the only nitrogenous products identified and measured. The methane reactant was completely recovered and consequently was not a reactant, but acted only as an inert bath gas. Exhaustive searches for hydrogen, methylamine, and/or hydrazine were made with several runs made over the range of temperatures, and were always negative. Thus the hydrazoic acid-methane system represents merely the non-explosive pyrolysis of HN_3 with apparently no chemical interaction with the methane.

The nitrogen and ammonia product concentrations were investigated as a function of the parameters of temperature, reaction time, and reaction vessel surface conditions and surface area. Data from runs where only non-condensibles were analyzed are presented in Table XI. Each run represents fresh reactants, introduction to the furnace for the time specified, and withdrawal of the total contents for analysis, rather than withdrawal of an aliquot. Table X may be divided into four sections: (1) Runs 1.-10.: $p(HN_3)$ and $p(CH_4)$ were constant and reaction time at the higher temperatures used in this study was varied. (2) Runs 11.-14.: the same as (1) except $p(HN_3)$ is halved and 'seasoned' and fresh Pyrex vessels were used. (3) Runs 15.-19.: the partial pressures of reactants were varied at higher temperatures. (4) Runs 20.-31.: the temperature was gradually decreased for reactions in Pyrex and 'seasoned' vessels. No trend was noted in the $(HN_3)_i/(N_2)$ ratio for either 'seasoned' or Pyrex vessels at the higher temperatures; in fact the ratio was quite invariant to all conditions listed in Table X at temperatures above 400°C. However, the rapid falloff of nitrogen production in a Pyrex vessel at lower temperature (run 23.) relative to the 'seasoned' vessel, and the total absence of N_2 at 180°C after an hour in the furnace (run 31.) in the Pyrex vessel was indicative of a slower N_2 production rate in Pyrex vessels as compared to 'seasoned' vessels.

Runs in which both condensable and non-condensable analysis were carried out are entered in Table XII. At higher temperatures

Table XI. Hydrazoic acid-methane system.

Run #	Reactants[a]		Product Yield[a]	Product Ratio	Reaction Conditions[b]		
	$(HN_3)_i$	$(CH_4)_i$	(N_2)	$(HN_3)_i/(N_2)$	Time	Temp.	Remarks
1.	2.0	10.0	2.56	0.78	65	400	SV
2.	2.0	10.0	2.56	0.78	60	462	SV
3.	2.0	10.0	2.55	0.78	60	458	SV
4.	2.0	10.0	2.59	0.77	60	453	SV
5.	2.0	10.0	2.56	0.78	60	407	SV
6.	2.0	10.0	2.56	0.78	30	457	SV
7.	2.0	10.0	2.45	0.81	30	454	SV
8.	2.0	10.0	2.05	0.97	20	457	SV
9.	2.0	10.0	2.40	0.83	20	452	SV
10.	2.0	10.0	2.40	0.83	5	459	SV
11.	1.0	10.0	1.06	0.94	30	435	PV
12.	1.0	10.0	1.10	0.91	30	423	PV
13.	1.0	10.0	1.16	0.86	20	443	SV
14.	1.0	10.0	1.04	0.96	15	420	PV
15.	2.0	20.0	2.56	0.78	60	443	SV
16.	1.0	17.0	1.20	0.83	60	458	PB
17.	1.0	10.0	1.11	0.90	10	414	SV
18.	1.0	5.0	1.10	0.91	15	453	PV
19.	1.0	3.0	1.02	0.98	15	460	PV
20.	2.0	10.0	2.00	1.00	10	344	SV
21.	2.0	10.0	0.60	3.33	7	344	SV
22.	2.0	10.0	2.10	0.95	16	337	SV
23.	1.0	10.0	.10		30	320	PV
24.	1.0	10.0	1.06	0.94	17	310	SV
25.	1.0	10.0	0.60	1.67	15	290	SV
26.	1.0	10.0	0.40	2.50	15	280	SV
27.	1.0	10.0	0.20	5.00	15	255	SV
28.	1.0	10.0	.10		17	234	SV
29.	1.0	10.0	.05		15	180	SV
30.	1.0	10.0	.10		60	180	SV
31.	1.0	10.0	.00		60	180	PV

a. Reactants and products are tabulated as cc of gas at STP.
b. Time is in minutes, Temp. is in degrees Centigrade, SV is 'seasoned' vessel, PV is Pyrex vessel which was used in successive runs with no cleaning procedure, and PB is Pyrex break-off tube.

in both 'seasoned' and Pyrex vessels (runs 32.-41.) product ratios were independent of reaction time down to 15 minutes, and the particular vessel used. If long periods of reaction (runs 42.-45.) were used at lower temperatures the product yields were the same in 'seasoned' and Pyrex vessels. However, as shown in Table XI the rate of N_2 production was dependent upon the vessel even though the stoichiometry at complete reaction appears unchanged. Runs where the vessel surface was doubled (46.-49.) showed a trend toward diminished NH_3 yields, while (N_2) remained unchanged. After many experiments in untreated Pyrex vessels a non-volatile whitish material was noted on the walls of the vessel; similar deposits may have been in the 'seasoned' vessels too, since inspection could not be made there. The product ratios also evidenced a severe loss of equal numbers of N and H, and a complete mass balance could never be obtained under our conditions. This was presumably due to the polymerization product on the vessel walls. The product ratios from 'seasoned' and Pyrex vessels plus the 'missing' N and H lead to the overall stoichiometry

$$100\ HN_3 \rightarrow 15\ NH_3 + 115\ N_2 + 55\ (NH). \qquad (16)$$

Two series of experiments were designed to observe nitrogen production as a function of reaction time in a 'seasoned' and a Pyrex vessel, the same vessel being used throughout a series with total analysis done at each reaction time. Intermediate temperatures were chosen where the reaction was sufficiently slow

Table XII. Hydrazoic acid-methane system.

Run #	Reactants[a]		Product Yields[a]		Product Ratios		Reaction Conditions[b]		
	$(HN_3)_i$	$(CH_4)_i$	(N_2)	(NH_3)	$(HN_3)_i/(N_2)$	$(NH_3)/(N_2)$	Time	Temp.	Remarks
32.	1.0	10.0	1.20	0.18	0.83	0.15	120	448	SV
33.	2.0	10.0	2.40	0.30	0.83	0.12	19	443	SV
34.	1.0	10.0	1.09	0.15	0.92	0.14	15	465	SV
35.	1.0	10.0	1.32	0.22	0.76	0.17	15	457	SV
36.	1.0	10.0	1.24	0.18	0.81	0.14	15	443	SV
37.	1.0	10.0	1.24	0.14	0.81	0.11	15	440	SV
38.	1.0	10.0	1.11	0.14	0.90	0.13	15	432	SV
39.	1.0	10.0	1.14	0.17	0.88	0.15	60	455	PV
40.	1.0	10.0	1.16	0.17	0.86	0.15	18	459	PV
41.	1.0	10.0	1.13	0.16	0.88	0.14	15	468	PV
42.	1.0	10.0	1.17	0.16	0.86	0.14	137	355	PV
43.	1.0	10.0	1.11	0.24	0.90	0.22	137	355	SV
44.	1.0	10.0	1.12	0.17	0.89	0.15	90	360	SV
45.	1.0	10.0	1.11	0.20	0.90	0.18	90	355	SV
46.	1.0	10.0	1.16	0.11	0.86	0.09	5	460	PV with 2-fold surface
47.	1.0	10.0	1.15		0.87		5	450	PV with 2-fold surface
48.	1.0	10.0	1.16	0.10	0.86	0.08	2	461	PV with 2-fold surface
49.	1.0	10.0	1.14	0.05	0.88	0.04	2	460	PV with 2-fold surface

a. Reactants and products are tabulated as cc of gas at STP. b. Time is in minutes, Temp. is in degrees Centigrade, SV is 'seasoned' vessel, PV is Pyrex vessel.

so that the rate could be followed. The averaged data, representing 2-4 determinations, is given in Tables XIII and XIV along with reaction conditions.

Table XIII. 'Seasoned' vessel studies.

Time (Min)	15	21	30	40	45	60	130
(N_2) (cc) yield	0.27	0.40	0.65	0.61	0.66	0.83	1.10

Surface/volume = 1.9 cm^{-1}. Temperature = 285 $\pm$ 5°C.

$(HN_3)_i$ = 1.0 cc. $(CH_4)_i$ = 10.0 cc.

Table XIV. Pyrex vessel studies.

Time (Min)	15	30	45	58	75	90	120	137
(N_2) (cc) yield	0.20	0.40	0.62	0.73	0.81	0.88	1.01	1.17

Surface/volume = 1.8 cm^{-1}. Temperature = 355 $\pm$ 5°C.

$(HN_3)_i$ = 1.0 cc. $(CH_4)_i$ = 10.0 cc.

This data has been treated kinetically using Powell's method[46] of dimensionless parameters. The stoichiometry given by (16) and by that reported by other authors[104] was used to convert the rate of nitrogen formation to the rate of HN_3 decomposition. Conventional plots for 0, 1/2, 1, 3/2, and 2 order HN_3 decomposition were made using the reported stoichiometry. In no case could a reaction order be firmly elucidated, but the data appear to approach first order behavior. A typical Powell type plot for this data is given in Fig. 6.

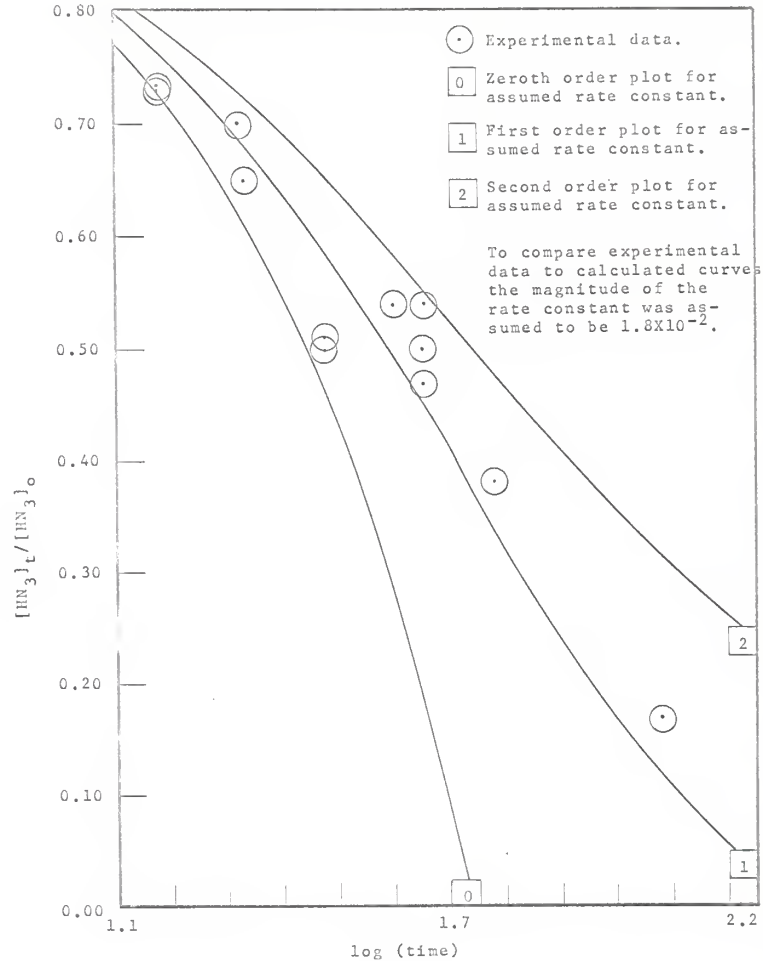

Figure 6. Powell plot $[HN_3]_t/[HN_3]_o$ vs log (time). Stoichiometry assumed: $HN_3 \rightarrow 1/3NH_3 + 4/3N_2$. Data from runs in 'seasoned' vessel at 285±5°C.

The severe loss of (NH) in the overall stoichiometry, the effect of vessel surface, and the difficulty in determining kinetic order, all point to a system in which at least part of the initiating reaction is heterogeneous.

From TABLES XI and XII a number of points may be summarized: (1) The N_2 and NH_3 product yields are, within experimental error, the same at complete reaction for either low or high temperature, and for decomposition in 'seasoned' and Pyrex vessels a fairly constant stoichiometry is obtained. (2) The decomposition rate is faster in 'seasoned' vessels than in Pyrex vessels. (3) The trend appears to be toward a reduced ammonia yield in vessels with added surface area. (4) There is no interaction between the pyrolysis products of HN_3 and methane. (5) The decomposition is somewhat heterogeneous.

C. Pyrolysis of Hydrazoic Acid with Deuterium. Hydrazoic acid at a partial pressure of 40 cm was pyrolyzed with deuterium at a total pressure of 2.5 atm and 450°C. Quantitative analysis of the ammonia product indicated no change in the yield compared with the methane system. Nitrogen analysis was prevented by the inability of Molecular Sieve to completely adsorb D_2., making quantitative transfer of the nitrogen product impossible. In one run, the condensibles were trapped, and qualitative analysis was carried out on a mass spectrometer. Analysis in the m/e range 16-20 indicated no isotopically labelled ammonia, i.e., no NH_2D, NHD_2, or ND_3 was detected.

D. Pyrolysis of Hydrazoic Acid With Ethane. HN_3-C_2H_6 and HN_3-C_2H_6-CH_4 mixtures were pyrolyzed under conditions previously described. Ammonia and nitrogen were the only nitrogenous products found; they were present in similar proportions to the HN_3-CH_4 system. The main interest in this system involved the attempted isolation of product ethylamine. None was found. Small amounts of C_2H_4 and butane were detected; these arose mainly from pure ethane pyrolysis as indicated by blank determinations. The results from this system are summarized in Table XIV.

E. Pyrolysis of Hydrazoic Acid With Propane. Propane was used as a substrate in an attempt to facilitate (lower secondary C-H bond energy) the formation of propylamine. No amine was detected in this system by analysis with the Gas Chrom CL + 20% Carbowax + 5% NaOH column. Ammonia and nitrogen were the only nitrogen containing products recovered. Further product analysis was not attempted. Results from two runs are given in Table XVI.

F. Pyrolysis of Hydrazoic Acid with Ethylene. The results with methane have shown that at least part of the reactions are heterogeneous. These may be the surface decomposition of HN_3 followed by either surface reactions or gas phase reactions of NH and other radicals. Ethylene was used as a substrate to gain positive evidence for gas phase NH. Ethylene has been used as a scavenger for NH radicals (see Appendix III and references therein). Complete description of the reactions in this system is very difficult,

Table XV. Hydrazoic acid-ethane system

$(HN_3)_i$	$(C_2H_6)_i$	$(CH_4)_i$	(N_2)	(NH_3)	(C_2H_4)	(C_4H_{10})	$(HN_3)/(N_2)$	$(NH_3)/(N_2)$	Time	Time	Remarks
									35 min.	458°C	Pyrex vessel
0.68cc	5.42cc			0.10cc					20	428	Pyrex vessel
0.61	5.70			0.09					10	455	Pyrex vessel
0.50	5.40			0.08	0.02cc				10	462	Pyrex vessel
0.50	5.50			0.11	0.03						
	0.4										
	4.80				0.01	0.01cc			10	450	Pyrex vessel
0.50	4.0				0.01	0.01			10	460	Pyrex vessel
1.05	11.0				0.01				15	367	Seasoned vessel
2.14	10.0			0.50	0.04				10	461	Seasoned vessel
2.00	10.1			0.40					10	460	Seasoned vessel
1.00	1.00	10.0cc	1.09cc	0.16			0.92	0.15	30	425	Seasoned vessel
1.00	1.00	10.0	1.08	0.16			0.93	0.15	32	440	Seasoned vessel

Table XVI. Hydrazoic acid-propane system[a]

$(HN_3)_i$	$(C_3H_8)_i$	$(CH_4)_i$	(N_2)	(NH_3)	$(HN_3)/(N_2)$	$(NH_3)/(N_2)$	Time	Temp.
1.0 cc	1.0 cc	10.1 cc	1.06 cc	0.14 cc	0.94	0.13	30 min.	426°C
1.0	1.0	10.0	1.02	0.14	0.98	0.14	30	434

a. Seasoned vessel used.

even for merely the nitrogen containing products; the reactions are not certain. With the GLPC columns used in this study quantitative analysis for most nitrogen containing products was possible.

Hydrazoic acid-C_2H_4 and NH_3-C_2H_4-CH_4 mixtures were pyrolyzed above 400°C. Under such conditions, complete decomposition took place in less than 2 minutes. Fresh vessels became coated with oils and/or polymeric materials after one reaction. This system is very complex, as evidenced by the myriad products separated by gas chromatography. Important nitrogen containing products determined using the Gas Chrom CL + 20% Carbowax 400 +5% NaOH column were CH_3CN, and NH_3, and using a molecular sieve column N_2; analysis did not include, or did not find HCN, an expected product, but HCN may have complexed with NH_3 to form NH_4CN. A tabulation of some typical data is given in Table XVII.

Table XVII. The Hydrazoic acid-ethylene system.

Reactants[a]			Products[a]			Time[b]	Temperature[c]
$(HN_3)_i$	$(C_2H_4)_i$	$(CH_4)_i$	(N_2)	(NH_3)	(CH_3CN)		
1.0	1.0	10.0	0.96			30	430
1.0	1.0	10.0	0.93			30	440
2.1	10.0		2.58	0.39		2	460
2.1	5.0		3.40		0.34	5	470
2.1	10.0		2.55		0.20	5	470
1.0[d]	10.0		1.28	0.39	0.23	4	460
2.1[d]	10.0		2.80	0.40	0.27	2	450
1.0[d]	5.0		0.86	0.31	0.10	2	460
2.0[d]	5.0		2.62	0.55	0.23	2	460

a. Concentrations are in cc of gas at STP. b. Time is in minutes. c. Temperature is in degrees Centigrade. d. These experiments were designed to reflect a competition between the $(CH_3CN)/(NH_3)$ product ratio vs. the initial $(HN_3)/(C_2H_4)$ reactant ratio. For these runs starting at the top the product ratios are 0.6, 0.7, 0.3, 0.4 respectively, and the reactant ratios are 0.1, 0.2, 0.2, 0.4 respectively.

The product of NH_3 in the C_2H_4 system was a little surprising. Some experiments, indicated by footnote 'd' in TABLE XVII, were done with a varying ratio of HN_3/C_2H_4 to test whether the ratio of the yield of NH_3/CH_3CN showed any correlation to the starting HN_3/C_2H_4 ratio. The ratio of CH_3CN/NH_3 is 0.6, 0.3, 0.7, and 0.4, respectively, for these runs, and does not constitute crucial evidence one way or the other, although a strong relationship apparently does not exist.

In order to gain a further understanding of the HN_3-C_2H_4 system a number of reactions were run with the same conditions as Table XVII 2.0 cc HN_3 - 10 cc C_2H_4 mixtures were pyrolyzed at 460°C for the objective of identifying as many products as possible. The condensible products were collected, and analyzed by gas chromatography with trapping of as many components as possible for mass spectroscopic identification. A general difficulty in this system is the proper choice of a column that will separate all the components of the product mixture; a one meter Porapak Q plus 6% polyethylene imine column was used in this analysis. This column at 80°C gives reasonable separation of high boiling polar compounds (H_2O and CH_3CN) and intermediate saturated and unsaturated hydrocarbons (C_3 and C_4). Low boiling polar compounds (NH_3) and light hydrocarbons (CH_4, C_2H_6, and C_2H_4) elute as an initial unresolved peak. Consequently products identified do not exhaust all the products that may be present in this system. A representative chromatogram of the products from this system and the operating conditions are given in Fig. 7. To trap all

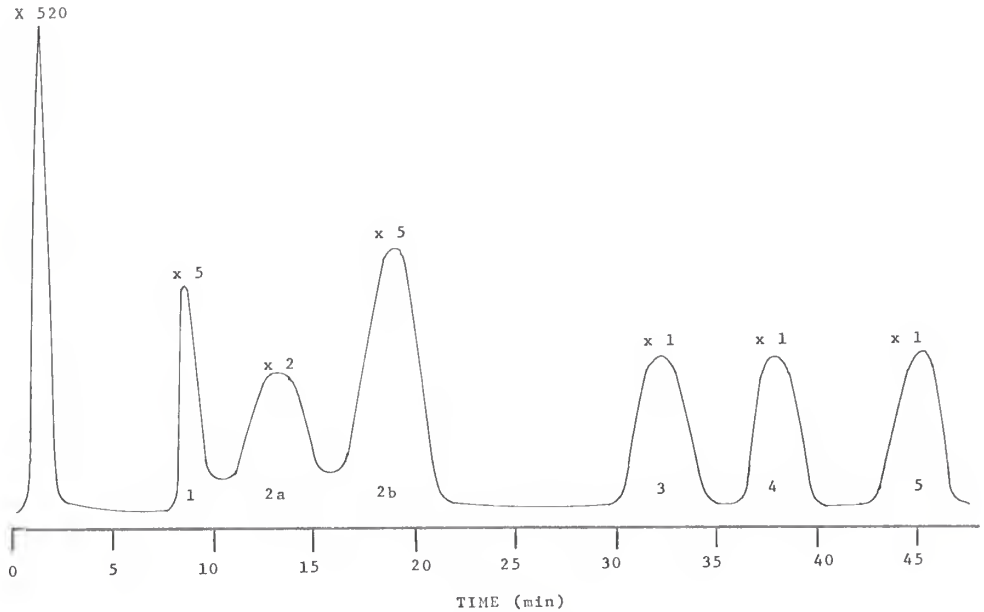

Figure 7. Chromatogram of condensable products from HN_3-C_2H_4 system. G. C. operating conditions: column, Porapak Q plus 6% polyethylene imine (1 meter, copper); filament current, 209 ma; detector temperature, 145°C; carrier gas, helium; tank pressure, 40 psi; head pressure, 8 psi; flow rate, 80 cc min^{-1}; column temperature, varied. Initial peak (x 520) is unresolved C_2H_4 and NH_3.

six peaks, multiple passes were required through the gas chromatograph. Such a tactic may introduce H_2O and CO_2 impurities from the He carrier gas.

The trapped peaks were subjected to mass spectral analysis. Relative intensity data and ASTM[46a] values for each peak of probable identity are given in Tables XVIII and XXI. A summary of the identifications is given as follows: Peak 1, propene; Peak 2a was not trapped in this series of experiments but was later identified in the HN_3-C_2D_4 system as propane; Peak 2b was identified as H_2O and CO_2 evidently present in the analysis apparatus or impurities in the reagent gases; Peak 3 was tentatively identified as n-butane; Peak 4 appears to be a butane; and Peak 5 was previously identified as acetonitrile.

Table XVIII. Mass spectrum of Peak 1.

m/e	Relative Abundance[a]	Propane[b]	Propene[b]
15	8	6	5
26	15	8	10
27	51	39	38
28	21	59	1
29	10	100	
37	18	3	13
38	30	5	19
39	79	17	71
40	30	2	29
41	100	13	100
42	72	6	68
43	10	23	2

a. At 70 eV. b. Literature values taken from ASTM[46a] tables for 70 eV mass spectrum.

Table XIX. Mass spectrum of Peak 3.

m/e	Relative Abundance	n-Butane[a]	Isobutane[a]
15	8	1	1
25	4		
26	20	3	
27	67	23	17
28	64	24	1
29	61	34	5
37	4		1
38	7	1	2
39	31	9	11
40	7	1	2
41	61	26	35
42	18	13	37
43	100	100	100
44	32	3	3
49	4		
50	6	1	
51	6	1	
52	4		
53	5	1	
54	4	1	
55	9	1	
56	15	1	
57	4	3	4
58	13	17	4

a. ASTM values

Table XX. Mass spectrum of Peak 4.

m/e	R.A.	1-Butene[a]	cis-2-Butene[a]	trans-2-Butene[a]	Isobutene[a]
26	23	6	7	7	3
27	68	18	20	21	13
28	95	22	24	24	17
29	28	11	13	17	9
37	15	2	2	2	3
38	13	3	3	3	5
39	48	28	30	30	36
40	25	6	6	5	9
41	100	100	100	100	100
42	8	3	3	3	4
43	13				
44	45				
50	15	4	6	6	5
51	13	4	5	5	4
52	10	1	2	2	1
53	15	6	8	9	5
54	13	2	4	4	2
55	25	22	27	27	20
56	48	47	57	54	52

a. Taken from ASTM tables

Table XXI. Mass spectrum of Peak 5.

m/e	Ion	Relative Abundance	Acetonitrile[a]
12	C^+	5	5
13	CH^+	4	3
14	CH_2^+, N^+	12	11
15	CH_3^+	4	2
16		2	
17		5	
18		15	
24	C_2^+	3	1
25	C_2H^+	5	3
26	$C_2H_2^+, CN^+$	7	3
27	$C_2H_3^+, CNH^+$	5	2
28	CNH_2^+	10	3
29		3	
38	C_2N^+	13	11
39	$CHCN^+$	21	19
40	CH_2CN^+	52	52
41	CH_3CN^+	100	100
42		5	
43		2	
44		6	

a. Taken from ASTM tables.

G. Pyrolysis of Hydrazoic Acid with Ethylene -d_4. Isotopic labelling often offers itself as a powerful method in determining reaction mechanisms. The HN_3-C_2D_4 system was initially thought to present this capability. Reaction, separation, and mass spectral analysis were carried out in the same manner as for C_2H_4. Cracking pattern data of the deuterated ethylene, and the product peaks are given in Tables XXII-XXIII. The C_2D_4 sample is obviously of high purity.

Table XXII. Mass spectrum of ethylene -d_4.

m/e	Ion	Relative Abundance[a]	Literature Values[b]
12	C^+	1	3.78
14	CD^+	4	6.26
16	CD_2^+	4	10.2
17	OH	2	
18	H_2O	6	
24	C_2^+	3	3.04
26	C_2D^+	8	10.4
27		3	
28	$C_2D_2^+$	53	63.7
29		4	
30	$C_2D_3^+$	48	60.8
31		6	
32	$C_2D_4^+$	100	100.0

a. At 70 eV. b. V. H. Dibeler, F. L. Mohler, M. deHemptinne, J. Research Natl. Bur. Standards, 53, 107 (1954).

Table XXIII. Mass spectra of peaks from deuterated experiments.[a]

m/e	Relative Abundance			
	Peak 1 (Propene)	Peak 2a (Propane)	Peak 3 (Butane)	Peak 5 (acetonitrile)
12	3	5	4	4
13				2
14		8	3	7
15	3	11	4	7
24				2
25				1
26	4	6	4	6
27	16	17	11	4
28	27	67	40	12
29	11	51	19	4
30	20	70	21	1
31	2	95	15	
32	5	87	19	
33		100	17	
34		32	10	
38	7	14	3	16
39	16	14	6	21
40	20	25	8	49
41	33	56	17	100
42	46	46	16	84
43	28	44	17	43
44	100	84	100	19
45	32	21	22	
46	42	16	19	
47	15	22	11	
48	21	40	14	
49	2	32	42	
50		36	23	
51		16	3	
52		3	2	
53,54			2	
55			4	
56			6	
57			5	
58			6	
59,65			4	
66			9	
67			8	
68			4	

a. Peaks 2b and 4 have not been included.

Full, detailed conclusions would be presumptuous from this limited amount of data; however, a few points may be made. Formstion of CH_3CN (Peak 5) in an HN_3-C_2D_4 system of this purity is impossible. The analysis may have succumbed to the danger of exchange involved with polar compounds. This process may have been facilitated by the basicity of the polyethylene imine substrate on the Porapak Q column used.

The unreliable intensities at m/e = 44 for peaks 1, 2a, and 3 in the face of possible CO_2 contamination is undeniable. However, other intensity data do point to a complex process. The m/e = 45 peak in component 1 points to a possible C_3HD_4 ion, and similarly m/e = 47 ($C_3HD_5^+$) points to propene containing a hydrogen. The complexity of the spectrum may indicate a mixture of labelled propenes. The data for component 2a also indicate a propane containing hydrogen (m/e = 33, C_2D_4H). The data for component 3 also indicate a butane containing H (e.g. m/e = C_3D_6H). In view of the high purity of the initial C_2D_4, these results strongly suggest the occurrence of processes involving hydrogen atoms.

H. Pyrolysis of Hydrazoic Acid with Nitric Oxide. The NH_3-NO-CH_4 pyrolysis system was briefly investigated in a qualitative manner to determine whether NH may react with NO. The following scheme may be considered (based on thermochemical data, see Appendix I):

$$NH + NO \rightarrow N_2 + OH \qquad \Delta H = -93 \text{ kcal} \qquad (16)$$

$$OH + CH_4 \rightarrow H_2O + CH_3 \qquad \Delta H = -15 \text{ kcal} \qquad (17)$$

$$OH + HN_3 \rightarrow H_2O + N_3 \qquad \Delta H = -34 \text{ kcal} \qquad (18)$$

NO was purified by distilling a sample of tank NO at liquid oxygen temperatures to a trap at liquid nitrogen temperatures. The mixtures of HN_3-NO-CH_4, 2:1:10cc and 1:2:10cc, were pyrolyzed in a 'seasoned' vessel at 450°C for two minutes. Non-condensibles were analyzed as usual. Gas chromatographically H_2O was detected among the condensibles on the Porapak Q plus polyethylene imine column operated at 80°C. Further analysis of products on a Porapak Q plus tetraethylenepentamine column operated at room temperature identified ammonia and an unknown peak noted to elute early. Mass spectrometric analysis of the unknown peak failed to establish its identification. Nitrogen analysis was determined on the two runs and were 1.3cc and 3.3cc respectively. The nitrogen yields do not differ appreciably from pure hydrazoic acid decomposition. NH_3 was not quantitatively determined in these experiments.

In view of the lack of NH_3 determination and the inconclusiveness of merely identifying H_2O (which may come from the analysis apparatus) no conclusions may be drawn.

DISCUSSION

A. Introduction. The thermal decomposition of hydrazoic acid and the subsequent reactions of the NH radical, are complex, even in the methane system. In the discussion of experimental results it will be necessary to refer to the previous literature to acquire an overall view and point out some implications. An overall qualitative view will evolve, but only after discussion of a number of details. Each section then will not necessarily come to a definite conclusion.

However, one conclusion is apparent at the onset: the pyrolysis of hydrazoic acid is not a useful source of NH radicals for kinetic studies.

B. Experimental results and the primary process in HN_3 thermal decomposition. The primary reaction in the thermal decomposition of HN_3 may possibly be (19) or (20).

$$HN_3 \rightarrow H + N_3 \qquad \Delta H = 86 \text{ kcal} \qquad (19)$$

$$HN_3 \rightarrow NH(3\Sigma) + N_2 \qquad \Delta H = 9 \text{ kcal} \qquad (20)$$

$$\rightarrow NH(^1\Delta) + N_2 \qquad \Delta H = 45 \text{ kcal} \qquad (21)$$

A review of the existing pyrolysis studies in Appendix III concludes that at least in the non-explosive region, the primary gas phase process is formation of NH and N_2. At the low temperatures of these studies, the thermochemistry certainly supports this conclusion. The CH_4-HN_3 pyrolysis studies of this thesis

showed products consistent with the data for the non-explosive decomposition of pure HN_3; N_2 and NH_3 were the only gaseous products. There was no H_2 produced under any of the experimental conditions. This itself is not a crucial test for the presence of H-atoms. However, two reasonable reactions involving H-atoms can be envisioned.

$$H + HN_3 \rightarrow NH_2 + N_2 \qquad \Delta H = -69 \text{ kcal} \qquad (21)$$

$$\rightarrow H_2 + N_3 \qquad \Delta H = -5 \text{ kcal} \qquad (22)$$

The relative rates for (21) and (22) are unknown as, in fact, are the rates of all radical reactions with HN_3. The higher temperature of our work would tend to help the abstraction reaction (22), and the exothermicity of (21) would certainly deem it reasonable. The lack of knowledge of relative abstraction versus addition rates for radicals with HN_3 poses a serious problem. In a similar system of HNCO[47] where two primary processes are operative, H_2 is always an appreciable product. It apparently does not arise by abstraction reactions, but from either H + radical reactions or from HNCO + H-atom reactions (see Appendix III for a summary). Thus, this system is not of much direct help toward an understanding of the HN_3 case, but it is hard to imagine no H_2 production if appreciable concentrations of H-atoms were present in the HN_3 system. Nevertheless, the lack of H_2 formation, the thermochemistry of the possible primary steps, and previous work in the literature favor the formation of NH and N_2 as the major primary step. The possibility of a small heterogeneous

reaction to give H-atoms, followed by fast addition to the π-bond system of HN_3, (21), cannot be entirely eliminated.

In experiments with CH_4, C_2H_6, and C_3H_8 no insertion products could be found despite a careful search. The experiments were done at pressures > 1 atm, and the RRKM calculations at 280° and 450° show that if methyl amine were formed, the stabilization to decomposition ratios would be greater than 5 and 1, respectively. The lack of insertion products and the presumable formation of NH_2 and NH_3 by H-abstraction from the weak $H-N_3$ bond strongly suggest that the reactive species in these systems in the NH radical in its triplet ground state. Formation of $NH(3\Sigma)$ from HN_3 decomposition can be explained by a nonadiabatic reaction path, similar to the well studied nitrous oxide case.[18]

Path (20a) is thermodynamically least unfavorable, but forbidden by spin-correlation rules. Path (20b) is spin allowed, but thermodynamically more unfavorable than (20a) (the thermochemistry was only published as our work was being completed), and kinetically requires a greater activation energy. This scheme is represented pictorially in Fig. 8. By analogy with N_2O thermal decomposition, where the separation between $O(^1D)$ and $O(^3P)$ is 45 kcal, and with CH_2N_2, where the separation for CH_2 $(^1\Delta)$ and $CH_2(^3\Sigma)$ is about 5 kcal, hydrazoic acid with a recently determined separation between $NH(^1\Delta)$ and $NH(^3\Sigma)$ of 37 kcal would be expected to behave like N_2O. This mode of reaction proceeds by a nonadiabatic process corresponding to a transition between

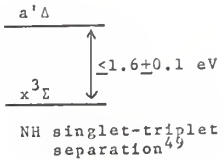

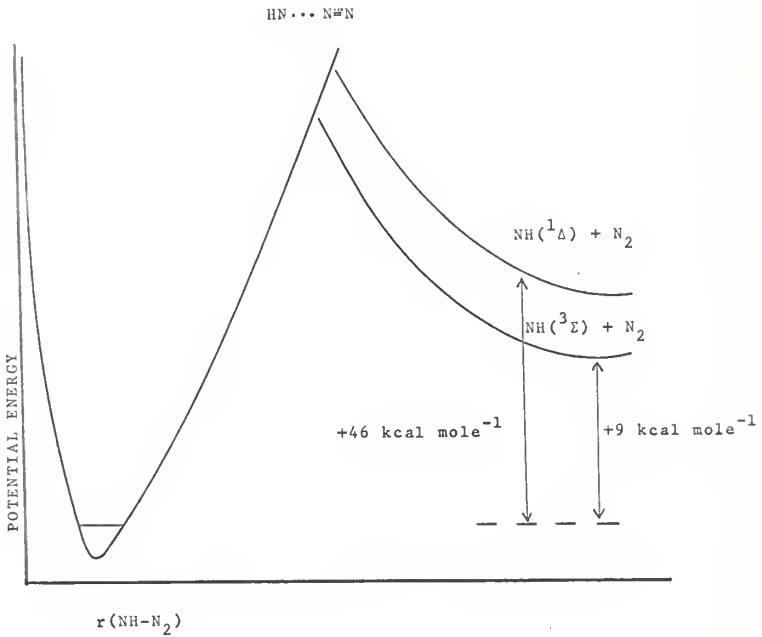

Figure 7. Two-dimensional schematic representation of potential surfaces for hydrazoic acid, singlet and triplet NH.

two potential surfaces at some point. This would be represented in Figure VIII by a transition or crossing point between the HN_3 and $NH(^3\Sigma)$ surfaces where they intersect or very nearly approach each other. Such an intercombination, i.e., singlet-triplet intersystem crossing, in accordance with the multiplicity forbiddeness selection rule, is ordinarily[48] less probable by a factor of about 10^3. This is reflected in low preexponential factors expected for nonadiabatic reactions. Hydrazoic acid decomposition with no kinetic data available has not been established as a nonadiabatic decomposition by measurement of the preexponential factor. However, the recent spectroscopic determination[49] of the large separation of the $^3\Sigma$ and $^1\Delta$ NH states, and the present interpretations of the reactiona of NH, support decomposition via the triplet surface.

C. Supporting evidence from the ethylene-hydrazoic acid system. Qualitative experiments in the presence of ethylene show no evidence for formation of the addition product, ethylenimine, expected to arise via rapid singlet NH addition to C_2H_4. In fact the contrary was found, namely, production of CH_3CN, which is associated with triplet NH radical reactions with C_2H_4.[50] The literature dealing with $NH^3\Sigma$ and C_2H_4 ia aummarized in Appendix III.

Unfortunately, the C_2H_4 system is too complicated to aid much more in understanding the primary HN_3 decomposition process. Moreover, the HN_3-C_2H_4 results suggest that H-atoms are

part of the reactive system; however, they may arise from secondary rather than primary reactions, or they may arise from heterogeneous sources.

D. Heterogeneity problems. The severe loss of (NH) in the overall stoichiometry in the CH_4-HN_3 system, and the buildup of polymer on the vessel wall, are indicative of a surface consumption of NH (23),

$$NH + Y(NH) \rightarrow (NH)_x \quad . \tag{23}$$

A simple ratio of the ammonia product to the 'missing' (NH), assuming an ideal stoichiometry, i.e., $3HN_3 \rightarrow NH_3 + 4N_2$, indicates that about 1/2 of the reaction may have taken place on the surface. Similar conclusions have been reached in pure HN_3 pyrolysis studies.[1,3]

The possibility that the decomposition of HN_3 took place completely on the surface is precluded by obtaining the same results for complete decomposition in under two minutes at 460°C. For a complete surface reaction, the controlling process would be diffusion of the reactive species to the wall. Such a process could not occur completely in under two minutes at the pressures (>2 atm) in this study. Furthermore, the formation of CH_3CN in the HN_3-C_2H_4 system also supports the presence of gaseous NH.

E. The approach to explaining product formation in the HN_3-CH_4 system. It will be assumed that the formation of NH_3 and N_2 is

mainly the result of gas phase reactions. There is no real proof of this assumption.

In the HN_3-CH_4 system, no interaction with the methane could be detected from end product analysis, and the ammonia is presumed to have arisen entirely by NH interaction with the parent HN_3 molecules. Thermochemical considerations provide a rationale, assuming an abstraction mode of reaction for NH. The bond dissociation energy of CH_4 is about 104 kcal $mole^{-1}$ (See Appendix I). The H-bond dissociation energy of hydrazoic acid, i.e., $D(H\text{-}N_3)$, is about 86 kcal $mole^{-1}$. Abstraction would consequently be more facile from the HN_3 molecule. The same arguments apply to the HN_3-D_2 system. Presumably no ND_2H or NDH_2 was observed because (24),

$$NH + D_2 \rightarrow NHD + D \qquad (24)$$

requires breaking a 106 kcal bond, and abstraction from HN_3 again is more favorable. Data for the C_2H_6-HN_3 system indicate no NH abstraction from the substrate molecule; however, the experimental analysis was at its lower limit of detection, and this result for abstraction is not as conclusive. The system is thus one of reaction of HN_3 at low temperature, and involves an understanding of NH interactions with HN_3 and secondary steps. Before proceeding to construct a mechanism for N_2 and NH_3 formation, the pertinent reactions from the literature will be presented.

F. Brief literature survey in relation to experimental results. Spectroscopic observations of intermediates in hydrazoic acid photlysis[51] and shock tube systems[52] have observed NH and NH_2 directly. The NH has usually been observed in it $^3\Sigma$ ground state. Thus the existence of the radicals is well estsblished. Also the absorption spectrum of the azide radical has been observed.[53] However, reactions of N_3 are not known. Dissociation of N_3 from its $^2\pi$ ground state to form a nitrogen atom and nitrogen molecule (25),

$$N_3\ (^2\pi) \rightarrow N(^4S) + N_2\ (^1\Sigma) \quad \Delta H = 7 \text{ kcal} \tag{25}$$

is not too endothermic (about 7 kcal) and is tempting to consider. However, such a step is spin forbidden and probably slow. Reaction in pairs, (26),

$$N_3\ (^2\pi) + N_3\ (^2\pi) \rightarrow 3N_2\ (^1\Sigma) \quad \Delta H = -210 \text{ kcal} \tag{26}$$

to form molecular nitrogen is allowed and exothermic by about 210 kcal mole^{-1}.

Diimine, N_2H_2, has been isolated in low temperature matrices and studied by a variety of methods (Appendix III). From these studies its formstion (by NH association) in sn NH system is implied,

$$NH + NH \rightarrow N_2H_2 \qquad \Delta H = -109 \pm 10 \text{ kcal} \tag{27}$$

Isolation st room temperature is highly unlikely due to its thermal instability. Decomposition of diimide is unclear. A highly

excited N_2H_2 may dissociate to $N_2H + H$, a more likely mode of N_2H_2 decomposition compared to back dissociation, since $D(N_2H\text{-}H)$ will undoubtedly be less than the energy necessary for HN - NH bond rupture. Decomposition through a four-center complex to form molecular hydrogen and nitrogen is another possibility. The reactions of the N_2H radical are virtually unknown. One possibility was given by Diesen,[54]

$$N_2H + NH_2 \rightarrow NH_3 + N_2 \quad \Delta H = -136 \text{ kcal.} \tag{28}$$

Formation of hydrazine by NH_2 association has never been established in an hydrazoic acid system, although the NH_2 combination-disproportionation ratio is between 0.18 and 0.40, and the combination rate constant has been measured[71a] as about 10^{12} cc $mole^{-1}$ sec^{-1}.

G. Unified Mechanism. In this experimental low temperature study of HN_3 pyrolysis no hydrogen was detected. This has import not only as far as the primary mechanism is concerned but it also is important when considering diimine formation. If diimine formed from $NH + HN_3 \rightarrow N_2 + N_2H_2$ or the combination of NH radicals at temperatures in the range 285° - 470°C further decomposition would have undoubtedly taken place to give possibly a polymerization product or $N_2 + H_2$. A mode of diimine decomposition to give N_2 and H_2 is ruled out, because no H_2 was ever found in the system. A mode of diimine decomposition to give N_2H and H would be ruled out, if H-atoms undergo third order recombination at these temperatures and presaures and/or abstract

H from HN_3 sufficiently fast to form hydrogen. A possible mechanism is

$$HN_3 \rightarrow NH + N_2 \qquad \Delta H = 9 \text{ kcal} \qquad (29)$$

$$NH + HN_3 \rightarrow NH_2 + N_3 \qquad \Delta H = -7 \text{ kcal} \qquad (30)$$

$$\rightarrow N_2H_2 + N_2 \qquad \Delta H = -104 \text{ kcal} \qquad (31)$$

$$NH + N_3 \rightarrow N_2 + N_2H \qquad \Delta H = -100 \text{ kcal} \qquad (32)$$

$$NH_2 + HN_3 \rightarrow NH_3 + N_3 \qquad \Delta H = -17 \text{ kcal} \qquad (33)$$

$$NH_2 + N_2H \rightarrow NH_3 + N_2 \qquad \Delta H = -136 \text{ kcal} \qquad (34)$$

$$NH_2 + NH_2 \rightarrow N_2H_4^* \qquad \Delta H = -56 \text{ kcal} \qquad (35)$$

$$NH_2 + NH_2 \rightarrow NH_3 + NH \qquad \Delta H = -10 \text{ kcal} \qquad (36)$$

$$N_2H_2 \xrightarrow{S} (NH)_x \qquad (37)$$

$$NH + NH \xrightarrow{S} (NH)_x \qquad (38)$$

$$N_3 + N_3 \rightarrow 3N_2 \qquad \Delta H = -210 \text{ kcal} . \qquad (39)$$

The reactions of H with HN_3 can be added if later information shows that they are desirable.

As an aside, it is interesting to speculate about the mechanism which may apply to the explosive decomposition of HN_3. By analogy with known explosions which are chemically sensitized

some branching chain process usually becomes important above certain limits of temperature and pressure. Such reactions, though, are difficult to envision in the HN_3 system. Steps such as (40) and (41),

$$NH + NH \rightarrow NH_2 + N \qquad \Delta H = -8 \text{ kcal} \qquad (40)$$

$$NH + NH \rightarrow N_2H + H \qquad \Delta H = -24 \text{ kcal} \qquad (41)$$

qualify as branching chains, but so little is known about how these species will react with HN_3 or each other that further comment is not useful.

The RRKM calculations for hydrazine and methylamine show that if either $N_2H_4^*$ or $CH_3NH_2^*$ were formed in the HN_3-CH_4 system, a significant fraction of the formed complexes would be stabilized at the temperatures and pressures of this study. Methylamine, as shown previously, did not form in the absence of NH singlets in the HN_3-CH_4 system. The fact that hydrazine was not detected requires more careful examination, in view of the exhaustive searches made for it and the postulated NH_2 participation in the overall mechanism. In a first glance at this mechanism, hydrazine would be expected to form.

Application of a steady state assumption to the HN_3 decomposition mechanism of necessity requires a certain reliance on data from hydrocarbon systems, because reliable kinetic data is not available for nitrogen-hydrogen radicals. Consequently one can only utilize analogous data from other systems at best.

The nature of the steady state treatment to this system at this time involves detailed assumptions, but these are based on analogy with hydrocarbon systems.

The particular objective is to determine on a rough basis the relative rates, v, of NH_2 disappearance, in the hope that one mode of NH_2 removal will be so fast that NH_2 combination is negligible. For this estimation rates 30 and 31 can be combined and will simply be designated as k_{30}. The mechanistic steps to consider are (29), (30), (33), and (35). Other radical NH_2 removal reactions will reduce the $[NH_2]$ and diminish the importance of (35). Since interest is on an upper limit to $[NH_2]$, those processes will be ignored. The two paths of NH_2 removal to compare first are the abstraction-combination ratio, i.e., H-abstraction by NH_2 from HN_3 (33), versus NH_2 combination to form hydrazine (35), or mathematically

$$\frac{v_{33}}{v_{35}} = \frac{k_{33}[HN_3]}{k_{35}[NH_2]} \quad . \tag{XIII}$$

The important unknown in (XIII) is the $[NH_2]$ steady state. This may be obtained from (29), (30), (33), and (35), and is

$$[NH_2] = \frac{-k_{33}[HN_3] \pm \sqrt{k_{33}[HN_3]^2 + 4k_{35}k_{30}[HN_3]\,[NH]}}{2k_{35}} \quad . \tag{XIV}$$

The procedure is to obtain a value for the $[NH_2]$ steady state from (XIV), and use this value in (XIII) to obtain the relative rates of abstraction to combination.

In order to solve (XIV) each term must be reasonably accounted for. The steady state for NH from (29) and (30) is

$$[NH] = k_{29}/k_{30} \cdot \qquad (XV)$$

The HN_3 unimolecular rate constant, k_{29}, is computed at half HN_3 decomposition (at 723°K) as if the decomposition wss 1st order. The NH abstraction rate constant, k_{30}, can be estimated using Semenov's method to estimate the activation energy, and using a near normal preexponential factor modified[56] by a 0.1 steric factor. The value obtained is $k_{30} = 10^{12} \exp(-11 \text{ kcal/RT})$. There are some literature data which can be related to k_{33}. Michel[57] has obtained a rate constant for NH_2 abstraction from hydrazine, and this should be similar to NH_2 abstraction from hydrazoic acid, since the bond energies are similar. However, the value $10^{13.5} \exp(-17 \text{ kcal/RT})$ cc mole^{-1} sec^{-1}, appears to have too high a preexponential factor and too high an activation energy. Gray and Thynne[58] report $10^{11} \exp(-5 \text{ kcal/RT})$ cc mole^{-1} sec^{-1} for CH_3 abstraction from hydrazine. This latter value seems more reasonable, and will be used for k_{33}. The NH_2 combination rate constant, k_{35}, comes reasonably (cf. calculation section) from simple collision theory assuming a steric factor of 0.01 and a small activation energy (1 kcal). These numbers are computed at 723° and compiled in Table XXIV.

Table XXIV. Data summary for $[NH_2]$ steady state approximation.

$k_{29} = 1.73 \times 10^{-2}$ sec^{-1}	$k_{35} = 4.6 \times 10^{11}$ cc mole^{-1} sec^{-1}
$k_{30} = 4.7 \times 10^{8}$ cc mole^{-1} sec^{-1}	$[NH] = 3.68 \times 10^{-11}$ mole cc^{-1}
$k_{33} = 3.08 \times 10^{9}$ cc mole^{-1} sec^{-1}	$[HN_3]^a = 2.09 \times 10^{-6}$ mole cc^{-1}

a. $[HN_3]$ at half decomposition.

Using these numbers in equation (XIV), the NH_2 steady state concentration is computed to be 5.6×10^{-12} mole cc^{-1}. Using this value, and appropriate numbers from Table XXIV, the V_{33}/V_{35} ratio from equation (XIII) is found to be 2.5×10^{3}. In other words, the abstraction rate, V_{33}, may be 10^3 times faster than the combination rate, V_{35}. Such a feature may account for the lack of hydrazine formation. In addition, this simplified treatment has neglected reactions (34) and (36), whose inclusion may decrease the NH_2 steady state even more and increase the V_{34}/V_{36} ratio.

H. Interpretation of the results from the hydrazoic acid-ethylene system. The following products have been identified in this system: nitrogen, methane, propane, propene, butane, a butene, acetonitrile, and ammonia. It is not feasible to develop a unique mechanism at the present time; the total products present may not have been completely identified, and there are too many possible intermediates to reach a unique solution

from simple end product analysis. However, one conclusion is evident. Hydrogen atoms are involved in this system, and the question as to how they may be generated is important. From the data in the HN_3-CH_4 pyrolysis system it is not apparent that H-atoms are generated in the primary or secondary processes occuring in HN_3 decomposition. The formation of H-atoms, consequently, may arise from interaction with ethylene. Admittedly, the complexity of this system outweighs the study given it, however, hints of the overall mechanistic route can be obtained.

The reaction of NH with ethylene has been studied and interpreted by Cornell et al.[50] in a photolysis system. To explain the spectroscopic observation of NH and CN in flash experiments, and the chromatographic separation of HCN and CH_3CN among the end products in steady photolysis experiments, the following interaction was suggested.

$$NH + CH_2 = CH_2 \rightarrow \underset{\underset{NH}{|}}{CH_2} - CH_2 \rightarrow \begin{array}{c} H\ H \\ | \quad | \\ H-C-C-H \\ | \quad | \\ N\ H \end{array} \qquad (42)$$

Their experimental observations were explained when three bonds to the α-carbon break in the flash experiments, and two bonds to α-carbon break in the isothermal experiments.

$$\begin{array}{c} H\ H \\ | \quad | \\ H-C-C-H \\ | \quad | \\ N\ H \end{array} \begin{array}{l} \nearrow\ HCN + CH_4\ (CH_3 + H) \\ \searrow\ CH_3CN + H_2\ (2H) \end{array} \qquad (43)$$

However, this scheme has not been verified. In fact, in parallel systems some researchers have reported only acetronitrile formation, and others only HCN formation (Appendix III).

In the HN_3-C_2H_4 pyrolysis system of this study CH_3CN was identified, but HCN analysis was not possible, and consequently this work cannot bear further on Lwowski's mechanism.

Since the HN_3-C_2H_4 pyrolysis system displayed such a complexity, comparison of the products and/or product distributions to known systems may be worthwhile. The distribution of C_3 and C_4 products in the pyrolysis system bear a resemblance to H + C_2H_4 systems.

The product distribution and labelling experiments indicate the presence of H-atoms. It becomes important to suggest a possible source of H-atoms in this system. Assuming thermalized NH radicals, reactions (44) and (45),

$$NH + C_2H_4 \rightarrow CH_3CN + H_2 \qquad \Delta H = -53 \text{ kcal} \tag{44}$$

$$NH + C_2H_4 \rightarrow HCN + CH_4 \qquad \Delta H = -76 \text{ kcal} \tag{45}$$

are not exothermic enough to provide the necessary energy for H-H or C-H bond rupture. In fact, a reasonable source of H-atoms is difficult to envision in this system with the present data. The mechanism given by Cvetanovic[59] for H + C_2H_4 in an Hg-photosensitized system is

$$H + C_2H_4 \rightarrow C_2H_5^* \tag{46}$$

$$C_2H_5^* \rightarrow C_2H_4 + H \quad (47)$$

$$C_2H_5^* \xrightarrow{M} C_2H_5 \quad (48)$$

$$C_2H_5 + C_2H_5 \rightarrow C_2H_6 + C_2H_4 \quad (49)$$

$$\rightarrow C_4H_{10} \quad (50)$$

$$C_2H_5 + H \rightarrow C_2H_6^* \rightarrow CH_3 + CH_3 \quad (51)$$

$$\rightarrow C_2H_6 \quad (52)$$

$$C_2H_5 + CH_3 \rightarrow C_3H_8^* \xrightarrow{M} C_3H_8 \quad (53)$$

Above 10 cm Hg pressure the excited species would certainly be stabilized.[33,60] For example, at 10 cm and 300°C, ethane S/D[60] is 4.7 for CH_3 combination and 0.19 for H + C_2H_5. Excited ethyl radical formed from H + C_2H_4 at 300°C and 10 cm has an S/D of 3.5. Carrying the mechanism through for H + C_2D_4 would yield products with a complicated deuterium substitution. A similarity does exist between the products so far identified and the products identified by Halstead and Quinn[61] in the shock tube pyrolysis of ethylene at 798° - 924°K (525° - 651°C). The following products were reported: hydrogen, methane, propane, propene, n-butane, 1-butene, cis-2-butene, trans-2-butene, butadiene, 1-pentene, cyclopentane, cyclopentadiene, 1-hexene, cyclohexene, 1,3-cyclohexadiene, benzene, and toluene. Now it is important to note the possible close similarity between the pyrolysis system in this present study and the shock tube conditions. As

stated previously, complete reaction occurred in less than two minutes, and at the temperatures of this study (450°C) and the partial pressure of HN_3(=20cm), the system was close to the explosion limit. Under such conditions, rapid decomposition may have occurred, accompanied by adiabatic heating. The measured temperature merely represents the temperature of the furnace in the region of the reaction vessel and not the reaction temperature. In blank experiments, some decomposition of ethylene was noted over 15 minutes at 450°C. However, blank experiments under two minutes showed no detectable products. Assuming the temperatures attainable in the limit of an explosion the possibility exists of a simultaneous decomposition of ethylene. Products in ethylene shock tube studies are usually explained by the following incomplete mechanism, which involves H-atom production in several steps.[62]

$$C_2H_4 + C_2H_4 \rightarrow C_2H_3 + C_2H_5 \quad (54)$$

$$C_2H_5 + C_2H_4 \rightarrow C_4H_9 \quad (55)$$

$$C_4H_9 \rightarrow C_4H_8 + H \quad (56)$$

$$C_2H_3 + C_2H_4 \rightarrow C_4H_7 \quad (57)$$

$$C_4H_7 \rightarrow C_4H_6 + H \quad (58)$$

$$H + C_2H_4 \rightarrow C_2H_5 \quad (59)$$

Thus the HN_3-C_2H_4 pyrolysis system in this study may be complicated by two simultaneous primary decompositions, viz., HN_3 and

C_2H_4. However, the mechanism of ethylene pyrolysis does not involve the H from HN_3 and hydrogen-deuterium substituted products would not be found. The possibility of ethylene pyrolysis would have to be investigated further before a more complete evaluation could be made. Another objection to all mechanisms written here is lack of a path for propene formation.

Another interesting observation of NH_3 as a product raises the question as to how it was formed. A number of possibilities can be put forth, but more data is desirable. The previous NH abstraction mechanism in the CH_4-HN_3 reaction is possible, but one would think that NH addition to ethylene would be competitive if not faster than H abstraction from HN_3. H-atoms could arise from

$$NH + NH \rightarrow N_2H_2^* \rightarrow N_2H + H \qquad (59a)$$

followed by H-atom addition to ethylene. H-atom-substrate reactions were not observed in the methane system because the reaction,

$$H + HN_3 \rightarrow NH_2 + N_2 \qquad (59b)$$

is faster than H-abstraction from CH_4. Other possibilities for H-atom formation include the following

$$NH + HN_3 \rightarrow H\text{-}N{=}N\text{-}N{=}N\text{-}H \qquad (59c)$$

$$\rightarrow N_2H + N_2H \rightarrow 2N_2 + 2H$$

I. Relation of the RRKM calculations to previous work on unimolecular reactions of N_2H_4 including chemical and thermal activation systems. The RRKM calculations for hydrazine are of further interest in so far as they relate to the literature. In this section the existing literature is reviewed in depth and analyzed in relation to the present calculations. This discussion is really in two parts: one concerns attempts to measure the thermal unimolecular rate constant for hydrazine decomposition and the second deals with NH_2 recombination-dissociation reactions.

The low temperature (350 - 780°C) decomposition of hydrazine is heterogeneous in part.[63] Ammonia, nitrogen, and a trace of hydrogen were the products formed. The stoichiometry was closely approximated by (60).

$$3N_2H_4 \rightarrow 4NH_3 + N_2 \qquad \Delta H = -64 \text{ kcal} \tag{60}$$

The decomposition kinetics were first order in hydrazine, and the unimolecular rate constant determined in Szwarc's[63a] N_2H_4 decomposition in a toluene flow reactor was given as $4X10^{12}$ exp (-60 kcal/RT) sec^{-1}. The mechanism for decomposition in this system was formulated by Szwarc[63a] and has not changed with more recent study.

$$N_2H_4 \rightarrow NH_2 + NH_2 \qquad \Delta H = 56 \text{ kcal} \tag{61}$$

$$N_2H_4 + NH_2 \rightarrow NH_3 + N_2H_3 \qquad \Delta H = -30 \text{ kcal} \tag{62}$$

$$N_2H_3 + N_2H_3 \rightarrow N_2 + 2NH_3 \qquad \Delta H = -113 \text{ kcal} \tag{63}$$

Hydrazine enriched with ^{15}N showed[63b] no randomization in the product nitrogen. The nitrogen yield depended critically on surface conditions.

The failure of low temperature thermal systems to provide suitable conditions for hydrazine decomposition, i.e., heterogeneity problems, has led to shock tube investigations. The decomposition of pure hydrazine under shock tube conditions proceeded with a low activation energy. A typical reported[64] first order rate constant in this type system has been given as $10^{10.33}$ exp(-36.2 kcal/RT) sec^{-1}. The low activation energy has been interpreted in terms of a steady state chain mechanism by Adams and Stock[65], and is consequently not of much interest.

There have been several alleged homogeneous, non-chain induced decomposition sutdies[66-68]. For the present purposes the interesting studies seem to be those by Michel and Wagner[67] and McHale, Palmer, and Knox[68]. Both studies were done at pressures of 2.3-8.6 atm., and combining both studies the temperature range covered was 970-1500°K. The data were analyzed according to the mechanism below.

$$N_2H_4 + M \rightarrow 2NH_2 + M \tag{64}$$

$$NH_2 + N_2H_4 \rightarrow NH_3 + N_2H_3 \qquad \Delta H = 30 \text{ kcal} \tag{65}$$

$$N_2H_3 + M \rightarrow N_2 + H_2 + H + M \tag{66}$$

$$H + N_2H_4 \rightarrow NH_3 + NH_2 \qquad \Delta H = -46 \text{ kcal} \tag{67}$$

McHale, et al., followed the N_2H_4 rate of loss by end product analysis in a mass spectrometer, and found a N_2H_4 first order rate constant of $10^{13.0}$ exp (-54 kcal/RT) sec^{-1}. Michel and Wagner reported an upper limit for the preexponential factor for N_2H_4 decomposition, and using Szwarc's activation energy estimated the first order rate constant as $10^{14.0}$ exp(-60 kcal/RT) sec^{-1}.

In another study by Michel and Wagner[69] the relative ammonia product concentration was followed by absorption spectroscopy. The first order rate constant for hydrazine was found to have a slight dependence on the total gas density. Rate constants reported were: $10^{12.8}$ exp(-52 kcal/RT) sec^{-1} at a pressure of 7.4 atm (1200°K) and $10^{12.0}$ exp (-48 kcal/RT) sec^{-1} at 2.5 atm (1200°K).

Using time-of-flight mass spectral analysis techniques, Diesen[54] studied the shock tube decomposition of hydrazine. Argon was used as a diluent in the temperature region 1400-2400°K. Species identified in the mass spectrometer were hydrazine, ammonia, nitrogen, hydrogen, and the NH_2 radical. A non-chain mechanism was proposed.

$$N_2H_4 + M \underset{}{\overset{}{\rightleftharpoons}} N_2H_4^* + M \tag{68}$$

$$N_2H_4^* \overset{c}{\rightarrow} NH_2 + NH_2 \qquad \Delta H = 56 \text{ kcal} \tag{69}$$

$$N_2H_4^* \rightarrow NH_3 + NH \qquad \Delta H = 45 \text{ kcal} \tag{70}$$

$$NH_2 + NH_2 \overset{d}{\rightarrow} NH_3 + NH \qquad \Delta H = -10 \text{ kcal} \tag{71}$$

$$NH + NH \rightarrow N_2H_2^* \rightarrow N_2 + H_2 \quad (72)$$

$$N_2H_2^* \rightarrow N_2H + H \quad (73)$$

$$N_2H_2^* \rightarrow N_2 + 2H \quad (74)$$

$$H + NH_2 \rightarrow NH + H_2 \qquad \Delta H = -12 \text{ kcal} \quad (75)$$

$$N_2H + NH_2 \rightarrow NH_3 + N_2 \qquad \Delta H = -136 \text{ kcal} \quad (76)$$

$$NH_2 + H_2 \rightarrow H + NH_3 \qquad \Delta H = 1 \text{ kcal} \quad (77)$$

The concentration of the intermediate NH_2 was found to increase with an increase in temperature and with a decrease in the partial pressure of hydrazine. From the kinetic data reaction (68)was found to be in the second order falloff region. The rate constant at 1400°K was 2.99×10^3 sec^{-1}.

A summary of the reported rate constants for N_2H_4 decomposition and experimental conditions is given in Table XXV.

Table XXV. Reported rate constants for N_2H_4 decomposition.

Reference	Rate Constant (sec^{-1})	Conditions
Szwarc	4×10^{12} exp (-60 kcal/RT)	630-780°C, 0.013 atm.
Eberstein	$10^{10.33}$ exp (-36.2 kcal/RT)	800-1000°K
Michel & Wagner	$10^{14.0}$ exp (-60 kcal/RT)	1100°-1550°K, 2.6-8 atm
McHale et al	$10^{13.0}$ exp (-54 kcal/RT)	970°-1100°K, 2.6-8 atm
Michel & Wagner	$10^{12.8}$ exp (-51 kcal/RT)	1100°-1600°K, 6.8-9.8 atm
	$10^{12.0}$ exp (-48 kcal/RT)	1100°-1600°K,2.3-3.3 atm
Diesen	2.99×10^3	1400°K

The models for the RRKM calculations in this thesis were chosen to represent upper and lower bounds within which the true unimoleculsr rste constant msy be found. The limiting values in Arrhenius form st 1000°K are $k = 3.08 \times 10^{16} \exp(-60.4 \text{ kcal/RT}) \text{ sec}^{-1}$, and $k = 6.04 \times 10^{17} \exp(-61.0 \text{ kcal/RT}) \text{ sec}^{-1}$, based on determining K_{eq} and k_{bi} for a steric factor of 0.01 and 0.1 respectively. The value for the critical energy ϵ° was chosen as the bond energy plus one kcal[56.8]. The experiments of Palmer and Knox and Michel and Wagner are at relatively high pressures and purported to be in the first order region; Diesen's work is admittedly in the second order region. However, the pre-exponential factors in the higher pressure studies seem too low for this kind of reaction, which usually shows a positive entropy of activation. In fact the entropy of activation for the rate constant reported by McHale et al. is negative, a rate constant property unreasonable for a dissociative type reaction. The component entropies of activation for the two model rate constants cited above are 13.91 and 18.43 eu. respectively. In addition RRKM thermal falloff curves from k/k_{∞} [equivalent to $S/(S + D)$] plots indicate that according to the models used in this thesis the first order region is not reached even at 8 atm. The discrepancy between the limiting values, and the literature values may be due to the possibility that previous work was not done at high enough pressures, and the rate constants previously determined may be in the falloff region. The activation energies are near the expected high pressure values, but small errors

in the activation energies of the 6-8 atm. experiments would increase the preexponential factors so that the absolute values of the rate constants are not in large disagreement with our models.

Approaching this problem in the opposite sense, a number of investigators have concerned themselves with the NH_2 combination problem. This approach, however, is somewhat more complex. Hanes and Bair[70] used a pulsed radio frequency discharge in ammonia, and followed the NH_2 concentration by U. V. absorption spectroscopy. The data were originally discussed in terms of a simple bimolecular sssociation process. The error in this simplified treatment was pointed out by Diesen, who seems to be the first to recognize the importance of NH_2 radical disproportionation reactions. In his shock tube study at 1900-2400°K the rate constant for disproportionation was given as 2.5×10^{13} cc $mole^{-1}$ sec^{-1}, and k^d/k^c was estimated as 0.4. A recent room temperature flash photolysis study of NH_3 by Bair and Salzman[71] has also been interpreted in terms of combination-disproportion reactions. This study revealed that the rate of NH_2 disappearsnce from absorption measurements was dependent on total NH_2 concentration and that their previous study was in error. The disproportionation rate constant was given as 0.46×10^{12} cc $mole^{-1}$ sec^{-1}. An uncorrected value for combination was 2.5×10^{12} cc $mole^{-1}$ sec^{-1}. These data would give an NH_2 disproportionation combination ratio of 0.18, a reasonable value by comparison with alkyl radical d/c kinetics.

Recently Carbaugh, Munno, and Marchello[72] have examined the NH_2 d/c kinetic in an ammonia glow discharge flow system. The reaction products were observed using both optical spectroscopy and gas chromatography. The combination rate constant was found to be 6.33×10^5 cc mole^{-1} sec^{-1}; the disproportionation rate constant was 6.92×10^5 cc mole^{-1} sec^{-1}. These rate constants appear frightfully low, and lead to a d/c of 1.0, which is slightly high.

The results, however, from all these experiments neglected the back dissociation of chemically activated N_2H_4 formed in these systems. The results from the RRKM calculations (compiled in Table XII) show that there would be significant decomposition of N_2H_4 formed at the temperatures and pressures of these studies. The neglect of N_2H_4 back dissociation would cause the measured k_d/k_c ratio to be higher than the true value. To obtain the true k_d/k_c ratio experiments should be done at pressures above one atm pressure at room temperature. One further consideration may be given to hydrazine systems where the following process is considered.

$$H + N_2H_3 \rightarrow N_2H_4^* \qquad \Delta H = -93 \text{ kcal} \qquad (78)$$

Such a process is highly energetic, imparting about 93 kcal to the chemically activated hydrazine. Based on the RRKM calculations, hydrazine from this process would never be stabilized under ordinary conditions. At room temperature and 10^6 cm Hg the S/D ratio is only 3.96 and 7.25 for models (I) and (II)

respectively. These values decrease a factor of 10 for every factor of 10 decrease in the pressure. The instability of $N_2H_4^*$ under such conditions is in agreement with Ghosh and Bair[71b] who consider the process,

$$H + N_2H_3 \rightarrow NH_2 + NH_2 \qquad \Delta H = -36 \text{ kcal} \quad . \qquad (79)$$

important in the reaction system of hydrazine with atomic hydrogen.

J. The RRKM Calculations for Methylamine and the literature. The methylamine calculations are less applicable to published data because of a lack of information for such a chemically activated system. However, it should be noted that the CH_3NH_2 results are comparable to CH_3CHO and C_2H_6 calculations[29,60]. For radical combination at 300°K the calculated half stabilization pressure of these similar models are all about 0.1 cm. This is expected since for CH_3NH_2 and CH_3CHO the number of degrees of freedom are the same, the E_o are similar, and both are assumed to dissociate via loose complexes. In contrast, ethane has an additional degree of freedom and a higher minimum energy. The CH_3NH_2 calculations may be extrapolated to propylamine results in a photolysis study[73] of HNCO in the presence of propane. Formation of methylamine by singlet NH insertion in methane is exothermic by about 102 kcal of energy. The S/D ratio at this energy would be 1.27×10^{-2} at 10 cm and ambient temperatures. However, propylamine with two more methyl groups would be expected[74] to lower the specific rate constant, k_e, by about 10^2, and give an S/D ratio of about 1.30. Under such conditions

propylamine should have been observed; that it was not may indicate the absence of singlet NH in the reaction system.

APPENDIX I

THERMOCHEMISTRY

A. Enthalpies of formation and bond dissociation values. A summary of the thermochemistry pertinent to NH systems is given in TABLES I-I and II-I. The enthalpies of formation were taken from the JANAF Thermochemical Tables[75] and the National Bureau of Standards Technical Note 270-1.[76] ΔH_f° is the standard enthalpy at 0°K, and ΔH_f° is the standard enthalpy at 298.15°K. The bond dissociation data is primarily from Benson.[77] Tentative values for certain radicals have been added to the tables from other sources, and a note of caution is introduced in fully accepting certain values.

The ΔH_f° (N_3) is presently in dispute, and has not been definitely determined. Gray[79] summarized work on the azide radical to 1963. The heat of formation of N_3 may be computed from the enthalpy of formation of the azide anion, N_3^-, and the electron affinity of gaseous N_3. ΔH_f° (N_3^-) has been given as 38.8 $\pm$ 0.1 kcal[80] and 45 kcal[76]. Values for $E(N_3)$ have been taken from three independent sources by Gray and averaged to 69 $\pm$ 7 kcal. Obtaining ΔH_f° (N_3) = ΔH_f° (N_3^-) $\pm$ $E(N_3)$, ΔH_f° (N_3) may be taken in the range 104 $\pm$ 7 to 114 $\pm$ 7 kcal. An early semi-empirical calculation by Singh[82] set the value at 113 kcal. Gray's best value was given as 105 kcal and will be used in this thesis. Based on the bond dissociation energy of N_2-N one could in principle calculate the heat of formation of the N_3

radical in reaction (1)-I from the

$$N_3 \rightarrow N_2 + N \qquad (1)\text{-I}$$

known thermochemistry of N and N_2 and the equation

$$D(N_2\text{-}N) = \Delta H_f^\circ(N_2) + \Delta H_f^\circ(N) - \Delta H_f^\circ(N_3) \quad . \qquad (I)\text{-I}$$

A recent value for $D(N_2\text{-}N)$ has been given[86] in the range 131-161 kcal, which not only indicates a tightly bound N_3 radical, but would give $\Delta H_f^\circ(N_3) = -38$ kcal. This recent value appears to be spurious, and has been questioned.[87] A value of 105 kcal $mole^{-1}$ leads to $D(H\text{-}N_3)$ of 87 kcal $mole^{-1}$ which is certainly reasonable.

Currently published values for $D(N_2H_3\text{-}H)$ run the gamut from 76[88] - 93[85] kcal. The 76 kcal value is based on mass spectrometric data,[84] and the 93 kcal value appears to arise out of an intuition that 76 is too low,[89] and that the bond dissociation energy should be nearer to ammonia ($D(NH_2\text{-}H) = 103$ kcal). By comparison with the bond energy change in going from CH_4 to C_2H_6, the 93 kcal value for hydrazine appears more reasonable than 76 kcal.

A current discussion is centered indirectly on the D(H-CN) value. By determining the $\Delta H_f(CN)$ by emission spectroscopy[90a], mass spectrometry[90b], and absorption spectroscopy[90c], a value near 103 kcal has been given. These recent determinations then make the $D(H\text{-}CN) \leq 124$ kcal $mole^{-1}$, a few kcals below the previous value.[75]

Table I-I. Enthalpies of Formation (kcal mole^{-1}).

Species	ΔH^o_o	ΔH^o_{298}	Reference
H	51.63	52.102	(75)
N	112.52	113.0	(75)
N_2	0	0	(75)
H_2	0	0	(75)
N_3		105	(79)
		113	(82)
HNCO	-27.2	-27.9	(75)
HN_3	71.82	70.3	(76)
NH	81	81	(75)
NH_2	40.987	40.3	(75)
NH_3	-9.362	-11.04	(75)
NCO	62[c]	61[c]	
N_2H_4	26.18	22.80	(76)
$NH_4N_{3(c)}$		27.6	(76)
HCN	32.39	32.3	(76)
NO	21.46 $\pm$ 0.04	21.58 $\pm$ 0.04	(75)
CH_4	-15.991	-17.895	(75)
CH_3	32.805	31.94	(75)
C_2H_4	14.578	12.540	(75)
C_2H_5	30.0	26.2	(83)
CH_2NH_2	-3.2[b]	-5.49	(76)
$C_2H_5NH_2$	-6[c]	-11.5[b]	
N_2H_2		48.7 $\pm$ 5	(84)
N_2H_3	67[b]	64[b]	
N_2H		86[a]	

Table I-I. Continued.

Species	ΔH^o_o	ΔH^o_{298}	Reference
OH	9.290 ± 0.3	9.432 ± 0.3	(75)

a. Calculated assuming $D(N_2H-H)$ = 90 kcal. b. Values calculated in this work using appropriate known thermochemical data. c. Calculated assuming D(H-NCO) = 86 kcal.

Table II-I. Bond Dissociation Data (kcal $mole^{-1}$).

Bond	D^o_{298}	Ref.	Bond	D^o_{298}	Ref.
H-H	104.2	(77)	H_2N-NH_2	56 ± 4[b]	(75)
D-D	106.0	(77)	HN=NH	109 ± 10	(84)
CH_3-CH_3	88	(77)	N≡N	226	(77)
C_2H_5-H	98	(77)	NH_2-H	103	(77)
CH_3-H	104	(77)	NH-H	91[c]	
CH_3-CN	122	(77)	N-H	83[e]	(75)
HC≡N	164	(77)	$HN-N_2$	9[c]	
H-CN	124		$H-N_3$	86[c]	
CH_3-NH_2	79[a]	(77)	N_2H_3-H	93	(85)
CH_3NH-H	92	(78)	N_2H_2-H	37[c]	
$C_2H_5-NH_2$	78		N_2H-H	90[d]	
$nC_3H_7-NH_2$	78		OCN-H	86[d]	

a. $D(CH_3-NH_2)$ calculated to be 77 kcal $mole^{-1}$ at 0°K. b. $D(NH_2-NH_2)$ calculated to be 56 kcal $mole^{-1}$ at 0°K. c. Values calculated in this work from appropriate known thermochemical data. d. Assumed by analogy with $D(H-N_3)$. e. Seal and Gaydon[81] report a value of 74 ± 3.8 for NH bond dissociation energy, but this value seems too low.

B. NH Electronic States. Ionization and dissociation[44] of HN_3 by electron impact established $D(N_2\text{-}NH)$ at 9.2 kcal $mole^{-1}$. Such a small energy for the $HN\text{-}N_2$ bond would lead to spontaneous decomposition at room temperature, an unobserved phenomenon. In addition to the activation energy barrier, another factor inhibiting decomposition may be prohibition invoked by spin correlation rules for the dissociation of HN_3 into NH and N_2 in their ($^3\Sigma$) and ($^1\Sigma$) ground states respectively, as for N_2O. Directly related to the thermochemistry is the exact separation between the triplet and singlet states of NH. Until only recently the energy separation has not been known with much certainty. The separation was theoretically calculated by Hurley[91] using atomic orbitals, and found to be 1.76 $\pm$ 0.2 eV. Free imine was finally detected by mass spectrometry[92] and the NH appearance potential plot indicated superposition of two appearance potential curves, assigned as $NH(a^1\Delta)$ and $NH(^3\Sigma)$. Depending on the analytical method applied to the data, the separation was placed in the range 1.7-2.2 eV. Okabe and Lenzi[49] observed the fluorescence of NH following the photodissociation of NH_3 in the vacuum U. V. From this work the best value for the electronic separation is 1.6 $\pm$ 0.1 eV (36.9 $\pm$ 2.3 kcal). A pictorial diagram of the energy levels of NH is given in Fig. 1-I after a diagram by Okabe and McNesby[93], the states of nitrogen in these energy regions[94] are given for comparison.

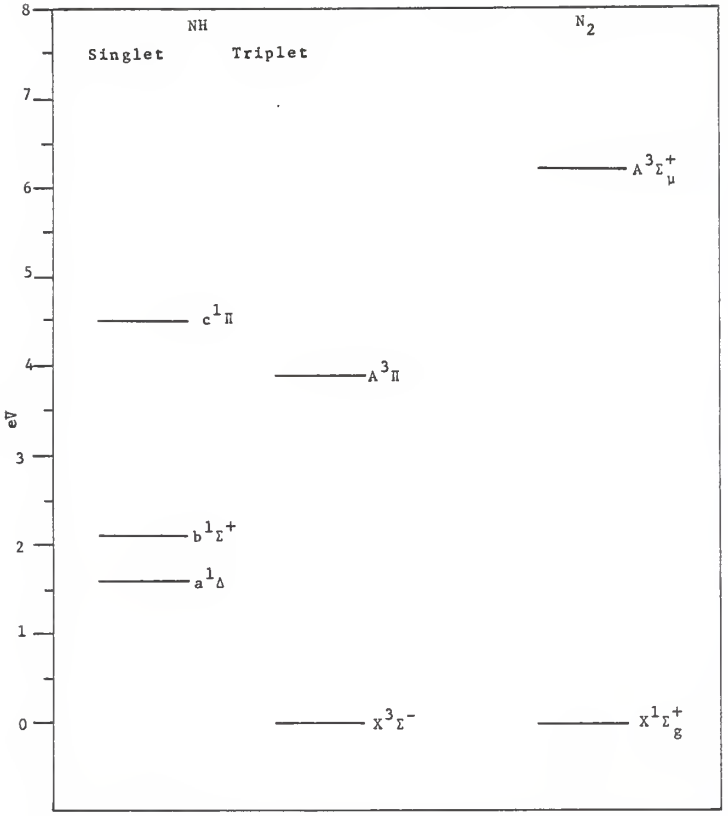

Figure 1-I. Spectroscopic states of NH (after a diagram by McNesby and Okabe[93]) and N_2[94].

APPENDIX II

Molecular parameters of hydrazine and methylamine. The data necessary for RRKM computations for N_2H_4 and CH_3NH_2 are compiled in the following tables.

Table I-II. Vibrational frequencies and vibrational assignments for N_2H_4 [95a] and NH_2 [96].

	Vibrational frequency (cm^{-1})	Vibrational assignment
N_2H_4	3350	N-H atretching
	3325	N-H stretching
	3297	N-H stretching
	3160	N-H stretching
	1607	H-N-H bending
	1493	H-N-H bending
	1275	N-N-H rocking
	1098	N-N-H rocking
	950	N-N-H wagging
	882	N-N stretching
	780	N-N-H wagging
	377	torsional oscillation
NH_2	3220	H-N-H stretching
	3173	H-N-H atretching
	1499	H-N-H bending

Table II-II. Moments of inertia for N_2H_4 [95] and NH_2 [97].

Molecule	I, g cm^2 x 10^{40}	Radical	I, g cm^2 x 10^{40}
N_2H_4	6.18	NH_2	1.18
	35.3		2.16
	37.0		3.42

Table III-II. Vibrational frequencies and vibrational assignments for CH_3NH_2[98a].

	Vibrational frequency (cm^{-1})	Vibrational assignment
CH_3NH_2	3387	N-H stretching
	3369	N-H stretching
	2962	C-H stretching
	2842	C-H stretching
	1622	H-N-H bending
	1460	CH_3 bending
	1410	CH_3 bending
	1244	CH_3 bending
	1129	CH_3 rocking
	1044	CH_3 rocking
	779	C-N stretching
	600	H-N-H rocking
	235	torsional vibration

Table IV-II. Vibrational frequencies and vibrational assignments for CH_3[33].

	Vibrational frequency (cm^{-1})	Vibrational assignment
CH_3	3056	C-H stretching
	3056	C-H stretching
	3056	C-H stretching
	1400	CH_3 bending
	1400	CH_3 bending
	730[a]	CH_3 out-of-plane deformation

a. Observed in a solid matrix at 14°K by Andrews and Pimentel[99].

Table V-II. Moments of inertia for CH_3NH_2[100] and CH_3[a].

Molecule	I, g cm^2 x 10^{40}	Radical	I, g cm^2 x 10^{40}
CH_3NH_2	8.136	CH_3	2.82
	37.08		2.82
	38.66		5.63

a. Calculated assuming a planar configuration and a C-H distance of 1.02A.

The barrier height to internal rotation for hydrazine has been reported[95b] as greater than 890 cm^{-1} (> 2.5 kcal $mole^{-1}$). For methylamine[98b] the barrier is about 691 cm^{-1} (1.9 kcal).

APPENDIX III

The Production and Reactions of NH and NH_2 Radicals.

This appendix is a review of gas phase NH and NH_2 radical chemistry. Since little kinetic information is available, attention is focused on the thermochemistry of the reactions. Unless otherwise stated, thermochemistry of $NH(^3\Sigma)$ was used for computing the enthalpies of reaction.

NH Radical Production and Chemical Reactions. Thermal Decomposition of HN_3 as a Source of NH. The thermal decomposition (290°C) of hydrazoic acid was first investigated by Ramsperger[1]. A white solid and a noncondensable gas, considered to be ammonium azide and nitrogen respectively, were noted to form. The extent of reaction was followed by pressure measurements of noncondensable gas at liquid air temperature. At an acid pressure of 4 cm, 9-11% decomposition occurred in 25 minutes. By increasing the surface 4 fold, 12% decomposition was experienced in eight minutes, indicating a profound effect of surface. The first thorough investigation of the slow thermal decomposition was carried out by Meyer and Schumacher;[2] a first order rate law was found, and N_2, NH_3, and a trace of H_2 were the products. Since the rate was found to be slower in a quartz vessel, the initial decomposition step was assumed to be somewhat heterogeneous. An overall stoichiometry was reported as (1)-III.

$$3HN_3 \rightarrow NH_3 + 4N_2 \qquad \Delta H^\circ = -74 \text{ kcal} \qquad (1)\text{-III}$$

The mechanism proposed was similar to that suggested for the photochemical[5] decomposition of hydrazoic acid.

$$HN_3 \rightarrow NH + N_2 \qquad \Delta H = 9 \text{ kcal} \qquad (2)\text{-III}$$

$$NH + HN_3 \rightarrow N_2H_2 + N_2 \qquad \Delta H = -106 \text{ kcal} \qquad (3)\text{-III}$$

$$NH + HN_3 \rightarrow 2N_2 + H_2 \qquad \Delta H = -153 \text{ kcal} \qquad (4)\text{-III}$$

$$N_2H_2 + HN_3 \rightarrow NH_3 + 2N_2 \qquad \Delta H = -128 \text{ kcal} \qquad (5)\text{-III}$$

A calorimetric study[3] of the explosive decomposition yielded -70.9 ± 0.5 kcal mole^{-1} as the heat of reaction for (6)-III,

$$2HN_3 \rightarrow H_2 + 3N_2 \qquad \Delta H = -144 \text{ kcal} \qquad (6)\text{-III}$$

although modern thermochemical values give -71.8 kcal mole^{-1}. The stoichiometry for the explosive decomposition excluded ammonia, and this is still believed to be the case. However, the above discrepancy remains unexplained.

The papers cited are felt to be the major early contributions on the thermal pyrolysis, and are included for an historical bent. A more inclusive review including solution work to 1943 is given by Bonnemay.[101]

A resurgence of investigation of HN_3 decomposition and NH radical reactions was initiated in the United States by a very interesting observation reported by Rice and Freamo[102] in 1951. When HN_3 was passed at low pressures (0.05-0.2 mm) through a heated (1000°C) quartz tube with a liquid nitrogen cooled finger

at the exit of the tube, a paramagnetic blue solid collected on the finger. Upon warming the blue solid to -125°C ammonium azide was formed. The condensed blue species was tentatively identified as the NH radical with a half-life of about $9X10^{-4}$ sec. Rice and co-workers[103-106] attempted a mass balance, and established the absorption spectrum of the blue solid (a broad maximum at 6500$^{o}_{A}$) and a small band between 3400 and 3500$^{o}_{A}$). The mass balance study established the production of one mole of gaseous hydrogen and seven moles of gaseous nitrogen for each six-moles of hydrazoic acid decomposed. To balance the stoichiometry the term 4(NH) was required to complete the equation, (7)-III.

$$6HN_3 \rightarrow 7N_2 + H_2 + 4(NH) \qquad (7)\text{-III}$$

Upon warming the material collected on the cold finger transformed to ammonium azide, (8)-III.

$$4(NH) \rightarrow NH_4N_3 \qquad (8)\text{-III}$$

A compilation of the data is given in Table I-III. Later it waa concluded that the ammonium azide had been formed from undecomposed hydrazoic acid and ammonia which was produced in the thermal decomposition. If (7)-III is then reinterpreted and corrected by substracting one HN_3 from both sides of the equation, an overall stoichiometry for HN_3 that has decomposed ia given by equation (9)-III,

$$5HN_3 \rightarrow NH_3 + 7N_2 + H_2 \qquad (9)\text{-III}$$

Table I-III.

	Average	Calculated
HN_3 consumed (g)	1	1
Non-condensible gas (g)	1.32	1.33
N_2 (g)	1.16	1.17
H_2 (g)	0.162	0.167
NH_4N_3 measured after transition (g)	0.168	0.167

Many investigations and speculations have been made on the blue material, but no definitive conclusions have been reached. The early conclusions associating it with NH are certainly in error.

Gray and Waddington[12] in 1957 studied the thermal explosion of HN_3 in quartz vessels. Conditions of pressure of HN_3 versus temperature for the explosion limits were determined, and a new mode of decomposition was observed. Under conditions too mild for an explosion, yet near the explosion boundary, decomposition was accompanied by a whitish luminescence. The explosive decomposition products were N_2 and H_2 only; no NH_3 was observed. Reaction (2)-III, followed by steps (10)-III and (11)-III, was suggested.

$$NH + NH \rightarrow N_2 + H_2 \qquad \Delta H = -162 \text{ kcal} \qquad (10)\text{-III}$$

$$NH + HN_3 \rightarrow 2NH + N_2 \qquad \Delta H = 9 \text{ kcal} \qquad (11)\text{-III}$$

Diimide is often suggested in the mechanism of HN_3 pyrolysis and it has been the subject of a number of inveatigations and a short general review on gas phase work.[107] Diimine thought to arise from reactions such as (12)-III and (13)-III was first directly observed by Foner and Hudson[108] in a mass

$$NH + HN_3 \rightarrow N_2H_2 + N_2 \qquad \Delta H = -95 \text{ kcal} \qquad (12)\text{-III}$$

$$NH + NH \rightarrow N_2H_2 \qquad \Delta H = -109 \text{ kcal} \qquad (13)\text{-III}$$

spectrometric study of an electrical discharge of HN_3 in a flow system. HN_3, N_2, NH_3 and a parent peak at m/e = 30 were detected in the mass range 14-100. The m/e = 30 peak waa aasigned as N_2H_2 and from the appearance potential the heat of formation was given as 48.1 kcal $mole^{-1}$. The same peak was observed in the products from the thermal and electrical decomposition of hydrazine.

Guenebaut, Pannetier, and co-workers[51,52] found intense NH emission from the $^3\pi$-$^3\Sigma$ band when HN_3 was decomposed in a shock tube. A continuum at 4200°_{A} was assigned as the NH_2 radical. In the deuterated study[52] the $^3\pi$-$^3\Sigma$ system of ND was obaerved. NH $^1\pi$-$^1\Delta$ emission was also observed, but attributed to secondary reactions.

The explosive decompoaition of hydrazoic acid can be initiated by an electrical apark. Such a study[109] has been done in the presence of argon, nitrogen, hydrogen, carbon dioxide, methane, benzene, toluene, n-hexane, n-heptane, and n-octane. The effectiveness of inhibition of the explosion was found to be

in the above order, with n-octane 16 times more effective than argon. The foreign gas was thought to disrupt the radical chains probably occuring in the explosion. In previous spark initiated decomposition sutdies[110,111] a yellow emission was observed above an acid pressure of 5 mm. The foreign gases nitrogen, hydrogen, argon, and water vapor were also found to inhibit explosion. Spectral analysis[111] of the system generated by the spark decomposition of deuterated HN_3 showed evidence for $ND(X^3\pi\text{-}B^3\Sigma)$ emission. An electrical discharge through HN_3 in a flow system with ammonia added downstream was found to yield hydrazine.[112,113] Injecting ammonia before the discharge increased the yield. Reaction (14)-III was suggested.

$$NH + NH_3 \rightarrow N_2H_4 \qquad \Delta H = -46 \text{ kcal} \quad (14)\text{-III}$$

The decomposition flame[114-116] of hydrazoic acid yielded a second order process with an activation energy of about 23 kcal $mole^{-1}$. The unimolecular decomposition to NH and N_2 (reaction III-2) was inferred, but at low pressure and high temperature the production of active HN_3^* through bimolecular collisions became insufficient to maintain a stationary concentration and the activation phenomenon of order two controlled the overall rate.

To summarize, decomposition in thermal systems can occur in two extreme ways which lead to two different sets of products. Slow thermal decomposition yields ammonia and nitrogen; the explosive decomposition yields hydrogen and nitrogen. Apparently two different mechanisms for decomposition exist. The slow

thermal pyrolysis has been studied in more detail; the initial step of decomposition seems to be $HN_3 \rightarrow NH + N_2$. The explanation of the change to explosive conditions is not known. The explanation may involve a change in primary processes or of secondary reactions of NH or perhaps a combination of both. Heterogeneity problems have been known from the beginning but a detailed study has not been made. Spectroscopic observations of intermediates in HN_3 decomposition in shock tubes and by electrical spark have detected the NH radical and the NH_2 radical. Isolation of intermediates in low temperature matrices produced evidence for N_2H_2 formation, and its presence is implied in gas phase reactions. An overall picture of the primary and secondary processes in HN_3 thermal decomposition is not complete. Part of the problem is the experimental difficulties of gas phase studies of these inorganic compounds (glpc analysis, acid-base complexes, etc.) and surface reactions encountered in these systems.

B. Photolytic decomposition of hydrazoic acid. Hydrazoic acid absorption begins at 2250A and reaches a maximum at 1990A. Photons of this energy (128 kcal) are sufficient to give either singlet or triplet NH radicals and N_2 in the primary photolytic step, which is usually agreed to be (15)-III.

$$HN_3 + h\nu \rightarrow NH + N_2 \qquad (15)\text{-III}$$

Also, sufficient energy is present for H-atom and azide radical formation. The gas phase data are considered first, and then the low temperature matrix isolation work will be summarized.

In 1928 Beckman and Dickinson[4] studied the photolysis of hydrazoic acid, and identified nitrogen, hydrogen, and ammonium azide among the products. Resction (15)-III was the favored primary process. Subsequent work in 1930 and 1935 on the aluminum spark (λ = 1990Å) initiated decomposition[5] and the mercury photosensitized decomposition[6] confirmed these products. A primary quantum yield of about 3 was deduced, and found to be independent of pressure in the region 2-130 mm. No chain reactions were discernible. The following mechanism was suggested.

$$NH + HN_3 \rightarrow H_2 + 2N_2 \ (18\%) \qquad \Delta H = -77 \text{ kcal} \qquad (16)\text{-III}$$

$$NH + HN_3 \rightarrow N_2H_2 + N_2 \ (82\%) \qquad \Delta H = -104 \text{ kcal} \qquad (17)\text{-III}$$

$$N_2H_2 + HN_3 \rightarrow NH_3 + 2N_2 \qquad \Delta H = -130 \text{ kcal} \qquad (18)\text{-III}$$

$$NH_3 + HN_3 \rightarrow NH_4N_3 \qquad \Delta H = -34 \text{ kcal} \qquad (19)\text{-III}$$

An important study was the high intensity flash photolysis[53] of HN_3. Absorption spectra of NH ($^3\pi$-$^3\Sigma$) and NH_2 free radicals were identified, and a previously unobserved band at 2700Å, more intense than either NH or NH_2, was assigned to the N_3 radical. A recent high-resolution study[117] of these bands and a U.V. photolysis study[118] of HN_3 have confirmed the assignment of N_3. The proposed mechanism for N_3 formation utilized (15)-III as the primary

step followed by

$$NH + HN_3 \rightarrow NH_2 + N_3 \qquad \Delta H = -7 \text{ kcal} \qquad (20)\text{-III}$$

$$NH_2 + HN_3 \rightarrow NH_3 + N_2 \qquad \Delta H = -17 \text{ kcal} \qquad (21)\text{-III}$$

$$N_3 + N_3 \rightarrow 3N_2 \qquad \Delta H = -210 \text{ kcal} \qquad (22)\text{-III}$$

Thrush[53] pointed out that reaction (22)-III may have occurred in two steps, involving a novel source of nitrogen atoms in a static system.

$$N_3 \rightarrow N + N_2 \qquad \Delta H = 7 \text{ kcal} \qquad (23)\text{-III}$$

$$N + N_3 \rightarrow 2N_2 \qquad \Delta H = -217 \text{ kcal} \qquad (24)\text{-III}$$

Recent bond energy estimation[86] for $D(N\text{-}N_2)$ would preclude process (23)-III, as being too endothermic, but this has not been confirmed.[87]

The observation of $(^3\pi\text{-}^3\Sigma)$ NH absorption raises the interesting and important question of whether the initial dissociation of HN_3, (15)-III, takes place with conservation of spin to give $NH(^1\Delta)$ followed by spin inversion (collision induced or spontaneous) or whether resction (15)-III gives directly the $NH(^3\Sigma)$ state. The presence of the triplet state in flash photolysis has recently been confirmed by Cornell, et al.[50]

Recent photolysis[119] investigations in the vacuum U.V. region have shown fluoresence from $NH(^1\Pi)$. In the vacuum U.V. photolysis of HN_3 at 1236A, 1470A, and 1600-2000A, Welge[120] proposed that

HN_3 dissociated in part according to (25)-III.

$$HN_3 + h\nu \rightarrow NH(C^1\pi,\ v = 0.1) + N_2(X\ ^1\Sigma_g^+) \qquad (25)\text{-III}$$

A threshold energy of about 122 kcal was obtained for this spin allowed process. Photolysis[121] of HN_3/NO mixtures at 1420A and 1236A produced NO ($A^2\pi$) γ-band fluorescene. This was explainable by formation of $N_2(A^3\Sigma)$ in the photodissociation of HN_3 according to (26)-III,

$$HN_3 + h\nu \rightarrow NH(X^3\Sigma) + N_2(A^3\Sigma), \qquad (26)\text{-III}$$

a process capable of providing the excitation energy of 126 kcal required for the population of the NO ($A^3\Sigma$) state from the NO ($X^2\pi$) state.

The matrix isolation method has yielded important information on the primary and secondary processes in the photolytic and electrical discharge decomposition of HN_3. Mador and Williams[122] spectroscopically examined products deposited at 4 and 77° from the electrical discharge decomposition of HN_3. In other experiments HN_3 was photolyzed at 2537A during and after deposition. Infrared spectral features were consistent with reactant HN_3 and product NH_4N_3. In the visible and ultraviolet region, absorption bands attributed to NH and NH_2 were observed at 3500A and 6500A, which disappeared upon warming above 148°K. Photodecomposition[123] of HN_3 at 4.2°K in Kr and Xe matrices gave products whose electronic spectra were clearly due to NH and NH_2 radicals. N_3 was

also suggested. Dows, et al.,[7] examined the condensed products from the glow discharge decomposition of HN_3 by infrared spectroscopy. Ammonium azide, HN_3, NH_3 and two intermediates were observed. As the temperature of the matrix increased another species with absorption at 3230 cm^{-1} and 860 cm^{-1} was noted. After a certain temperature was reached, the bands disappeared. The intermediates were tentatively assigned as NH, $(NH)_x$, and N_2H_2, where diimine was the temperature dependent species arising from NH diffusion and reaction as the temperature was increased. These dependent bands[124] were later attributed to triazene (N_3H_3), but further work[125] has suggested that a water impurity was involved and at present they seem to have no real significance. Photolysis[126] (3320A) of HN_3 deposited on a window at 66°K gave only NH_4N_3 if pure HN_3 was used. Whereas photolysis in a Xe matrix indicated NH radical isolation, Ar and N_2 matrices gave more evidence for other undetermined intermediates. Further work from this laboratory in 1960[127] gave more evidence for the isolation of NH during the photolysis of HN_3 in a nitrogen matrix at 20°K. In addition, the possibility of NH_2 and N_3, N_2H_2, and NH_2N_3 (azide amine) could not be eliminated. In a definitive study Milligan and Jacox[128] directly observed the NH and ND fundamental vibration at 3133 cm^{-1} and 2323 cm^{-1} respectively in Ar and N_2 matrices at 4°, 14°, and 20°K. Ultraviolet absorption spectra established the presence of NH and ND (in the deuterated case) in their ground $^3\Sigma$ states. Rapid relaxation of the initially formed $^1\Delta$ state to the $^3\Sigma$ state was used to explain the presence

of triplet rather than the singlet state NH. In a CO matrix, HN_3 photolysis yielded HNCO, HOCN, and HCO.[129] The formation of HCO was thought to imply some H-atom production, probably by (27)-III

$$HN_3 + h\nu \rightarrow H + N_3 \qquad \Delta H = 86\text{kcal} \qquad (27)\text{-III}$$

Milligan and Jacox dealt with the subsequent fate of NH from the viewpoint of NH attack on HN_3, possibly leading to the formation of N_2H_2 and N_4H_2, (28)-III.

$$NH + HN_3 \rightarrow H\text{-}N{=}N\text{-}N{=}N\text{-}H \qquad (28)\text{-III}$$

NH_2N_3 may have formed by (29)-III,

$$NH_2 + N_3 \rightarrow NH_2N_3 \qquad (29)\text{-III}$$

but it was thought to readily decompose.

The latest careful work from Pimentel's laboratories[130] confirmed Milligan and Jacox's NH detection in Ar and N_2 matrices, and also firmly established trans-N_2H_2 with absorption at 1286 cm^{-1} and cis-N_2H_2 with absorption at 3074 cm^{-1} and 1279 cm^{-1}.

Application of electron spin resonance[8] to the photolyzed matrix of HN_3 with Ar, Xe, and Kr at 4.2°K detected H-atoms and N-atoms. Based on several kinetic arguments their production was ruled out as occuring from secondary photolysis steps (30)-III and (31)-III.

$$NH + h\nu \rightarrow N + H \qquad \Delta H = 81\text{ kcal} \qquad (30)\text{-III}$$

$$HN_3 + h\nu \rightarrow H + N_3 \qquad \Delta H = 86 \text{ kcal} \qquad (31)\text{-III}$$

Unidentified secondary chemical reactions as a result of NH diffusion through the matrix were thought to be responsible for the N- and H-atoms, which were not formed in the primary process.

From the many photolysis studies it can be definitely concluded that the significant primary process is formation of NH and N_2. Some authors feel that the presence of the triplet NH is due to rapid quenching of the initially formed singlet state. The possibility of formation of H-atoms and N_3 in a primary process cannot be completely discounted although it is likely a minor process. The secondary reactions of NH with HN_3 differ in the gas phase and the matrix work. Isolation of ethylenimine in the $HN_3 + C_2H_4$ + Ar matrix photolysis (to be discussed in the next section) is the only clear addition reaction of NH reported. However, the detailed behavior of NH in gas phase and matrix photolysis systems has not been characterized sufficiently to be well understood. Successive abstraction of NH and NH_2 to give NH_3 seems established but addition reactions with π bonded molecules are also likely to be important especially at low temperatures.

C. Reactions of NH with substrates studied by HN_3 photolysis. Matrix isolation studies using I. R. absorption spectra as the analytical tool have been carried out utilizing reactive matrices enabling one to study radical reactions with various substrates. A summary of low temperature NH-substrate reactions studied is given in Table II-III.

Table II-III. Reactions of NH with substrates in solid matrices.

Reaction	Reference
(a) $NH + C_2H_2 \rightarrow CH_2{=}C{=}N{-}H$	(131)
(b) $NH + C_2H_4 \rightarrow \overbrace{CH_2CH_2NH}$	(131)
(c) $NH + CO \rightarrow HNCO$	(129)
(d) $NH + CO \rightarrow HOCN$	(129)
(e) $NH + CO_2 \rightarrow NH \cdot CO_2$	(132)
(f) $NH + F \rightarrow NHF$	(133)
(g) $NH + F_2 \rightarrow NHF + F$	(133)
(h) $NH + O_2 \rightarrow$ HONO (cis) and HONO (Trans)	(134) (135)
(i) $ND + CO_2 \rightarrow DNO + CO$	(136)

The reactions of NH and ND in a CO_2 matrix were unusual in that HNO and DNO were observed[136]. This was explained by

$$NH + CO_2 \rightarrow NH \cdot OCO \rightarrow HNO + CO \qquad (32)\text{-III}$$

The most pertinent work to this thesis is that by Jacox and Milligan[131] with $HN_3 - C_2H_4$ and $HN_3 - C_2H_2$ photolyses at 4°K. Ethylenimine was identified by infrared spectroscopy as the sole product in the $HN_3 - C_2H_4$ system. Reaction (33)-III

$$NH + C_2H_4 \rightarrow \overbrace{CH_2CH_2NH} \qquad (33)\text{-III}$$

which is similar to the reaction of singlet methylene with ethylene to cyclopropane by an analogous mechanism, was suggested.

However, triplet CH_2 also reacts with spin inversion to give cyclopropane. Reaction with acetylene via a singlet NH would have been expected to proceed by the sequence (34)-III and (35)-III.

$$NH + C_2H_2 \rightarrow HC \equiv CHNH \qquad (34)\text{-III}$$

$$NH + C_2H_2 \rightarrow H_2NC \equiv CH \qquad (35)\text{-III}$$

For a triplet NH the following scheme would have been expected

$$NH + C_2H_2 \rightarrow H - C \equiv C - \underset{NH}{\diagdown\!\diagup} - H \qquad (36)\text{-III}$$

$$NH + C_2H_2 \rightarrow H - C - \underset{NH}{\diagdown\!\diagup} - C - H \qquad (37)\text{-III}$$

$$H - C - \underset{NH}{\diagdown\!\diagup} - C - H \rightarrow H_2C - \underset{NH}{\diagdown\!\diagup} - C: \qquad (38)\text{-III}$$

$$H_2C - \underset{NH}{\diagdown\!\diagup} - C: \rightarrow H_2C \equiv C \equiv NH \qquad (39)\text{-III}$$

The infrared analysis data were interpreted in terms suggesting ketenimine ($CH_2 \equiv C \equiv NH$) formation, hence a triplet NH precursor. Apparently, the reactions of singlet NH compete with its intersystem crossing to the triplet state, and in some cases both singlet and triplet NH may be important.

For C_2H_4 the low temperature results seem to be in conflict with the gas phase (see below). The explanation may be the better energy transfer from hot species in matrices or from different electronic states of NH in the two cases.

The room temperature gas phase reactions of NH generated photolytically from HN_3 in the presence of hydrocarbons have been qualitatively investigated.[9] Product analyses were difficult due to formation of white solids in the reaction vessel. With methane small amounts of HCN and C_2H_6 were detected by mass spectrometry but no evidence for the insertion product methyl amine could be found. In the presence of propane, n-butane, and isobutane, amines were reported. The attack of NH on hydrocarbons was found to increase as the number of carbons increased. Reaction with ethylene occurred to an appreciable extent. Hydrogen cyanide, C_2H_6, and CH_3CN were formed, but the main products were NH_4N_3, H_2, and N_2. There was no conclusive evidence for the formation of the addition product with ethylene. In these systems complete mass balance was lacking. Since N_2H_2 had recently been detected[84], the following reactions,

$$NH + HN_3 \rightarrow HN = NH + N_2 \qquad (40)\text{-III}$$

$$HN = NH + HN_3 \rightarrow NH_3 + 2N_2 \qquad (41)\text{-III}$$

were included.

An extensive investigation of NH radical reactions with olefins was carried out by Cornell et al.[50] using flash and steady photolysis. The total pressure in the photolysis cell was about 12 cm Hg (6 cm HN_3; 6 cm hydrocarbon); such conditions are near the explosion limit for experiments at higher temperature in some experiments extensive heating of the sample by the flash occurred. Flash kinetic absorption spectroscopy identified

$NH(A^3\Sigma \rightarrow X^3\Sigma)$ and $CN(B^2\pi \rightarrow X^2\pi)$ in the ethylene system. Singlet NH was not observed. In the isothermal photolysis of HN_3 - C_2H_4 mixtures, HCN, CH_3CN, CH_4, H_2, N_2, and an amorphous solid were observed products. Analyses for NH_3 and NH_4N_3 were not reported. The $(HCN)/(CH_3CN)$ ratio was insensitive to ethylene partial pressure in the range 8-56 cm, and equal to 0.8. The two products were thought to arise from the same precursor (the triplet adduct of NH with C_2H_4), and may have been generated according to the following set of triplet NH radical reactions.

$$NH + C_2H_4 \rightarrow CH_2CH_2NH \qquad (42)\text{-III}$$

$$CH_2CH_2NH \rightarrow CH_3CH_2N \qquad (43)\text{-III}$$

$$CH_3CH_2N \rightarrow HCN + CH_4 \qquad (44)\text{-III}$$

$$CH_3CH_2N \rightarrow CH_3CN + H_2 \qquad (45)\text{-III}$$

A bimolecular rate constant of 10^{10} cc $mole^{-1}$ sec^{-1} for NH disappearance by (42)-III was obtained.

It is apparent that NH is a reactive free radical since products are observed from its reactions at very low temperatures. The mechanisms in most cases are not established and the only tentative available rate constant is the one with C_2H_4 at room temperature.

D. Photolysis of isocyanic acid as a source of NH. In 1950 Herzberg and Reid[130] established the structure of cyanuric acid vapor as H-N=C=O, and properly renamed the compound isocyanic

acid. Compared to its analogs CH_2CO, CH_2N_2, and HN_3, isocyanic acid could possibly be expected to disaociate into NH and CO upon photolysis. The photochemistry has been extensively investigated in low temperature matrices by Jacox and Milligan[129] in the gaa phase by Back and co-workera,[47,73,139-142] and by Bradley.[143]

Infrared absorption spectra[129] of the products from the photolysis of HNCO and DNCO in an inert matrix at 4° and 20°K suggested the presence of OCN, OD, CO, OH, and CN. A new species, HO-C=N, was tentatively identified. Two mechaniams were suggested, and both involved formation of NH in the primary step, although dissociation into H and NCO was not neceaaarily eliminated. No HNOC was observed; if produced, it may have quickly rearranged to HOCN.

$$HNCO + h\nu \rightarrow NH + CO \qquad (46)\text{-III}$$

$$NH + \underline{C}O \rightarrow HNCO \qquad (47)\text{-III}$$

$$NH + C\underline{O} \rightarrow HNOC \qquad (48)\text{-III}$$

$$HNOC \rightarrow HOCN \qquad (49)\text{-III}$$

A mechanism for formation of HOCN involved the conversion of singlet to triplet NH, (50)-III - (53)-III.

$$HNCO + h\nu \rightarrow NH\ (^1\Delta) + CO \qquad (50)\text{-III}$$

$$NH\ (^1\Delta) \rightarrow NH\ (^3\Sigma) \qquad (51)\text{-III}$$

$$NH\ (^3\Sigma) + CO \rightarrow CONH \qquad (52)\text{-III}$$

$$CONH \rightarrow HOCN \qquad (53)\text{-III}$$

Further work[118] coupling both infrared and ultraviolet spectroscopy led to identification of the NCO radical generated by vacuum - U. V. photolysis of HNCO suspended in an Ar matrix at 4° and 14°K. In the vacuum U. V. Photolysis the HNCO was thought to split into H + NCO in the primary step. The observation of NH in this system was attributed to a secondary reaction between N and H atoms, and not to a primary dissociation.

It should be noted that NH has been observed directly in the gas phase photolysis of HNCO[144], thus supporting a primary split into NH and CO. NCO, and NH_2 have also been observed.[145]

The steady state gas phase photolysis of HNCO has been extensively studied by Back and co-workers.[47,73,139-140] Early work[139,140] reporting a single primary process and an abstraction mechanism has yielded to recent reexamination by Woolley and Back[47]. Conclusions regarding both primary and secondary steps differ from the earlier work. The latest work measured the quantum yield of CO, N_2, and H_2 to be 1.0, 0.40, and 0.13; in addition, NH_3 or its equivalent was formed and complexed with HNCO to form NH_4NCO. The most remarkable feature of the latest study is the finding that the H in HNCO is abstracted by CH_3 radicals with a considerably lesser rate than H from $(CH_3)_2N_2$. Thus it was concluded that formation of NH_3 by successive abstraction of H by NH and NH_2 was unlikely. In order to explain

the data two primary processes are needed,

$$\text{HNCO} + h\nu \begin{cases} \rightarrow \text{NH} + \text{CO} & \Delta H = 81 \text{ kcal} \\ \rightarrow \text{H} + \text{NCO} & \Delta H = 86 \text{ kcal} \end{cases} \quad (54)\text{-III}$$

each with a quantum yield of about 0.5.

The secondary reactions were not well defined. Two possible sets of reactions were suggested. The first utilizes N_2H_2 as a means of producing NH_3.

$$2\text{NH} \rightarrow [\text{HN} = \text{NH}]^* \rightarrow N_2 + 2\text{H} \quad (55)\text{-III}$$

$$2\text{NH} \xrightarrow{\text{M or surface}} N_2H_2 \quad (56)\text{-III}$$

and

$$N_2H_2 + \text{NH} \rightarrow N_2 + NH_3 \qquad \Delta H = -139 \text{ kcal} \quad (57)\text{-III}$$

or

$$3N_2H_2 \xrightarrow{\text{surface}} 2NH_3 + 2N_2 \quad (58)\text{-III}$$

Other reactions between NH, NCO, and H atoms were suggested to explain the observed $H_2/CO/N_2$ stoichiometry. A second set of reactions was

$$\text{H} + \text{HNCO} \rightarrow H_2\text{NCO} \quad (59)\text{-III}$$

$$\text{H} + H_2\text{NCO}^* \rightarrow NH_3 + \text{CO} \quad (60)\text{-III}$$

and

$$H + H_2NCO \rightarrow H_2 + HNCO \qquad (61)\text{-III}$$

$$NH + H_2NCO \rightarrow NH_2 + HNCO \qquad (62)\text{-III}$$

It was argued that the H_2N-CO bond is quite strong and the NH_2CO radical, consequently, was relatively stable.

The data also suggest that NH reacts with HNCO probably to give N_2H_2 + CO. The N_2H_2 then reacts according to (57)-III.

In a parallel study Bradley, et al.,[143] photolysed HNCO at 30°C. Products reported were CO, N_2, H_2, and a solid polymer; no ammonia or hydrazine was detected by mass spectrometry. Deuterium was added in some experiments as a test for hydrogen atoms. The results were interpreted in terms of two primary splits, a polymerization reaction, and a non-abstractive mode of reaction for NH.

$$NH + HNCO \rightarrow N_2 + H_2 + CO \qquad \Delta H = -81 \text{ kcal} \qquad (63)\text{-III}$$

$$NH + HNCO \rightarrow (NH\ CONH)n \qquad (64)\text{-III}$$

$$H + HNCO \rightarrow H_2 + NCO \qquad \Delta H = -17 \text{ kcal} \qquad (65)\text{-III}$$

$$NCO + NCO \rightarrow N_2 + 2CO \qquad \Delta H = -70 \text{ kcal} \qquad (66)\text{-III}$$

Formation of $[NH_2CO^*]$ was ruled out in the absence of NH_3 and N_2H_4. An estimated 17% HNCO polymerized.

Friswell and Back[141] examined the mercury-photosensitized decomposition of HNCO vapor for the first time. A low ϕ CO, and the independence of ϕ CO and N_2/CO on HNCO pressure wereinterpreted in terms of a single primary process not involving NH.

$$Hg^{*} + HNCO \rightarrow Hg + H + NCO \qquad (67)\text{-III}$$

The mechanism was admittedly speculative. From experiments with added hydrogen a ratio of cross sections for reactive quenching was estimated, $^{\sigma}HNCO/^{\sigma}H_2 = 2.3$.

Woolley and Bsck[47] also investigated the photolysis of HNCO in the presence of ethylene. The following products were identified by gas chromatography; CH_4, C_2H_6, C_3H_8, $n\text{-}C_4H_{10}$, HCN, and C_2H_5NCO. No CH_3CN was found, and NH_3 was not mentioned among the products in this system. Some of the observed products were interpreted in terms of H-atom sddition to ethylene, and subsequent ethyl radical reactions.

$$C_2H_5 + C_2H_5 \rightarrow n\text{-}C_4H_{10} \qquad (68)\text{-III}$$

$$C_2H_5 + NH_2CO \rightarrow C_2H_6 + HNCO \qquad (69)\text{-III}$$

$$CH_3 + C_2H_5 \rightarrow C_3H_8 \qquad (70)\text{-III}$$

The addition of NH to C_2H_4 to give HCN + CH_3 was the suggested source of HCN. The absence of CH_3CN is puzzling in view of the work of reference[50]. The reaction of NCO with C_2H_4 was the favored source of CH_3 radicals.

$$NCO + C_2H_4 \rightarrow CO + [C_2H_4{\cdot}N] \qquad (71)\text{-III}$$

$$[C_2H_4{\cdot}N] \rightarrow HCN + CH_3 \qquad (72)\text{-III}$$

Support for this can be found in the reaction of N atoms with

C_2H_4 to give HCN + CH_3[24]. The C_2H_4 data in general support the formation of some H-atoms in the primary process.

In view of the recently amended interpretation of the mechanism of HNCO photolysis, the earlier results[73] from HNCO-alkane cophotolysis have little significance. In all cases the expected amines, formed by either H-abstraction followed by radical combination or by NH insertion, were absent. The failure to detect any amine was attributed to formation of the amines in high vibrationally excited states which decompose at the pressures of the experiments. In some cases it was proposed that C-H rupture was favored over C - C or C - N rupture. Even if the NH produced in the primary step was in the $^1\Delta$ state (which should favor C-H insertion), insufficient energy would be present to permit C-H bond rupture which is to be favored over C-CH_3 or C-NH_2 rupture. Furthermore, the calculations of this thesis show that at most pressures the amines ($C_2H_5NH_2$ or $C_3H_7NH_2$) would be stable to even C-C or C-N rupture regardless of whether they were formed by insertion of NH ($^1\Delta$) or by combination reactions. The likely explanation of these systems is a lack of understanding of the mechanism of the NH, H, NCO, etc. radical reactions rather than unimolecular reactions of the amines.

Recent work by Back and Ketcheson[142] with the photolysis of HNCO vapor in the presence of NO showed a reduction in the H_2 and CO yields (relative to pure HNCO photolysis) and an increased N_2 yield. Plausible reactions were suggested.

$$NH + NO \rightarrow N_2 + OH \qquad \Delta H = -93 \text{ kcal} \qquad (73)\text{-III}$$

$$OH + HNCO \rightarrow H_2O + NCO \qquad \Delta H = -32 \text{ kcal} \qquad (74)\text{-III}$$

$$NCO + NO \rightarrow N_2 + CO_2 \qquad \Delta H = -178 \text{ kcal} \qquad (75)\text{-III}$$

Experiments with ^{15}NO were carried out. A decline in $^{14}N\text{-}\,^{14}N$ with increasing ^{15}NO concentration supported NH and NCO reaction with NO. However, the system was complicated by the photolysis of NO. Condensible analysis detected trace amounts of CO_2 and N_2O, but there was difficulty in determining their origin.

Photolysis in the presence of oxygen[142] showed a parallel between O_2 and ethylene with regard to the suppression of H_2 formation. The yields of CO and N_2 were unchanged.

These studies of O_2 and NO mixed with HNCO seem to support the contention that H-atoms are the source of H_2 since both O_2 and NO are known to remove H-atoms quite readily. It also appears that no reaction between NH and O_2 takes place. The conclusion regarding the reaction between NH and NO is uncertain, and the increased N_2 production can have many explanations. Work involving the shock tube initiated oxidation of NH_3 is in conflict regarding whether or not NH reacts with O_2 and NO; in this author's opinion the evidence is in favor of no reaction.

E. Reactions of N and H Atoms with Hydrazoic Acid. Several qualitative investigations have shown that NH radicals are present in the reactions of N and H-atoms with hydrazoic acid. The HN_3/H atomic flame[146-148] yielded intense emission for both

the ainglet and triplet systems of NH. The HN_3/N atomic flame[149] displayed an intense gray-orange luminescence. Emission was observed for NH and NH_2. Analysis of the spectra for the $(^3\pi\text{-}^3\Sigma)$ NH emission gave a rotational temperature of 4500°K; for the singlet $(^1\pi\text{-}^1\Delta)$NH emission the rotational temperature was 2100°K. This delineated two separate mechanisms one giving $NH(^1\Delta)$ and the other giving $NH(^3\Sigma)$. The formation of the singlet was attributed to a reaction between atomic hydrogen and HN_3. The triplet system was thought to arise from the thermal decomposition of HN_3.

ND singlet and triplet were observed in the flame decomposition of deuterated hydrazoic acid.[150,151]

Stewart[152] decomposed hydrazoic acid in a non-luminous active nitrogen flow. Condensible products were collected downstream and analyzed. HN_3-substrate mixturea were also examined. No ammonia or hydrazine could be isolated from pure HN_3 decomposition products. Ammonia formed with H_2 as a substrate; aniline was formed in HN_3/C_6H_6 mixtures. $HN_3\text{-}C_2H_4$ mixtures yielded a volatile base which eluded further identification.

F. Amine Radical Chemistry. Hydrazine and ammonia photolytic and pyrolytic decompositions should be integrated into an overall picture of NH and NH_2 radical chemistry; more emphasis is placed on NH_2 radicals in these systems because they are more often encountered. The discussion of N_2H_4 and NH_3 will seek to amass

published evidence for the production of NH_2 by a variety of methods, and provide an overall, but by no means complete summary of work completed in these systems. Particular emphasis will be given to the leading studies relating to the disproportionation-combination problem of NH_2 radicals, which is of direct and major importance to this thesis. All work in hydrazine systems is plagued by a common problem, high adsorption-to-glass efficiency for N_2H_4. Heat is usually required for complete desorption.[153] This makes quantitative handling of small gaseous samples and gas chromatography analysis of N_2H_4 very difficult.

Low temperature matrix studies have detected the formation of NH_2 radicals in the decomposition of both hydrazine and ammonia. The electronic spectra of deposition products collected at 4.2°K when an electrodeless discharge was passed through N_2H_4[154] and ammonia[155], indicated NH_2 radicals. In the same hydrazine study absorption due to $NH(\Delta^3\pi\text{-}X^3\Sigma)$ has been noted.[156] Direct mass spectrometric analysis[84] of products and intermediates in the reaction zone of thermal and electrical discharge decompositions of N_2H_4 gave a myriad of species identified as H, N, H_2, NH_2, NH_3, N_2, N_2H_2, N_2H_3, N_2H_4, and N_3H_3. Such studies produced the first evidence for N_2H_2. If the discharge products were first condensed in a liquid nitrogen trap and then allowed to warm, tetrazene (N_4H_4) was observed, and concluded to arise from surface reactions in the condensed phase. A table of ionization potentials from the work of Foner and Hudson[84] of these rare species is given in Table III-III, along with more

Table III-III. Ionization potentials for some H and N species.

Species	I. P. (eV)[84]	I. P. (eV)[157]
H		13.8
N		14.6
NH		12.8
NH_2	11.4 ± 0.1	11.7
NH_3		10.2
N_2H_2	9.85 ± 0.1	9.9
N_2H_3	7.88 ± 0.2	7.6
N_3H_3	9.6 ± 0.1	
N_2H_4		8.8

recently determined values.[157] Diimine has been more thoroughly studied by decomposition of hydrazine with a microwave discharge. Condensation of products on a liquid nitrogen cooled window permitted study by infrared analysis; the spectrum was consistent with a planar N_2H_2 structure in a cis-geometry. The spectrum of the gas upon warmup did not permit structural elucidation. The repeated irrevocable demonstration of the trapping of diimine at low temperatures offers one example of the power of the matrix isolation method as a preparative method of normally unstable species, as a method for elucidating mechanisms, and as a method for allowing study of unstable species.

Photolysis of NH_3 and N_2H_4 are generally explained by formation of NH_2 radicals as the primary process.

$$NH_3 + h\nu \rightarrow NH_2 + H \qquad (76)\text{-III}$$

$$N_2H_4 + h\nu \rightarrow NH_2 + NH_2 \qquad (77)\text{-III}$$

Photolysis in both cases has been studied in the region from 1849Å to the vacuum U. V. Flash photolysis followed by kinetic absorption spectroscopy has directly identified NH_2 from both NH_3[160] and N_2H_4[161].

In the Schuman U. V.[162] photodissociation of ammonia produced NH_2 fluorescence with an onset at 843A. Reaction (78)-III,

$$NH_3 + h\nu \rightarrow NH_2(^2B_1) + H \qquad (78)\text{-III}$$

was suggested as the primary step. At the present time there seems to be no need to postulate a primary N-H rupture in the photolysis of N_2H_4 although such a reaction might be expected by analogy to ammonia, and is probably important at short wavelength.

The secondary reactions in the NH_3 radical system are not completely established; the main products are N_2, N_2H_4, and H_2. At 1470Å the quantum yield for ammonia loss was 0.45[163]. Flash photolysis results suggest that the hydrazine yield is independent of wavelength.[164] Investigators agree that the N_2H_4 yield and the NH_3 loss do not decline at low pressures. The first mechanism proposed is due to McDonald[165] who also compiled data at 1849A in both flow and static systems.

$$H + NH_2 \rightarrow NH_3^* \qquad \Delta H = -104 \text{ kcal} \qquad (79)\text{-III}$$

$$NH_3^* \xrightarrow{M} NH_3 \qquad (80)\text{-III}$$

$$NH_3^* \rightarrow NH_2 + H \qquad (81)\text{-III}$$

$$NH_2 + NH_2 \rightarrow N_2H_4 \qquad \Delta H = -56 \text{ kcal} \qquad (82)\text{-III}$$

$$N_2H_4 + H \rightarrow N_2H_3 + H_2 \qquad \Delta H = -11 \text{ kcal} \qquad (83)\text{-III}$$

$$N_2H_3 + H \rightarrow N_2 + 2H_2 \qquad \Delta H = -119 \text{ kcal} \qquad (84)\text{-III}$$

$$N_2H_3 + N_2H_3 \rightarrow 2NH_3 + N_2 \qquad \Delta H = -153 \text{ kcal} \qquad (85)\text{-III}$$

$$H + \text{wall} \rightarrow \tfrac{1}{2}H_2 + \text{wall} \qquad (86)\text{-III}$$

The pressure dependence for NH_3 loss was explained as a falloff in collisional deactivation of excited ammonia, NH_3^*, (80)-III. In the static photolysis the lack of hydrazine was attributed to reactions (83)-III - (85)-III, which became more important than in flow systems since hydrazine would remain for a longer time in the reaction zone. This requires that H-atoms react much more rapidly with N_2H_4 than with NH_3 which is reasonable in view of the much higher bond energy for the latter. Recent photolysis work by Husain and Norrish[161] as well as other investigations[54,70,71] have conclusively shown that NH_2 radical disproportionation reactions must be added to the above mechanism, either

$$NH_2 + NH_2 \rightarrow NH_3 + NH \qquad \Delta H = -10 \text{ kcal} \qquad (87)\text{-III}$$

or

$$NH_2 + H \rightarrow NH + H_2 \qquad \Delta H = -12 \text{ kcal} \qquad (88)\text{-III}$$

The subsequent fate of the NH is not known. The reaction (85)-III for N_2H_3 with itself seems also to be incorrect in view of recent work by Stief and De Carlo[166,167] which is discussed in the hydrazine mechanism considered below. The calculations in this thesis also suggest that the competition between redissociation and collisional deactivation of N_2H_4 should be considered at pressures $\leq$ 2 atm. Furthermore reaction (83)-III will give $N_2H_4^*$ which will dissociate to $2NH_2$.

A starting point for the secondary reactions in hydrazine to form N_2, H_2, and NH_3 is the mechanism proposed by Ramsay[160]

$$NH_2 + N_2H_4 \rightarrow NH_3 + N_2H_3 \qquad \Delta H = -6 \text{ kcal} \qquad (89)\text{-III}$$

$$N_2H_3 \rightarrow NH + NH_2 \qquad \Delta H = 54 \text{ kcal} \qquad (90)\text{-III}$$

$$N_2H_3 + N_2H_3 \rightarrow N_2 + 2NH_3 \qquad \Delta H = -153 \text{ kcal} \qquad (91)\text{-III}$$

$$N_2H_3 + NH_2 \rightarrow N_2 + H_2 + NH_3 \qquad \Delta H = -117 \text{ kcal} \qquad (92)\text{-III}$$

The second reaction, (90)-III can be discarded on the basis of modern thermochemistry. NH radicals are spectroscopically observed in the system[161], but can probably be better explained by reaction (93)-III.

$$N_2H_4 + h\nu \rightarrow NH + NH_3 \qquad (93)\text{-III}$$

However, some workers who used a mass spectrometer to identify the NH radical seem to favor a second primary process.

In their 1963 review Husain and Norrish[161] suggested that NH reacts with itself to form N_2 and H_2. This reaction currently is out of favor, but the real fate of NH is still uncertain. Undoubtedly some of the NH_2 radicals also recombine to N_2H_4.

Recent vacuum U. V. photolysis at 1236A and 1470A,[166] and an adiabatic flash heating study[167] of hydrazine have revised Ramsay's[160] suggested reactions of N_2H_3 with itself and with NH_2, (94)-III and (95)-III

$$N_2H_3 + NH_2 \rightarrow NH_3 + N_2H_2 \qquad \Delta H = -67 \text{ kcal} \qquad (94)\text{-III}$$

$$N_2H_2 \rightarrow N_2 + H_2 \qquad \Delta H = -48 \text{ kcal} \qquad (95)\text{-III}$$

Use of hydrazine and hydrazine-^{15}N mixtures indicated that nitrogen formation involved a process that maintained the integrity of the N-N bond of hydrazine. In light of this disproportionation of hydrazyl radicals (N_2H_3) was felt to be important, (96)-III.

$$N_2H_3 + N_2H_3 \rightarrow 2NH_3 + N_2H_2 \qquad \Delta H = -85 \text{ kcal} \qquad (96)\text{-III}$$

In this formulation, the combination reaction (91)-III is viewed as proceeding through formation of tetrazane (N_4H_6). In summary the best mechanism seems to include reactions (77), (89), (91), (92), (94), and (95)-III along with recombination of NH_2 radicals.

McDonald and Gunning[168] examined the mercury-photosensitized decomposition of ammonia at high light intensities in flow and static systems. The following mechanism,

$$Hg^* + NH_3 \rightarrow Hg + NH_2 + H \qquad (97)\text{-III}$$

$$H + NH_2 \rightarrow NH_3^* \qquad \Delta H = -103 \text{ kcal} \qquad (98)\text{-III}$$

$$NH_3^* + M \rightleftarrows NH_3 + M \qquad (99)\text{-III}$$

$$NH_2 + NH_2 \rightarrow N_2H_4 \qquad \Delta H = -57 \text{ kcal} \qquad (100)\text{-III}$$

which in view of present knowledge is deficient in NH_2 disproportionation, explained the initial stages of the decomposition. In this scheme NH_3^* contains enough energy to redissociate and based upon RRKM calculations for CH_4 could not be stabilized below a pressure of 10 atm. At long reaction times the hydrazine yield was found to diminish, probably by secondary attacks by H and NH_2, and nitrogen was formed. The quantum efficiency for the primary process was concluded to be unity, although direct measurement was hindered by back reaction (98)-III. Takamuku and Back[169] have attempted better measurement in the Hg-photosensitized decomposition by using lower light intensities and shorter reaction times. Secondary reactions still occurred, but the quantum yield was estimated to be below unity, and it increased with temperature. In the presence of propane the substrate was expected to provide a means of ΦNH_3 detection by efficiently scavenging hydrogen produced in the primary dissociation.

Although a very complex system was encountered, a significant finding was the suppression of nitrogen formation and increased methane yield. If methane arose from propyl radical decomposition, then (101)-III,

$$NH_2 + RH \rightarrow NH_3 + R \qquad (101)\text{-III}$$

was suggested to explain the data. Oxygen has been added to pure $Hg\text{-}NH_3$ systems as a free radical scavenger for both H and NH_2 radicals.[170] An upper limit was set at 0.3 for the primary quantum yield in (76)-III. There is no reason to believe that the $Hg(^3P_1)$ sensitization is any different than NH_3 photolysis, in terms of the primary and secondary reactions.

G. Mercury Photosensitization of Ethylenimine. Luner and Gesser[171] have studied the mercury photosensitized decomposition of ethylenimine with the objective of generating the $\overline{CH_2CH_2N}$ radical. Decomposition was found to yield H_2(70-75 mole%), N_2(20-30 mole%), CH_4(2-3 mole%), C_2H_4(93-97 mole%), NH_3(0.5-3 mole%), HCN(0.5-3 mole%), an m/e = 84 product peak attributed to the dimer of the CH_2CH_2N radical (0.5-3 mole%), and traces of ethane, propane, acetylene, and butane. A white, opaque, non-volatile polymer was also noted to form. Possible primary processes were suggested,

$$\overline{CH_2CH_2NH} + Hg(^3P_1) \rightarrow \overline{CH_2CH_2N} + H + Hg(^1S_0) \qquad (102)\text{-III}$$

$$\overline{CH_2CH_2NH} + Hg(^3P_1) \rightarrow CH_2CH_2 + NH + Hg(^1S_0) \qquad (103)\text{-III}$$

$$\overline{CH_2CH_2}NH + Hg(^3P_1) \rightarrow \overline{CH_2CHN}H + H + Hg(^1S_0) \qquad (104)\text{-III}$$

Jones and Lossing[172] have reported product yields determined from mass spectrometric analysis in an Hg photosensitized flow system: ethylene (83-90 mole%), hydrogen (33-41 mole%), nitrogen (8-12 mole%), acetonitrile (6-8 mole%), and methane (1-5 mole%), and ammonia (8 mole%). To cleverly clarify the primary process, the decomposition was carried out in mixtures with dimethyl mercury, which upon sensitization generates methyl radicals. Assuming an initial rupture of either C-H of N-H bonds in ethylenimine to give an H-atom plus some radical, CH_3 would 'trap' the radical by forming the combination product. Methyl titration in this manner resulted in formation of propylenimine, and thus was concluded to exclude (102)-III as occurring in this system. The power of this technique lay not only in the ability to distinguish (102)-III and (104)-III, but also by appropriate measurement of ethylenimine decomposed versus propylenimine formed, process (102)-III was shown to account for 5% of the decomposition. From the ethylene yield, reaction (103)-III was concluded to account for 83-90% of the decomposition, and the $Hg(^3P_1)$ sensitization of $\overline{CH_2CH_2}NH$ is established as a method of generating NH radicals.

In experiments with added CO,[172] the rate of ethylene appearance increased, while the methyl titration product was unaffected. Consequently they concluded that (104)-III proceeds via the formation of an electronically excited precursor,

while (103)-III results from an energy transfer analogous to quenching process observed in mercury sensitized alkane systems.

Typical, but unproven, secondary resctions for NH to form N_2, H_2, and NH_3 were proposed, (105)-III to (109)-III. Formation of HCN, CH_4, and CH_3CN

$$NH + NH \rightarrow N_2 + H_2 \qquad (105)\text{-III}$$

$$H + \overbrace{CH_2CH_2NH} \rightarrow H_2 + \overbrace{CH_2CH_2N} \qquad (106)\text{-III}$$

$$H + H \xrightarrow{M} H_2 \qquad (107)\text{-III}$$

$$NH + \overbrace{CH_2CH_2NH} \rightarrow \overbrace{CH_2CH_2N} + NH_2 \qquad (108)\text{-III}$$

$$NH_2 + \overbrace{CH_2CH_2NH} \rightarrow \overbrace{CH_2CH_2N} + NH_3 \qquad (109)\text{-III}$$

can be explained from secondary reactions of CH_2CH_2N and CH_3 radical abstraction reactions.

Klemm[173] investigated the Hg photosensitized decomposition of ethyleneimine and ethylenimine-d_4. Experiments were also performed with added ethylene. Ethylene, hydrogen, ammonia, nitrogen, methane, and ethane were observed products, but no propane, acetylene, acetonitrile, or hydrogen cyanide was detected. Using the deuterated ethylenimine, the primary process was again investigated. The breakdown of the isotopic hydrogen yield, H_2 67%, HD 33%, and D_2 0%, indicated the predominance of (102)-III as far as fragmentation to give a hydrogen was concerned. This is in sharp contradiction with the interpretation by Jones and Lossing[172] of the methyl titration results. Based

on a high activation energy for hydrogen abstraction from a carbon abstraction was assumed to be completely from the nitrogen. Possible competition with H-atom addition to ethylene implied an E_a of about 5 kcal for H-abstraction from ethylene-d_4

Decomposition via process (103)-III yielded only C_2D_4 in the deuterated system, and is exothermic by 43 kcal. It was interesting to note that H_2 and C_2H_4 rates of formation were nearly the same. This supports reaction (103)-III as the main path. With and without added ethylene, ammonia was observed unchanged in yield, and possibly arose from successive abstraction reactions from the parent. The strange isotopic distribution in the methane yield (CD_4 3%, CD_3H 33%, and CD_2H_2 63%) indicated a complex series of steps for its formation. Such a scheme was envisaged by analogy with the mercury photosensitized decomposition of cyclopropane and ethylene oxide, both of which are known to proceed via an excited molecule.

$$\overbrace{CD_2CD_2}NH + Hg(^3P_1) \rightarrow (\overbrace{CD_2CD_2}NH)^* + Hg(^1S_0) \qquad (110)\text{-III}$$

$$(\overbrace{CD_2CD_2}NH)^* \rightarrow (CD_3CD{=}NH)^* \rightarrow CD_4 + HCN$$
$$\rightarrow CD_3 + D + HCN \qquad (111)\text{-III}$$

$$(\overbrace{CD_2CD_2}NH)^* \rightarrow (CD_2NH = CD\ )^* \rightarrow CD_2H + D + DCN \qquad (112)\text{-III}$$

The results from the Hg photosensitized decomposition of ethyleneimine present themselves in a somewhat ambiguous manner. The system apparently affords NH radicals, but all the primary processes do not appear to be confirmed yet. The isotopic

ethylenimene-d_4 experiments would appear to be less suspect than the methyl radical titration experiments, however, more work is necessary. Assuming predominant hydrogen split off from the N-atom the latter could be explained by a rapid intramolecular hydrogen transfer relative to methyl combination i.e.,

$$\overbrace{CH_2CH_2N} \rightarrow \overbrace{CH_2CHNH} \quad . \qquad (113)\text{-III}$$

The ammonia product unchanged by added ethylene may require updating of previous views of ethylene as a scavenger for NH. In conclusion the Hg photosensitized decomposition of ethylenimene holds promise for the study of NH radicals.

ACKNOWLEDGEMENTS

The author wishes to gratefully acknowledge the continued asssistance of Dr. D. W. Setser, without whose role as prime mover this work would not have been possible.

The assistance of many other people is always necessary for such an undertaking, but rarely can be completely acknowledged. A few will be mentioned. My mother and father for perpetual encouragement, my sister, Kathie, for typing the tentative copy, my wife, Patricia, for understanding, Mr. G. Johnson for mass spec work, the members of the Group for helpful discussions of theory, and the members of W-301 for other interesting discussions and tolerance. The financial support of the Department of Health, Education, and Welfare through the Division of Air Pollution is also greatly appreciated.

REFERENCES

1. H. C. Ramsperger, J. Am. Chem. Soc., 51, 2134 (1929).

2. R. Meyer and H. J. Schumacher, Z. Physik. Chem., A170, 33 (1934).

3. P. Gunther, R. Meyer, and F. Muller-Skjold, Z. physik Chem. A175, 154 (1935).

4. A. O. Beckman and R. G. Dickinaon, J. Am. Chem. Soc., 50, 1870 (1928).

5. A. O. Beckman and R. G. Dickinson, J. Am. Chem. Soc., 52, 124 (1930).

6. A. E. Meyers and A. O. Beckman, J. Am. Chem. Soc., 57, 89 (1935).

7. D. A. Dows, G. C. Pimentel, and E. Whittle, J. Chem. Phys., 23, 1606 (1955).

8. P. H. H. Fischer, S. W. Charles, and C. A. McDowell, J. Chem. Phys., 46, 2162 (1967).

9. E. D. Miller, Ph.D. Thesis, Catholic University of America, 1961.

10. W. S. Frost, J. C. Cothran, and A.W. Browne, J. Am. Chem. Soc., 55, 3516 (1933).

11. D. A. Dows, E. Whittle, and G. C. Pimentel, J. Chem. Phys., 23, 1475 (1955).

12. P. Gray and T. C. Waddington, Nature, 179, 576 (1957).

13. W. B. DeMore and S. W. Benson, Advan. Photochem., 2, 219 (1964).

14. H. M. Frey, Progr. Reaction Kinetics, 2, 133 (1964).

15. D. W. Setser and B. S. Rabinovitch, Can. J. Chem., 40, 1425 (1962).

16. H. S. Johnston, J. Chem. Phys., 19, 663 (1951).

17. S. Glasstone, K. J. Laidler, and H. Eyring, "The Theory of Rate Processes", McGraw-Hill Book Co., Inc., New York, 1941.

18. E. K. Gill and K. J. Laidler, Can. J. Chem., 36, 1570 (1958).

19. S. W. Benson, Advan. Photochem., 2, 1(1964).

20. D. F. Ring and B. S. Rabinovitch, J. Am. Chem. Soc., 88, 4285 (1966).

21. (a) D. W. Setser, R. L. Littrell, and J. C. Hassler, J. Am. Chem. Soc., 87, 2062 (1965); (b) J. C. Hassler and D. W. Setser, J. Chem. Phys., 45, 3237 (1966).

22. L. I. Avramenko and R. V. Kolesnikova, Advan. Photochem., 2, 25 (1964).

23. F. Kaufman, Progr. Reaction Kinetics, 1, 1 (1961).

24. R. J. Cvetanovic, Advan. Photochem., 1, 115 (1963).

25. (a) H. Yamazaki and R. J. Cvetanovic, J. Chem. Phys., 41, 3703 (1964); (b) A. Kato and R. J. Cvetanovic, Can. J. Chem., 46, 235 (1968).

26. H. E. Gunning and O. P. Strausz, Advan. Photochem., 4, 143 (1966).

27. R. A. Marcus and O. K. Rice, J. Phys. and Colloid Chem., 55, 894 (1951).

28. L. S. Kassel, "The Kinetics of Homogeneous Gas Reactions", The Chemical Catalog Company, Inc., New York, 1932.

29. D. W. Setser, J. Phys. Chem., 70, 826 (1966).

30. H. Shaw, J. H. Menczel, and S. Toby, J. Phys. Chem., 71, 4180 (1967).

31. R. A. Marcus, J. Chem. Phys., 20, 359 (1952).

32. R. A. Marcus, J. Chem. Phys., 20, 352 (1952).

33. B. S. Rabinovitch and D. W. Setser, Advan. Photochem., 3, 1 (1964).

34. O. K. Rice, J. Phys. Chem., 65, 1588 (1961).

35. Z. Prasil and W. Forst, J. Phys. Chem., 71, 3166 (1967).

36. P. C. Haarhoff, J. Mol. Phys., 6, 337 (1963).

37. P. C. Haarhoff, J. Mol. Phys., 7, 101 (1963).

38. Glasstone, K. J. Laidler, and H. Eyring, op. cit.

39. K. Yang and T. Ree, J. Chem. Phys., 35, 588 (1961).

40. (a) E. Gorin, Acts Physicochim. U.R.SS., 9, 691 (1939); (b) H. S. Johnston and P. Goldfinger, J. Chem. Phys., 37, 700 (1962).

41. F. A. Cotton and G. Wilkinson, "Advanced Inorganic Chemistry", Interscience Publishers, New York, 1967.

42. M. E. Jacox and D. E. Milligan, J. Chem. Phys., 46, 184 (1967).

43. D. A. Dows and G. C. Pimentel, J. Chem. Phys., 23, 1258 (1955).

44. J. L. Franklin, V. H. Dibeler, R. M. Reese, and M. Krauss, J. Am. Chem. Soc., 80, 298 (1958).

45. C. Bighi and G. Saglietto, J. Chromatog., 18, 297 (1965).

46. A. A. Frost and R. G. Pearson, "Kinetics and Mechanism", Second Edition, John Wiley and Sons, Inc., New York, 1961.

46a. ASTM, Mass Spectral Data, American Petroleum Institute, Research Project 44, 1957.

47. W. D.Woolley and R. A. Back, Can. J.Chem., 46, 295 (1968).

48. (a) S. K. Lower and M. A. El-Sayed, Chem. Rev., 66, 199 (1966); (b) M. A. El-Sayed, Accounts of Chemical Research, 1, 8 (1968).

49. H. Okabe and M. Lenzi, J. Chem. Phys., 47, 5241 (1967).

50. D. W. Cornell, R. S. Berry, and W. Lwowski, J. Am. Chem. Soc., 88, 544 (1966).

51. H. Guenebaut, G. Pannetier, and P. Goudmand, Compt. rend., 251, 1166 (1960).

52. G. Pannetier, P. Goudmand, O. Dessaux, and H. Guenebaut, Compt. rend., 256, 3082 (1963).

53. B. A. Thrush, Proc. Roy. Soc. (London), A235, 143 (1956).

54. R. W. Diesen, J. Chem. Phys., 39, 2121 (1964).

55. N. N. Semenov, "Some Problems of Chemical Kinetics and Reactivity", Vol. 1, Pergamon Press, New York, 1958.

56. S. W. Benson, "The Foundations of Chemical Kinetics", McGraw Hill Book Company, Inc., New York, 1960.

57. K. W. Michel, Angew. Chem. internat. Edit., 4, 369 (1965).

58. P. Gray and J. C. J. Thynne, Trans. Faraday Soc., 60, 1047 (1964).

59. R. J. Cvetanovic, Advan. Photochem., 1, 115 (1963).

60. D. W. Setser and B. S. Rabinovitch, J. Chem. Phys., 40, 2427 (1964).

61. M. P. Halstead and C. P. Quinn, Trans. Faraday Soc., 64, 104 (1968).

62. S. W. Benson and G. R. Haugen,J. Phys. Chem., 71, 1735 (1967).

63. (a) M. Szwarc, Proc. Roy. Soc. (London), A198, 267 (1949); (b) A. Kant and W. J. McMahon, J. Inorg. Nucl. Chem., 15, 305 (1960).

64. I. J. Eberstein, Technical Report 708, 1964.

65. G. K. Adams and G. W. Stock, 4th Symp. Combust. Pittsburg, 1952, 239 (1953).

66. W. H. Moberly, J. Phys. Chem., 66, 366 (1962).

67. K. W. Michel and H.G.G.Wagner, Technical Summary Report No. 3, Contract No. AF61 (514)-1142, 1962.

68. E. T. McHale, B. E. Knox, and H. B. Palner, Technical Report PSU-12-P, 1964.

69. K. W. Michel and H. GG. Wagner, Symp. Combust. 10th, Univ. Cambridge, Engl. Cambridge, 1964, 79 (1965).

70. M. H. Hanes and E. J. Bair, J. Chem. Phys., 38, 672 (1963).

71. (a) J. D. Salzman and E. J. Bair, J. Chem. Phys., 41, 3654 (1964); (b) P. K. Ghosh and E. J. Bair, J. Chem. Phys., 45, 4738 (1966).

72. D. C. Carbaugh, F. J. Munno, and J. M. Marchello, J. Chem. Phys., 47, 5211 (1967).

73. J. L. Brash and R. A. Back, Can. J. Chem., 43, 1778 (1965).

74. D. W. Setser, J. Am. Chem. Soc., 90,582 (1968).

75. JANAF THERMOCHEMICAL TABLES, The Dow Chemical Company, Midland, Michigan, August 1965; Addendum 1, August 1966; Addendum 2, August 1967.

76. National Bureau of Standards, Technical Note 270-1, October, 1965.

77. S. W. Benson, J. Chem. Ed., 42, 502 (1965).

78. J. A. Kerr, Chem. Revs., 66, 465 (1966).

79. P. Gray, Quart, Rev., 17, 441 (1963).

80. P. Gray and T. C. Waddington, Proc. Roy. Soc. (London), A235, 481 (1956).

81. K. E. Seal and A. G. Gaydon, Proc. Phys. Soc. (London), 89, 459 (1966).

82. S. Singh, Proc. Roy. Soc. (London), A225, 519 (1954).

83. L. F. Loucks and K. J. Laidler, Can. J. Chem., 45, 2795 (1967).

84. (a) S. N. Foner and R. L. Hudson, J. Chem. Phys., 29, 442 (1958); (b) I. P. Fisher and G. A. Heath, Nature, 208, 1199 (1965).

85. P. Gray and A. Jones, Can. J. Chem., 45, 333 (1967).

86. J. J. Leventhal and L. F. Friedman, J. Chem. Phys., 46, 997 (1967).

87. W. B. Maier, II, J. Chem. Phys., 47, 859 (1967).

88. N. J. Friswell and B. G. Gowenlock, Advan. Free-Radical Chem., 2, 1 (1967).

89. P. Gray and J. C. J. Thynne, Trans. Faraday Soc., 60, 1047 (1964).

90. (a) D. H. Stedman and D. W. Setser, J. Chem. Phys., 49, 467 (1968); (b) V. H. Dibeler and S. K. Liston, J. Chem. Phys., 47, 4548 (1967); (c) D. D. Davis and H. Okabe, Preprint.

91. A. C. Hurley, Proc. Roy. Soc. (London), A249, 402 (1959).

92. S. N. Foner and R. L. Hudson, J. Chem. Phys., 45, 40 (1966).

93. J. R. McNesby and H. Okabe, Advan. Photochem., 3, 157 (1964).

94. F. R. Gilmore, RAND Memorandum, RM-4034-1-PR, April 1966.

95. (a) J. S. Ziomek and M. D. Zeidler, J. Mol. Spec., 11, 163 (1963); (b) A. Yamaguchi, I. Ichishima, T. Shimanouchi, and S. Mizushima, Spectrochim. Acta, 16, 1471 (1960).

96. D. E. Milligan and M. E. Jacox, J. Chem. Phys., 43, 4487 (1965).

97. D. A. Ramsey, Ann. N.Y. Acad. Sci., 67, 485 (1957).

98. (a) J. R. Barcelo and J. Bellanato, Spectrochim. Acta, 8, 27 (1956); (b) T. Nishikawa, J. Phys. Soc. Japan, 12, 688 (1957).

99. W. L. S. Andrew and G. C. Pimentel, J. Chem. Phys., 44, 2527 (1966).

100. T. Itoh, J. Phys. Soc. Japan, 11, 264 (1956).

101. M. Bonnemay, J. Chim. Phys., 40, 231 (1943).

102. F. O. Rice and M. Freamo, J. Am. Chem. Soc., 73, 5529 (1951).

103. F. O. Rice and M. Freamo, J. Am. Chem. Soc., 75, 548 (1953).

104. F. O. Rice and C. Grelecki, J. Am. Chem. Soc., 79, 1880 (1957).

105. F. O. Rice and R. B. Ingall, J. Am. Chem. Soc., 81, 1856 (1959).

106. F. O. Rice and T. A. Luckenbach, J. Am. Chem. Soc., 82, 2681 (1960).

107. S. Hunig, H. R. Muller, and W. Thier, Angew. Chem., 77, 368 (1965).

108. S. N. Foner and R. L. Hudson, J. Chem. Phys., 28, 719 (1958).

109. G.Pannetier, Ph. Mignotte, and M. Chevillon, Bull. soc. chim. France, 1960, 804.

110. G. Pannetier and M. Lecamp, Bull. soc. chim. France, 1954, 1068.

111. G. Pannetier, H. Guenebaut, and A. G. Gaydon, Compt. rend., 240, 958 (1955).

112. U. Wannagat and H. Kohnen, Angew. Chem., 69, 783 (1957).

113. U. Wannagat and H. Kohnen, Z. anorg. u. allgem. Chem., 304, 276 (1960).

114. I. Hajal and J. Combourieu, Compt. rend., 253, 2346 (1961).

115. I. Hajal and J. Combourieu, Compt. rend., 255, 509 (1962).

116. P. Laffitte, I. Hajal, and J. Combourieu, Symp. Combust. 10th, Univ. Cambridge, Engl. Cambridge, 1964, 79 (1965).

117. A. E. Douglas and W. J. Jones, Can. J. Phys., 43, 2216 (1965).

118. D. E. Milligan and M. E. Jacox, J. CHem. Phys., 47, 5157 (1967).

119. H. Okabe, A. C. S. Meeting, Atlantic City, September 1968.

120. K. H. Welge, J. Chem. Phys., 45, 4373 (1966).

121. K. H. Welge, J. Chem. Phys., 45, 166 (1966).

122. I. L. Mador and M. C. Williams, J. Chem. Phys., 22, 1627 (1954).

123. L. F. Keyser and G. W. Robinson, J. Am. Chem. Soc., 82, 5245 (1960).

124. H. A. Papazian, J. Chem. Phys., 32, 456 (1960).

125. H. A. Papazian and A. P. Margozyi, J. Chem. Phys., 44, 843 (1966).

126. E. D. Becker, G. C. Pimentel, and M. Van Thiel, J. Chem. Phys., 26, 145 (1957).

127. M. Van Thiel and G. C. Pimentel, J. Chem. Phys., 32, 133 (1960).

128. D. E. Milligan and M. E. Jacox, J. Chem. Phys., 41, 2838 (1964).

129. M. E. Jacox and D. E. Milligan, J. Chem. Phys., 40, 2457 (1964).

130. K. Rosengren and G. C. Pimentel, J. Chem. Phys., 43, 507 (1965).

131. M. E. Jacox and D. E. Milligan, J. Am. Chem. Soc., 85, 278 (1963).

132. D. E. Milligan and M. E. Jacox, J. Chem. Phys., 36, 2911 (1962).

133. M. E. Jacox and D. E. Milligan, J. Chem. Phys., 46, 184 (1967).

134. G. C. Pimentel, J. Am. Chem. Soc., 80, 62 (1958).

135. J. D. Baldeschwieler and G. C. Pimentel, J. Chem. Phys., 33, 1088 (1960).

136. D. E. Milligan, M. E. Jacox, S. W. Charles, and G. C. Pimentel, J. Chem. Phys., 37, 2302 (1962).

137. S. Krzyzanowski and R. J. Cvetanovic, Can. J. Chem., 45, 665 (1967).

138. G. Herzberg and C. Reid, Discussiona Faraday Soc., 9, 92 (1950).

139. J. Y. P. Mui and R. A. Back, Can. J. Chem., 41, 826 (1963).

140. R. A. Back, J. Chem. Phys.,40, 3493 (1964).

141. N. J. Friswell and R. A. Back, Can. J. Chem., 46, 527 (1968).

142. R. A. Back and R. Ketcheson, Can. J. Chem., 46, 531 (1968).

143. J. N. Bradley, J. R. Gilbert, and P. Svejda, Trans. Faraday Soc., 64, 911 (1968).

144. R. N. Nixon, Can. J. Phys., 37, 1171 (1959).

145. R. Holland, D. W. G. Style, R. N. Nixon, and D. A. Ramsay, Nature, 182, 336 (1958).

146. H. Guenebaut and M. Latour, Compt. rend., 250, 4358 (1960).

147. H. Guenebaut and G. Pannetier, compt. rend., 250,3613 (1960).

148. H. Guenebaut and M. Latour, J. Chem. Phys., 59, 970 (1962).

149. H. Guenebaut, Compt. rend., 249, 2778 (1959).

150. G. Pannetier, H. Guenebaut, and I. Hajal, Bull. Soc. chim. France, 1959, 1159.

151. G. Pannetier, H. Guenebaut, and I. Hajal, J. Chim. Phys., 56, 129 (1959).

152. K. Stewart, Trans. Faraday Soc., 41, 663 (1945).

153. B. E. Knox and E. T. McHale, Anal. Chem., 38, 487 (1966).

154. G. W. Robinson and M. McCarty, Jr., J. Chem. Phys., 28, 349 (1958).

155. G. W. Robinson and M. McCarty, Jr., J. Chem. Phys., 30, 999 (1959).

156. G. W. Robinson and M. McCarty, Jr., J. Chem. Phys., 28, 350 (1958).

157. C. E. Melton, J. Chem. Phys., 45, 4414 (1966).

158. E. J. Blau, B. F. Hochheimer, and H. J. Unger, J. Chem. Phys., 34, 1060 (1961).

159. E. J. Blau and B. F. Hochheimer, J. Chem. Phys., 41, 1174 (1964).

160. D. A. Ramsay, J. Phys. Chem., 57, 415 (1953).

161. D. Husain and R. G. W. Norrish, Proc. Roy. Soc. (London), A273, 145 (1963).

162. H. Okabe, H. D. Beckey, and W. Groth, Z. Naturforsch., a22, 1161 (1967).

163. H. Jucker and E. K. Rideal, J. Chem. Soc., 1957, 1058.

164. W. Groth and K. H. Welge, Bull. Soc. Chim. Belges., 71, 705 (1962).

165. C. C. McDonald, A. Kahn, and H. E. Gunning, J. Chem. Phys., 22, 908 (1954).

166. L. J. Stief, V. J. DeCarlo, and R. J. Matsloni, J. Chem. Phys., 46, 592 (1967).

167. L. J. Stief and V. J. DeCarlo, J. Phys. Chem., 71, 2350 (1967).

168. C. C. McDonald and H. E. Gunning, J. Chem. Phys., 23, 532 (1955).

169. S. Takamuku and R. A. Back, Can. J. Chem., 42, 1426 (1964).

170. M. Z. Hoffman, M. Goldwasser, and P. L. Damour, J. Chem. Phys., 47, 2195 (1967).

171. C. Luner and H. Gesser, J. Am. Chem. Soc., 62, 1148 (1958).

172. A. Jones and F. P. Lossing, Can. J. Chem., 45, 1685 (1967).

173. R. F. Klemm, Can. J. Chem., 45, 1693 (1967).

THERMAL DECOMPOSITION OF HYDRAZOIC ACID

by

WILLIAM C. RICHARDSON

B. S., Fordham College, 1965

AN ABSTRACT OF A MASTER'S THESIS

submitted in partial fulfillment of the

requirements for the degree

MASTER OF SCIENCE

Department of Chemistry

KANSAS STATE UNIVERSITY
Manhattan, Kansas

1969

ABSTRACT

The thermal decomposition of hydrazoic acid in the presence of methane, ethane, propane, deuterium, and nitric oxide was investigated over the temperature region 285°-470°C under a variety of pressures, and in vessels with different surface conditions. The decomposition proceeded in the same way as the low temperature pyrolysis of pure HN_3. Limited experiments were performed with ethene as a substrate; some products were formed by reaction of radical intermediates containing nitrogen with C_2H_4. Although the reaction products in these systems can, in part, be explained as arising from NH radicals, the pyrolysis of HN_3 is certainly not a clean source of NH radicals due to heterogeneity and complex secondary reactions of radicals with HN_3.

Since NH_2 radicals can be present in these systems it was important to have an estimate of the relative quantities of stabilization and decomposition products of hydrazine arising from the combination of NH_2. For this reason, RRKM calculations were done based on models designed to indicate the upper and lower bounds to the dissociation rate constants for chemically activated N_2H_4. The formation of chemically activated methylamine from NH interaction with methane was another possibility, and similar calculations were carried out for this species.